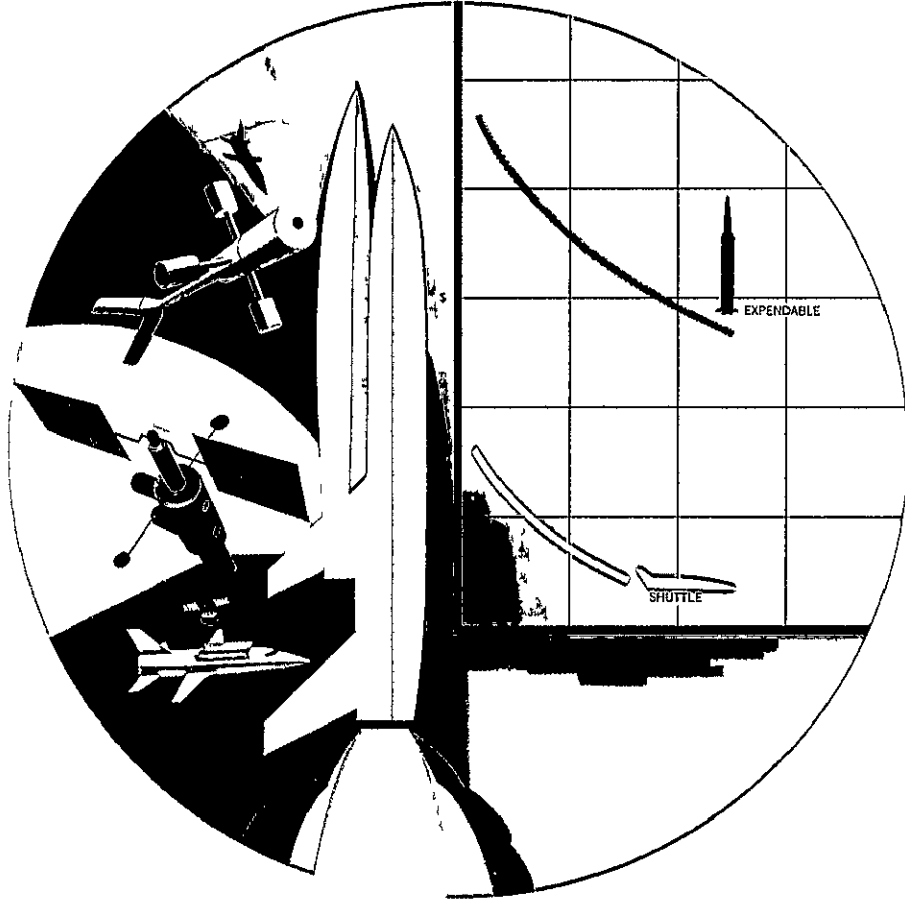


1-P



SD 70-9

# Space Shuttle Program Review

Bonn, Germany  
7 July 1970



Space Division  
North American Rockwell

Reproduced by  
NATIONAL TECHNICAL  
INFORMATION SERVICE  
Springfield Va 22151

5876974  
 22 JUL 1970  
 SPACE SHUTTLE PROGRAM

1-18438  
 (ACCESSION NUMBER)

GS  
 (THRU)

3  
 (CODE)

02-116600  
 (PAGES)

(NASA CR OR TMX OR AD NUMBER)

(CATEGORY)

FACILITY FORM 602

SD 70-9

# Space Shuttle Program Review

Bonn, Germany  
7 July 1970

Prepared by

B HELLO, Vice President and General Manager,  
Space Shuttle Program

J W SANDFORD, Project Director, Program Development  
and Plans, Space Shuttle Program

D A DOOLEY, Program Vice President, Booster Program,  
Convair GD

**Space Division**  
North American Rockwell

**Convair**  
General Dynamics

## FOREWORD

This paper was prepared by the Space Division of North American Rockwell Corporation and its team member the Convair Division of General Dynamics. It deals with details of the Phase B Space Shuttle Definition Program and the overall scope of the design and test activity being performed under the direction of NASA's Manned Spacecraft Center at Houston, Texas. The material contained in the paper was developed specifically for a National Aeronautics and Space Administration/European Launch Development Organization (NASA/ELDO) Shuttle conference held in Bonn, Germany 7-8 July 1970.

# CONTENTS

Section		Page
1	PROGRAM INTRODUCTION	1
2	SHUTTLE SYSTEM	9
3	SHUTTLE ORBITERS	15
	General Configuration	15
	Primary Orbiter Subsystems	25
	Orbiter Comparisons	31
4	SHUTTLE BOOSTER	35
	Booster Mission Profile	35
	Booster Characteristics	36
	Aerodynamic Characteristics	38
	Separation and Abort	39
	Structural and Thermal Protection Systems	41
	Booster Propulsion Systems	45
	Other Subsystems	50
5	OPERATIONS	55
	Baseline Operations Site	55
	Post-Landing Operations	56
	Maintenance and Refurbishment	56
	Prelaunch Operations	56
	Launch Operations	59
	Flight Operations	59
6	DEVELOPMENT PLAN	63
	Manufacturing and Assembly	63
	Ground Tests	65
	Horizontal Flight Tests	68
	Vertical Flight Tests	69
7	SUMMARY	71



## ILLUSTRATIONS

Figure		Page	Figure		Page
1-1	Presentation Outline	1	3-9	Cargo Center-of-Gravity	
1-2	Phase B Shuttle Team	2		Characteristics (Subsonic)	18
1-3	Introduction to North American Rockwell and General Dynamics	2	3-10	Orbiter Landing	19
1-4	Introduction to IBM, Honeywell, and American Airlines	3	3-11	Straight-Wing Orbiter Entry	19
1-5	Phase B Contract Plan	3	3-12	Maximum Temperatures and Materials	20
1-6	Major Elements of Phase B	4	3-13	Delta-Wing Orbiter, High Cross Wing	20
1-7	Shuttle Requirements	4	3-14	Orbiter Design Details	21
1-8	Shuttle Configuration Requirements and Concepts	5	3-15	Entry Flight Profile for High Cross-Range, Delta-Wing Orbiter	22
1-9	Reusable Shuttle Concept Options	6	3-16	Entry Flight Profile for High Cross-Range, Delta-Wing Orbiter	22
1-10	Baseline Configuration	7	3-17	Hypersonic Aerodynamic Characteristics, Delta-Wing Orbiter	22
2-1	Shuttle Mission Profile	9	3-18	Subsonic Aerodynamic Characteristics, Delta-Wing Orbiter	22
2-2	Integrated Vehicles	9	3-19	Cargo Center-of-Gravity Variations	23
2-3	Effect of Orbiter Gross Weight on Payload	10	3-20	Landing Characteristics	23
2-4	Number of Booster Engines	11	3-21	Landing Characteristics	23
2-5	Mated Configuration, Low Cross-Range Orbiter	11	3-22	Delta-Wing Orbiter Entry	24
2-6	Mated Configuration, High Cross-Range Orbiter	11	3-23	Maximum Temperatures and Materials	24
2-7	Payload and Mission Capability	12	3-24	Thermal Protection System Key Technology Factors	24
2-8	Flight Profile	13	3-25	Typical Thermal and Structural Tests	25
2-9	Ascent Trajectory Profile	13	3-26	Delta-Wing Orbiter Design Conditions and Load Intensity	25
3-1	Shuttle Orbiters	15	3-27	Large Structure Tests Major Structural Subassemblies	26
3-2	Straight-Wing Orbiter, Low Cross Range	15	3-28	Rocket Engine Systems	26
3-3	Orbiter Design Details, Straight-Wing Orbiter	16	3-29	Orbiter Main Propulsion System	27
3-4	Entry Flight Profile for Low Cross Range	17	3-30	Orbiter Attitude Control Propulsion System	27
3-5	Entry Flight Profile for Low Cross Range	17			
3-6	Straight-Wing Orbiter	18			
3-7	Subsonic Aerodynamic Characteristics, Low Cross-Range Orbiter	18			
3-8	Cargo Center-of-Gravity Characteristics (Hypersonic)	18			

Figure		Page	Figure		Page
3-31	On-Orbit Maneuvering System Schematic	28	4-19	Alternate Design Approaches	42
3-32	Integrated Electronics	28	4-20	Booster Design Conditions and Load Intensities	42
3-33	Integrated Avionics Characteristics	29	4-21	Booster Structural Features	43
3-34	Communications	29	4-22	Entry Corridor Comparison	43
3-35	Shuttle Orbiter Cockpit	30	4-23	Booster Temperature, Oxygen Tank Area Lower Surface 12.2 Meters From Nose	43
3-36	Apollo Crew Station and Equipment	30	4-24	Booster Temperature, Hydrogen Tank Area Lower Surface 27.4 Meters From Nose	44
3-37	Boost and Ascent Display	30	4-25	Booster Maximum Temperatures and Materials Distribution	44
3-38	Space Attitude Display	31	4-26	Acoustic Levels at Liftoff	45
3-39	On-Board Checkout	31	4-27	Booster Propulsion Systems	45
3-40	Baseline Vehicle Mass Characteristics, Gross Liftoff Mass = 1,587,000 Kilograms	32	4-28	Main Propulsion System	46
3-41	Structural and Subsystem Weight Distribution	32	4-29	Booster Main Propulsion System	46
3-42	Structural and Subsystem Weight Distribution	32	4-30	Number of Booster Engines	47
3-43	Comparison of Orbiter Fuselage Heating Histories, High and Low Cross-Range Entry	32	4-31	LO <sub>2</sub> Feed Duct Geometry Options	47
4-1	Baseline Booster After Staging	35	4-32	Attitude Control Propulsion System	48
4-2	Outline of Booster Briefing	35	4-33	Attitude Control Propulsion System Engine Characteristics Summary	49
4-3	Booster Flight Profile	36	4-34	Air-Breathing Propulsion System	49
4-4	Booster Flight Modes	36	4-35	Existing Versus New Air-Breathing Engines	50
4-5	Baseline Booster Configuration	36	4-36	Candidate High Bypass Ratio Turbofans	50
4-6	Characteristics of Baseline Booster	37	4-37	IAS Block Diagram	51
4-7	Baseline Booster	37	4-38	Crew Compartment	51
4-8	Booster Size Comparison	37	4-39	Environmental Control and Life Support Baseline	52
4-9	Booster Comparison Data	38	4-40	Power System Baseline	52
4-10	Baseline Vehicle Weight Characteristics (kg) Gross Liftoff Weight 1,587,000 kg	38	4-41	Main Landing Gear	53
4-11	Booster Stability Trends	39	4-42	Nose Landing Gear	53
4-12	Variation of Trim Angle of Attack	39	4-43	Landing Gear	53
4-13	Variations to Baseline Booster Nose	40	5-1	Ground and Flight Operations	55
4-14	Baseline Separation Concept	40	5-2	Baseline Operations Facilities	55
4-15	Baseline Separation Sequencing	40	5-3	Ground Operations	56
4-16	Intact Abort	41			
4-17	Booster Design and Packaging Considerations	41			
4-18	Booster Design and Packaging Considerations	41			

Figure		Page	Figure		Page
5-4	Booster Landing	57	6-6	Final Mating, Assembly, and Checkout	65
5-5	Booster in Safing Area	57	6-7	Final Orbiter Assembly	65
5-6	Post-Landing Operations Time Line (Booster)	57	6-8	Major Ground Tests	66
5-7	Post-Landing Operations Time Line (Orbiter)	57	6-9	Major Structural Tests (Booster)	66
5-8	Launch Preparation	58	6-10	Major Structural Tests (Orbiter)	66
5-9	Maintenance and Refurbishment Time Line	58	6-11	Structural Static/Fatigue Test of Booster Thrust Barrel	67
5-10	Towing Shuttle to Launch Site	58	6-12	Static Propulsion Test, Mississippi Test Facility	67
5-11	Space Shuttle in Vertical Launch Position	58	6-13	Integrated Avionics/Control Test	68
5-12	Prelaunch Operations Time Line	59	6-14	Horizontal Flight Test	68
5-13	Launch Operations Time Line	60	6-15	Horizontal Flight Test Objectives	68
5-14	Propellant Loading Operations	60	6-16	Vertical Flight Test	69
5-15	Ascent Flight Operations	60	6-17	Summary Program Plan	70
5-16	Docking Operations	60	6-18	Baseline Program Plan	70
5-17	Flight Operations Time Line (Hours)	61	7-1	Most-Critical Issues	71
6-1	Development Test Philosophy	63	7-2	Candidates for Participation	72
6-2	Program Functional Flow Plan	63	7-3	Timetable	72
6-3	LH <sub>2</sub> Tank Assembly Breakdown	64	7-4	Summary	73
6-4	Mated Tank Assembly Breakdown	64			
6-5	Fuselage Assembly Breakdown	64			

# 1. PROGRAM INTRODUCTION

The North American Rockwell Space Division and the Convair Division of General Dynamics welcome the opportunity to participate in this review of the Space Shuttle Program by the National Aeronautics and Space Administration (NASA) and the European Launch Development Organization (ELDO). It is encouraging to see the interest and enthusiasm that exists in Europe for the space program. It requires little imagination to envision the space shuttle being used to carry French, German, British, or, for that matter, any international payload into earth orbit, with flight crews and scientists from various nations. A further level of participation in the shuttle is also possible through teaming or subcontract arrangements. It is, therefore, timely at the outset of the Phase B to bring you up to date on details of the shuttle. The material discussed today will possibly provide a foundation for further communication between our governments and assist industry-to-industry discussions on programs of collaboration. Previous speakers have reviewed the primary reason why the United States strongly supports development of the space shuttle as the transportation system of the 70's and 80's. Therefore, this paper will summarize the major aspects of the Space Shuttle Phase B Definition Program contract that was recently awarded by NASA to an industrial team headed by Space Division. The material is divided into the seven major sections, as specified in Figure 1-1.

As will be seen from this outline, we will cover all aspects of the program, emphasizing the technical features of our baseline vehicles, operations, and the development program plan. In addition, we will briefly review the rationale we used in arriving at these baseline shuttle designs. The baselines provide a comprehensive definition of the total shuttle system - vehicles and the vehicle subsystems. These are to be used as points of departure, or as references, in investigating different approaches. During Phase B, the approaches will be compared to the baseline, and the system that meets the overall program cost objectives, the mission flexibility requirements, mission safety goals, and schedules will be selected. The contract for NASA will be performed by a team of major United States corporations

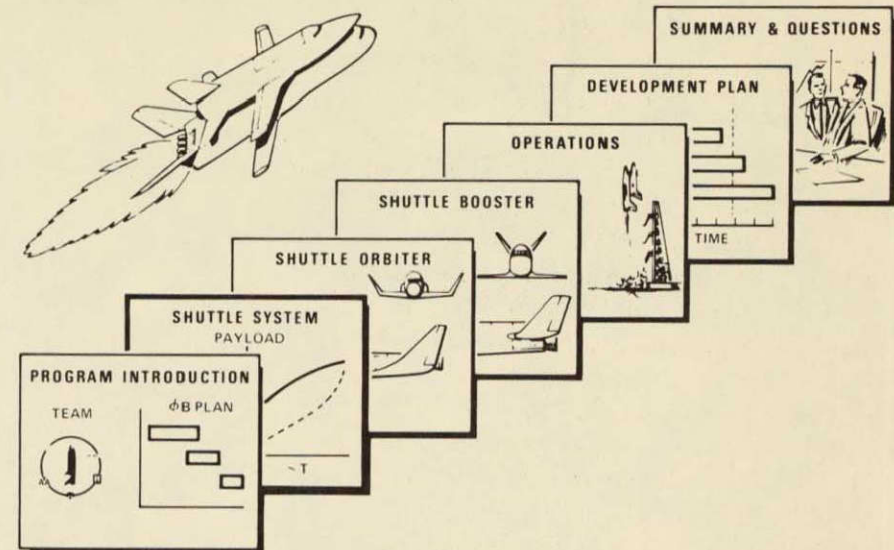


Figure 1-1. Presentation Outline

with extensive experience in the aircraft and space design, development, and operations fields. As Figure 1-2 illustrates, Space Division is the team leader and will be responsible for overall direction of Phase B contract. It will perform the overall program and system integration function and will be responsible for the preliminary design of the orbiter. This includes formulation of the development and operational plans and associated cost for this stage. Responsibility for the design and associated plans for the shuttle booster rests with Convair. The total integration of the avionics system for the shuttle will be carried out by Space Division. IBM will support in the area of data management systems. Honeywell will be responsible for the vehicle guidance control systems used on both the orbiter and booster. The team is rounded out by American Airlines. It will provide information pertaining to commercial aircraft operational experience and will support the program by studies on vehicle maintainability and the ground handling and turnaround.



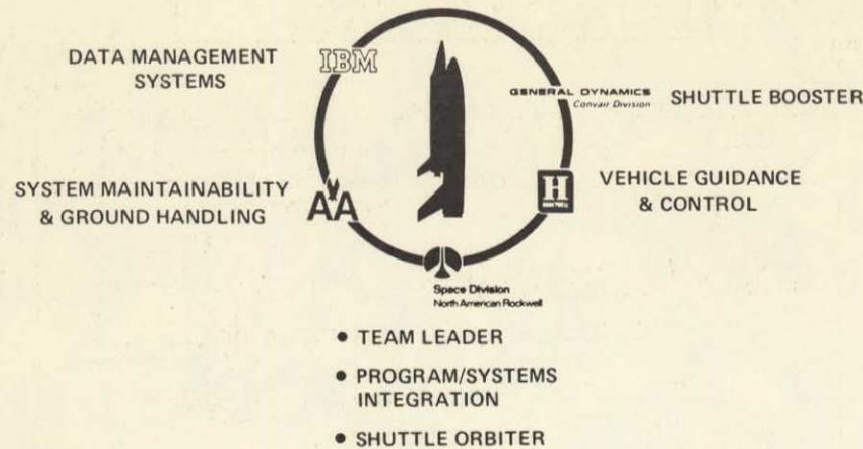
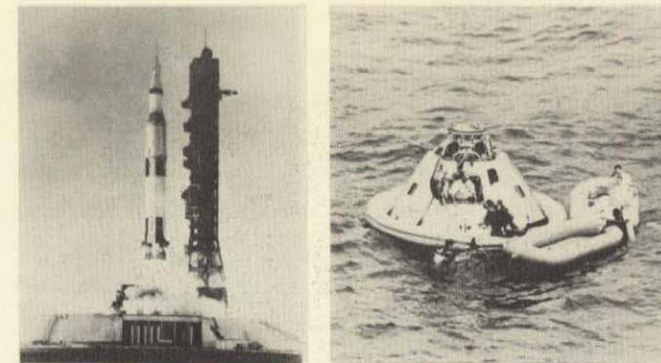


Figure 1-2. Phase B Shuttle Team

Space Division and Convair have long histories in aviation. Both have also made significant contributions to the United States space program. North American Rockwell built the X-15 airplane for NASA. This hypersonic research craft can be regarded as the first step in the shuttle program evolution in that it was a reusable rocket vehicle that explored a flight envelope similar to that the shuttle booster will fly on its normal mission. Referring to Figure 1-3, it will also be seen that Space Division's most recent space experience was gained through the development, production, and operations support of the Apollo command and service module and the S-II stage of the Saturn V launch vehicle. This performance provided in a most direct manner the technology and management experience necessary for undertaking a shuttle program. Convair Division of General Dynamics was a pioneer in development of launch vehicle and cryogenic upper stages. It designed and built the Atlas booster, which put the first American astronaut into earth orbit. In addition, Convair developed the Centaur upper stage used in the Surveyor lunar landing program. It is also planned as the stage that will boost many future deep space exploration and planetary spacecraft. Recent experience of our avionics and airline team members is summarized in Figure 1-4.

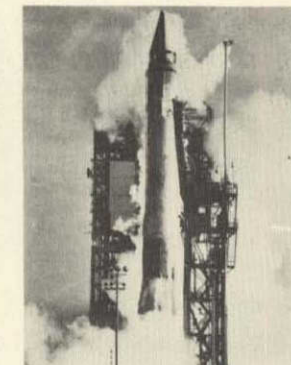


SATURN S-II  
B. Hello  
(VP, LAUNCH OPS)  
W. Ezeil  
(CHIEF ENGR)

APOLLO CSM  
C. FELTZ  
(ASST PROG MGR)  
B. HELLO  
(VP, LAUNCH OPS)  
A. KEHLET  
(SC MGR)



X-15  
C. Feltz  
(CHIEF ENGINEER)



ATLAS CENTAUR  
R. Keehn  
(ASSISTANT PROG MGR)

Figure 1-3. Introduction to North American Rockwell and General Dynamics

Thus, by working together over recent months, and because of the proved space and aircraft program capability, we feel confident that we have assembled a team that can perform the shuttle definition study and, of course, successfully compete later for the hardware development.





Figure 1.4. Introduction to IBM, Honeywell, and American Airlines

The contract awarded by the NASA is 12 months in duration. As Figure 1-5 illustrates, it is divided into three major parts: vehicle configuration selection, preliminary design and evaluation of the vehicle subsystems, and preliminary design and documentation. The latter phase includes generation of detailed program plans and overall resource requirements definitions. The Phase B contract will be supported by a substantial test program. The tests will provide supporting data that will assist in the overall configuration selection and design. Further, the tests will guide the detailed definition in critical technology areas such as (1) establishing high-temperature insulation material properties; (2) establishing the characteristics of long-life, high-temperature materials suitable for the external surfaces

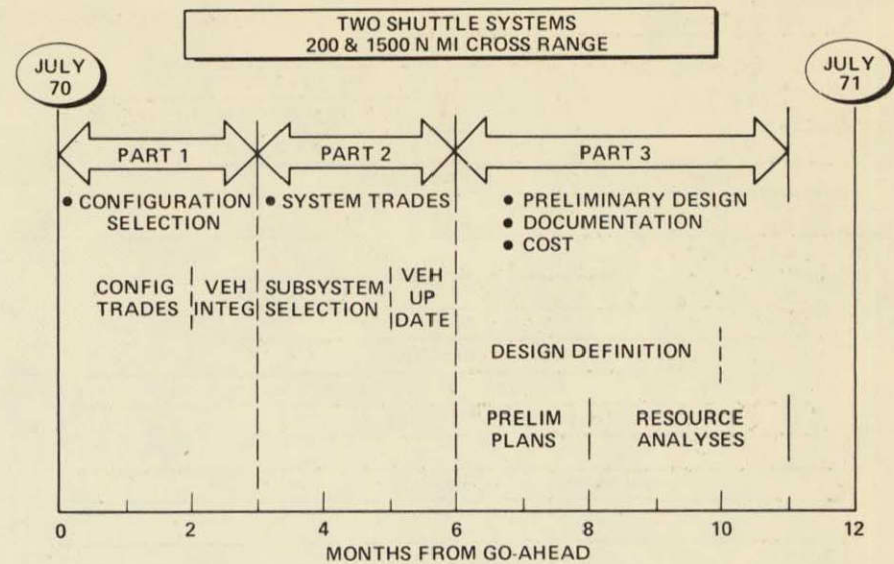


Figure 1-5. Phase B Contract Plan

of the vehicles; (3) developing design details, weight, and performance capabilities of integrated thermal protection systems; (4) verifying the aerodynamic characteristics of the vehicles; (5) predicting the thermal environment for vehicle design, and (6) evaluating the vehicle flight control systems. The phasing of these supporting tests, with respect to the vehicle design definition portions of the study, is illustrated in Figure 1-6. The contract performance will also be enhanced by the ongoing Phase B high-pressure main-rocket-engine studies and a large number of supporting technology development projects. Results of this companion effort will be fed continuously into the vehicle studies, as Figure 1-6 indicates.

Overall management aspects of the Phase B program having been described, we will concentrate on the technical aspects of shuttle design and operation. The study will consider only two-stage, fully reusable, shuttle systems that could be operational in the latter half of the 1970's. Figure 1-7 illustrates the major requirements that



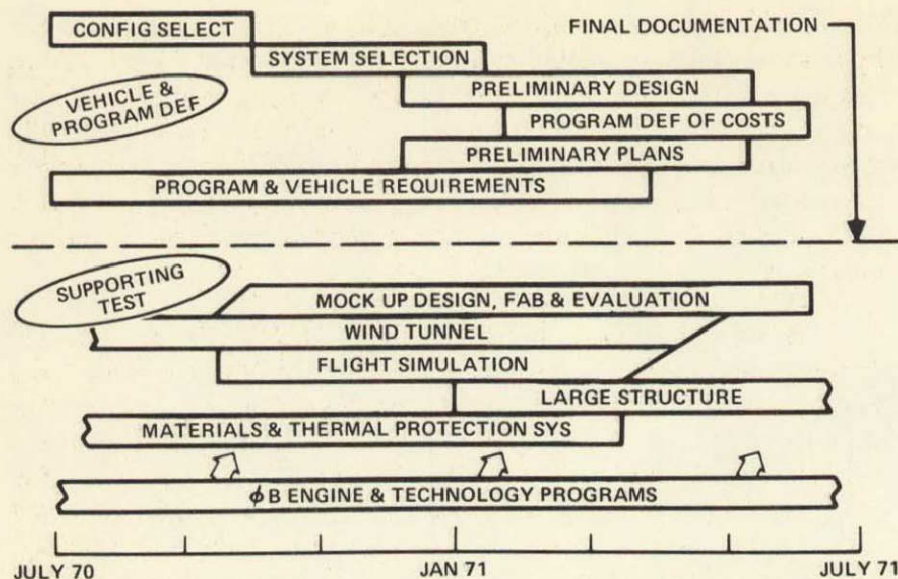


Figure 1-6. Major Elements of Phase B



- LIFTOFF WEIGHT  $1.587 \times 10^6$  Kg
- REF MISSION, SPACE STATION RESUPPLY - 500 Km X 55° ORBIT
- CROSS-RANGE - 200 & 1500 N MI
- COMMON MAIN ENGINE - 181,400 Kg THRUST
- CARGO BAY - 18.3M X 4.6 DIA M
- AT LEAST 100 MISSIONS/VEHICLE
- ORDER OF MAGNITUDE COST REDUCTION

Figure 1-7. Shuttle Requirements

were used in defining the current-shuttle system baselines we are studying for NASA. As the figure shows, the designs are based on a fixed gross liftoff weight of 1,587,000 kilograms. As a reference mission, it is assumed the shuttle will be used for crew rotation and logistics resupply of an earth orbiting space station. It should be noted, however, that, in the study, we will consider many other missions such as (1) satellite deployment; (2) satellite maintenance, repair, or retrievability; (3) transporting into earth orbit propulsion stages that would later be used for high-energy missions such as boosting a satellite to a geosynchronous orbit; (4) transporting propellants into orbit for loading into propulsion stages or space tugs, and (5) space rescue missions. As will be discussed in more detail later, two shuttle orbiters will be investigated in Phase B although only one will be developed. They will be designed to meet a cross-range requirement of 200 and 1500 nautical miles. (Cross range is defined here as the distance that the shuttle orbiter must be capable of aerodynamically traversing out of the plane of the orbit during entry.) The booster and orbiter will use the same basic  $LO_2/LH_2$  main rocket engine. It is a high-pressure, bell-nozzle engine that has a retractable nozzle. The contour of the nozzles may be uniquely configured to each stage beyond where the area ratio  $\epsilon = 6$ . Thrust level of this common engine is established as 181,400 kilograms at sea level. The shuttle orbiter is designed such that it can accommodate a payload or cargo canister that is 18.3 meters by 4.6 meters in diameter. The final major shuttle requirement is that each vehicle should be capable of performing at least 100 operational missions.

As noted, shuttle designs will be developed to meet two cross-range requirements. Referring to Figure 1-8, it will be seen that this is a major configuration driver. The necessity to meet a high cross range (1500 nautical miles) means that the orbiter must be flown at a high hypersonic lift-to-drag ratio ( $L/D \approx 1.8$ ) during a major portion of its earth atmospheric entry maneuver. Flying at this attitude over a large distance means that the vehicle exposes substantial areas of its surface to high heating rates for a long period

of time as compared to the short cross-range vehicle. Consequently, the high cross-range vehicle must be provided with greater thermal protection. In fact, the total heat load experienced by the high cross-range vehicle is five to seven times greater than that realized in the limited cross-range case. (A comparison of the specific heat loads for orbiters is given later in this paper.)

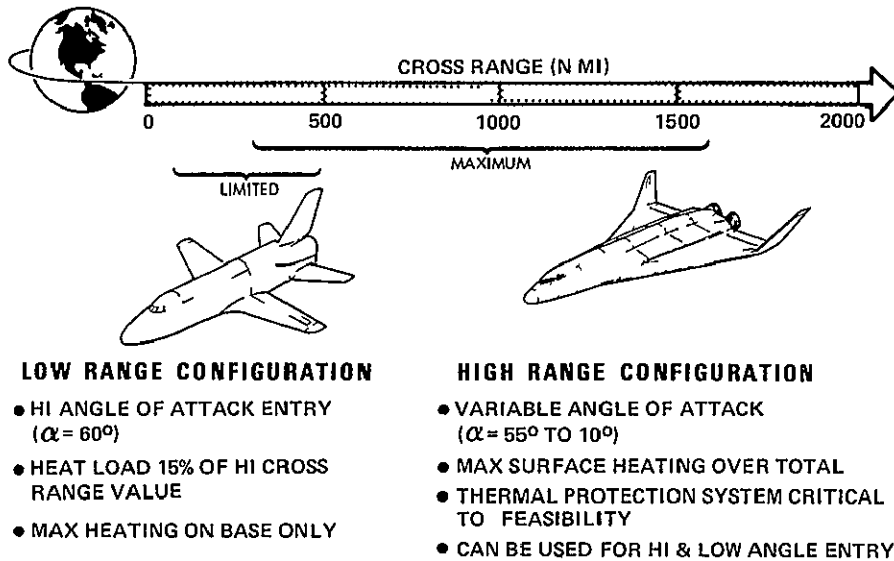


Figure 1-8 Shuttle Configuration Requirements and Concepts

For the limited cross range case, the vehicle is flown close to the maximum lift coefficient ( $C_{L_{max}}$ ) attitude (the  $L/D \approx 0.5$  at max  $C_{L_{max}}$ ), that is to say, at a high angle of attack, typically  $\alpha = 60$  degrees. At this attitude, the majority of the aerodynamic heating is experienced across the base of the vehicle, the upper surfaces being in the shadow of the primary shock system. As a result, only limited thermal protection is required on the sides and upper surfaces of the fuselage, wing, and empennage. Flying at a high angle of attack, a fixed straight-wing vehicle of the type selected can expect some shock interactions and interferences on the forward portion of the wing.

This could cause very high temperatures in localized areas. Limited hypersonic wind tunnel tests have been conducted by NASA to investigate this phenomenon on the straight wing orbiter.<sup>1</sup> In tests conducted at  $M = 10$  with the model at an angle of attack  $\alpha = 60$ , the shock interference effects were found to be only slightly more severe than observed on other shuttle configurations. As the authors noted, the tests were limited, but at least from our viewpoint, the results are promising.

Throughout most of the 1960's, NASA, Space Division, Convair, and other companies, both in the United States and Europe, have investigated shuttle configuration concepts.<sup>2</sup> This culminated last year in the award of Phase A studies on the Integral Launch and Reentry Vehicle (ILRV) and Space Transportation Systems (STS) by the NASA and Air Force, respectively. ILRV study results were presented to many of you at the Space Shuttle Symposium<sup>3</sup> held last October in Washington. These studies, supported by more than 200 man-years of engineering effort during the past 12 months and backed up by wind tunnel tests, extensive materials tests, and structures tests, resulted in selections of the baseline vehicles outlined in Figure 1-9. The concepts investigated ranged from lifting body shapes to variable-geometry wing configurations. The figure illustrates four generic classes of orbiters investigated. It also lists some of the major criteria used to arrive at the baseline designs. The check marks indicate factors that weigh

<sup>1</sup>Mini's, Maxi's and Mustard. Considerations in the Sizing of International Space Transportation Systems. Paper presented at the 16th Annual Meeting, American Astronautical Society, Anaheim, California (9 June 1970) by Raymond F. Creasey, Director of Advanced Systems and Technology, British Aircraft Corporation.

<sup>2</sup>Heating Studies on Manned Space Shuttle Concepts. Paper presented at the Space Technology and Heat Transfer Conference ASME, Los Angeles, California (21-24 June 1970) by Arthur Henderson, James C. Dunavant, and Robert A. Jones of NASA Langley Research Center, Hampton, Virginia.

<sup>3</sup>Integral Launch and Reentry Vehicle. Paper presented at the Space Shuttle Symposium, Washington, D.C. (16-17 October 1969) by George F. Fraser, Space Division of North American Rockwell Corporation.



favorably in the selection. Lifting-body vehicles have been studied and tested by NASA for a number of years. However, this class of vehicle was not competitive for the shuttle application because

- 1 The body shape did not lend itself to efficient packaging/installation of the large cargo bay, propellant tanks, and major subsystems
- 2 The double curvature of the body results in a vehicle that is complex to fabricate. Further, the body shape cannot be readily divided into subassemblies and thereby simplify manufacturing
- 3 The large base area yields a relatively low subsonic lift-to-drag ratio. Thus, the vehicle has a less attractive cruise capability and low-speed flight characteristics

The variable geometry designs were found to have many attractive features. These included low inert/burnout weight and the high hypersonic L/D necessary to meet the maximum cross range. The stowed-wing approach also permits the wing to be designed for the low-speed flight regime. It was found to be less attractive than the selected configurations because

- 1 The high vehicle weight to projected planform area ratio results in higher average base heat-shield temperatures, relative to the selected straight-wing design
- 2 Increased design and manufacturing complexity would result from the mechanisms required to actuate the wing and to transmit the flight loads

The selected orbiter vehicle designed to provide low aerodynamic cross-range capability has a low, swept, fixed wing configured to provide design simplicity, low weight, good handling, and good landing characteristics. The vehicle enters at a high angle of attack to minimize heating and to facilitate use of heat shield materials now available or in an advanced state of development. A delta-wing orbiter was selected for achieving high aerodynamic cross range. This system is designed to provide capability for time over a wide angle-of-attack range. This allows initial entry at a high angle of attack to minimize the severity of the entry environment. After peak heating, the vehicle is pitched down to a low angle of attack and banked to achieve cross range. This vehicle also exhibits good handling qualities and landing characteristics. The selected booster is also based on a fixed-wing design. This booster is common for either orbiter.

Artists' concepts of each baseline vehicle are illustrated in Figure 1-10. It should be stressed that these configurations will be used as points of departure at the beginning of the Phase B study. The primary objective of the Phase B study is to evaluate improvements in these designs so that a system can be developed consistent with the cost, mission capability, and safety objectives noted earlier.

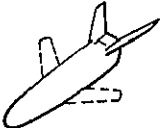
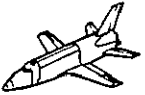


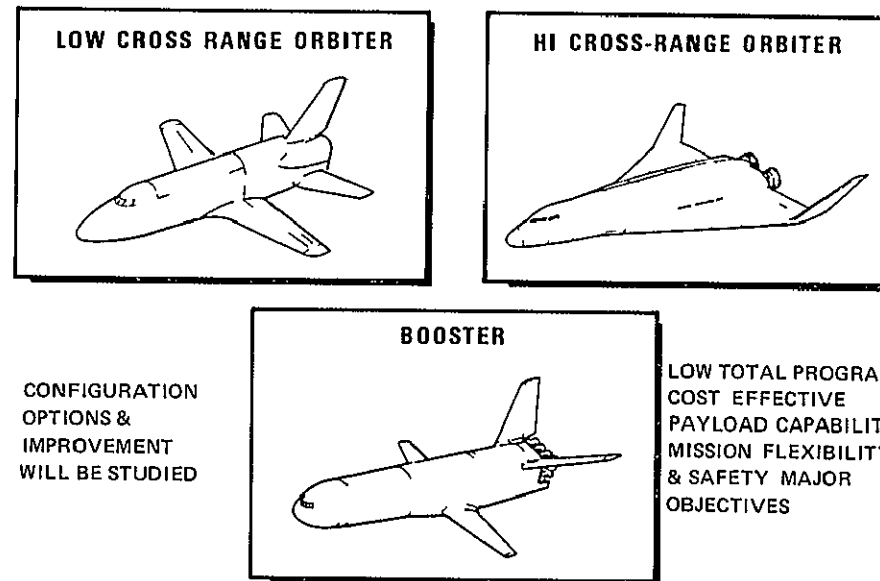
Φ A ILRV/STS & COMPANY STUDIES				
	STOWED WING/ VARIABLE GEOM 	STRAIGHT LOW SWEEP FIXED WING 	SWEPT DELTA WING 	LIFTING BODY 
HIGH RANGE ORBITER	✓ HIGH L/D <sub>HYP</sub> RANGE ✓ LOW WEIGHT ✗ HIGHER ENTRY ↑ ✗ POTENTIAL RISKS	✗ ADVERSE HEATING ✗ POTENTIAL STAB PROBLEM ✓ SIMPLE DESIGN ✓ LOW WEIGHT	✓ HIGH L/D <sub>HYP</sub> RANGE ✓ WIDE α TRIM ✗ POTENTIAL WT INCREASE	✗ DESIGN/DEVEL/ MFG COMPLEXITY & RISK
LOW RANGE ORBITER	✓ LOW WEIGHT ✗ HIGHER ENTRY ↑ ✗ POTENTIAL RISKS	✓ SIMPLE DESIGN ✓ LOW WT ✓ STALLED ENTRY LOW ↓ ✓ GOOD LANDING	✗ WT INCREASE FOR Δ	✗ DESIGN/DEVEL/ MFG COMPLEXITY & RISKS
BOOSTER	✓ LOW WEIGHT ✗ HIGHER ENTRY ↑ ✗ POTENTIAL RISK ✓ GOOD CRUISE	✓ SIMPLE DESIGN ✓ LOW WT ✓ STALLED ENTRY LOW ↓ ✓ GOOD CRUISE & LOGISTICS	✗ POTENTIAL WT INCREASE ✗ HIGH LANDING ATT	✗ DESIGN/DEVEL/ MFG COMPLEXITY RISK ✗ POOR CRUISE

Figure 1-9 Reusable Shuttle Concept Options



*Figure 1 10 Baseline Configurations*

## 2. SHUTTLE SYSTEM

The shuttle system consists of the vehicles illustrated in Figure 1-1 and all supporting equipment necessary to accomplish a variety of designated missions at a rate of 25 to 75 per year, assuming a two-week turnaround period. Figure 2-1 illustrates the shuttle's total mission cycle. The major events include the boost flight phase, on-orbit operations, orbiter and booster entry phase, and the ground operations cycle. In the shuttle vehicle design development, all elements of this mission profile must be taken into account if a system consistent with the cost and operational objectives is to be designed. One of the first steps in the vehicle and system evaluation process is the actual sizing of the vehicles, that is to say, determining the boost/payload performance capability, the optimum staging velocity, thrust-to-weight ratio at liftoff, number of engines, etc. (Figure 2-2). This optimization process was performed for the candidate integrated vehicles. The gross liftoff weight limit of  $1.587 \times 10^6$  kg was used, as was the requirement that the same basic

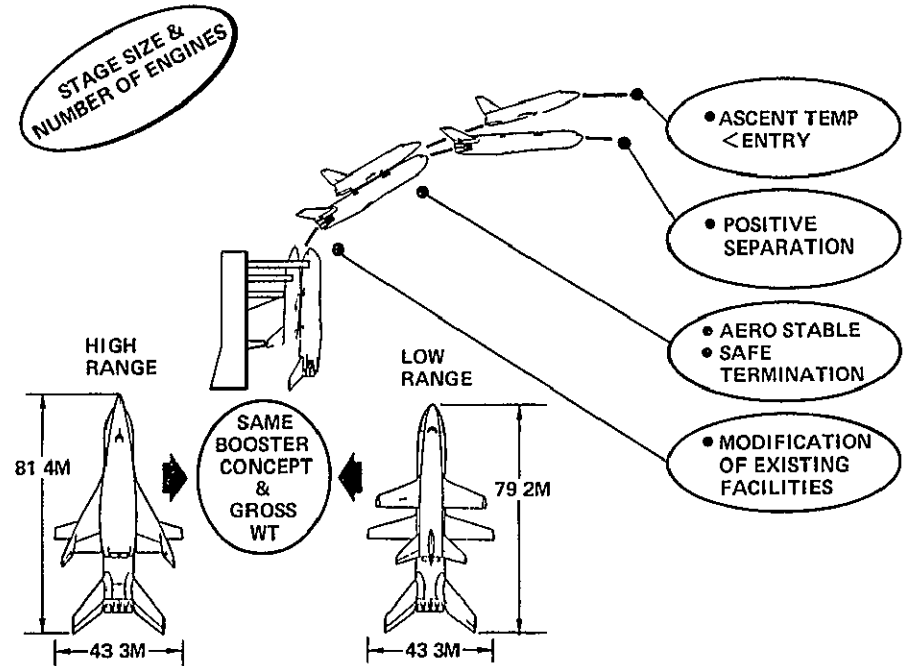


Figure 2-2 Integrated Vehicles

engine (184,000 kilograms sea level thrust each) be employed on both stages. Further considerations were:

- 1 The aerodynamic heating experienced during boost should (wherever practical) not exceed the values encountered during entry.
- 2 The stages should be capable of positive separation without use of special separation rocket systems of the type used on the Saturn vehicle.
- 3 The vehicle should be aerodynamically stable in the integrated configuration. This is required so that the

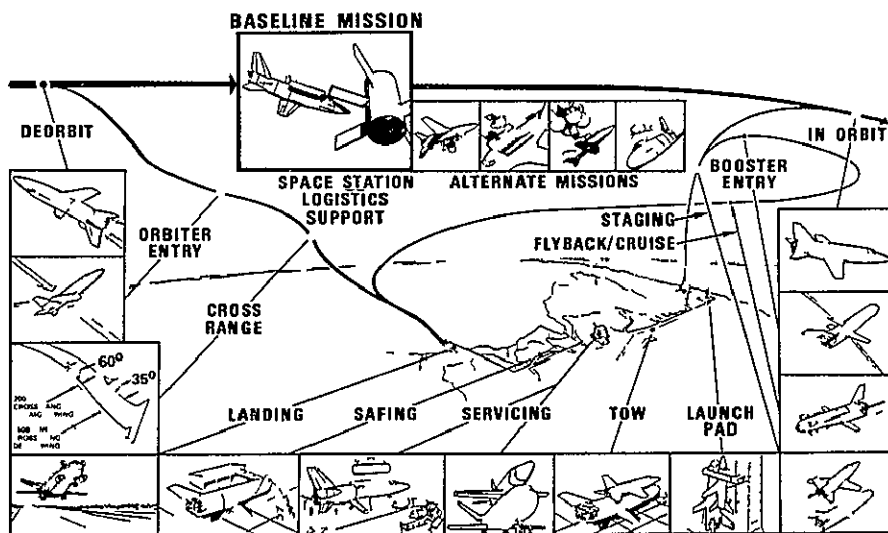


Figure 2-1 Shuttle Mission Profile

vehicles can coast with the main engines shut down. The coasting may be necessary during an abort. The vehicles could slow to a lower velocity, where safe separation could take place.

- 4 For safety, it was required that mission termination capability be incorporated. This is particularly important when a one-engine-out condition is considered on the orbiter immediately after separation from the booster. In fact, as will be seen later, this consideration limits the size and gross weight of the orbiter.
- 5 In the interest of lower cost, a goal was to minimize the modification to the existing launch facilities at Complex 39 of Kennedy Space Center (KSC). This constrained integrated vehicle designs as regards geometry and ground operations.

Figure 2-3 illustrates the typical vehicle performance and stage-size tradeoff studies that were performed. The figure on the left-hand side presents the payload capability to the reference orbit as a function of the orbiter gross weight. The data in the figure are for both the high and low cross-range orbiters. Also illustrated is the difference in payload that results from the use of two or three main rocket engines on the orbiter. By comparing the two upper curves on the left-hand graph, it will be seen that the highest payload performance results when two engines are used. The approximate difference in payload is around 20 percent. The payload decrement results principally from the additional engine and engine installation weight present in the three-engine arrangement. Of course, from a cost viewpoint, it is more desirable to use a smaller number of engines. That arrangement yields lower production, maintenance, and operation costs. The orbiter gross weight of 344,700 kilograms was selected in order that safe mission termination could be achieved in the one-engine-out condition. This results in a payload degradation of slightly over 10 percent for the low cross-range orbiter relative to the optimum case. The chart on the right-hand side of Figure 2-3

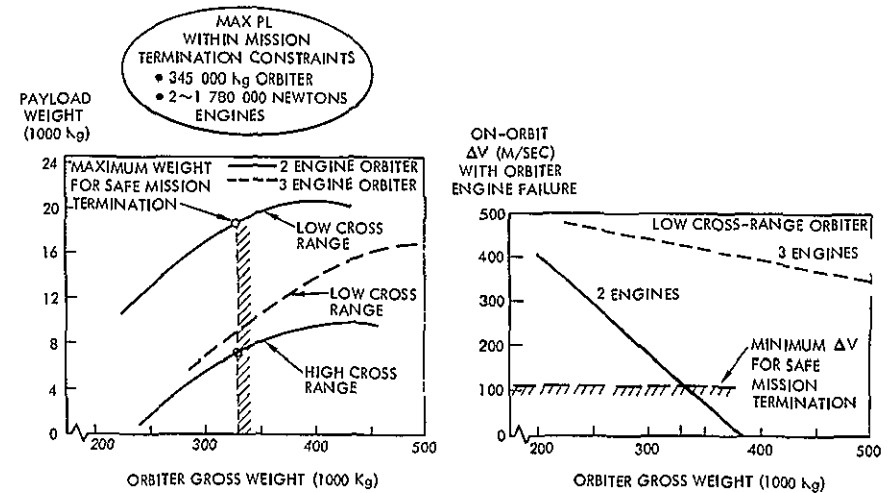


Figure 2-3 Effect of Orbiter Gross Weight on Payload

illustrates the on-orbit  $\Delta V$  capability of the orbiter (using both main and on-orbit propellants) as a function of the system gross weight. This is for the case of failure of one orbiter rocket engine immediately after separation from the booster. The slope of the line, or decreased  $\Delta V$  available, is a result of the higher gravity losses involved in achieving a safe orbit of 185 kilometers. The limit line on the curve is the  $\Delta V$  required to circularize the orbit, and retro-thrust out of orbit for the entry and return phase. Thus, taking the intercept of the capability versus the limit/requirement line, it will be seen that the orbiter gross weight must not exceed 344,700 kilograms.

To summarize the main points from this figure, the staging velocity/stage weights of the orbiter and booster are greatly influenced by the requirement for safe mission termination. Two engines on the orbiter were found to be optimum for the gross liftoff weight of  $1.587 \times 10^6$  kilograms and the main engine thrust limits specified. The next step in the evaluation is to consider the number of boost engines. Figure 2-4 illustrates the influence of liftoff thrust-to-weight ratio on the payload capability. The case presented is

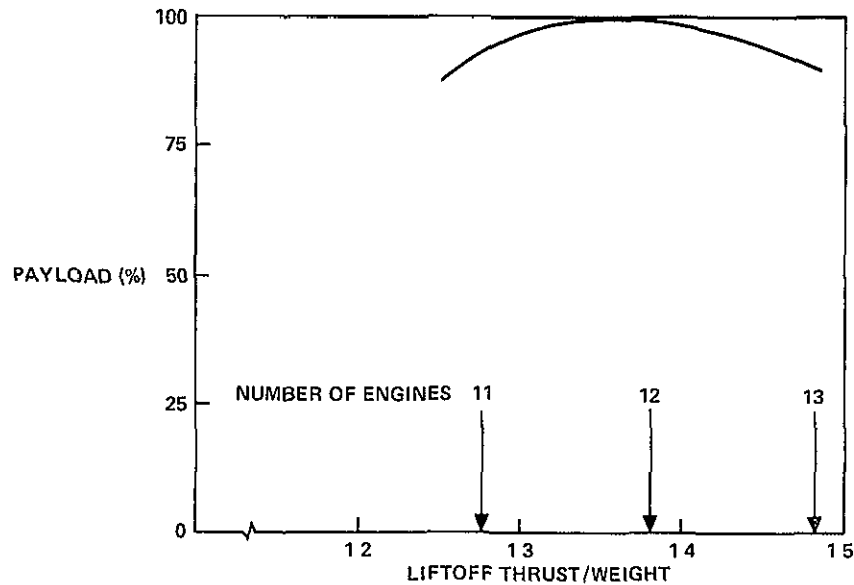


Figure 2 4 Number of Booster Engines

for the straight-wing orbiter. As this figure shows, the maximum payload is achieved with a thrust-to-weight ratio of approximately 1.35. This thrust level is achieved through the use of 12 engines with a thrust of 181,400 kilograms each.

When input data were developed for this tradeoff, various engine installation designs were considered, and the influence of the boost parameters such as gravity losses and drag were evaluated over a range of liftoff thrusts. A further consideration in selection of the number of engines is that the shuttle be able to accomplish its primary mission with a single booster engine out and that safe mission termination be achievable with two engines out. In both cases, it is assumed that the booster engines can be run at an over-thrust condition in the engine-out case.

As a result of the sizing processes and associated design analysis, the two integrated-system configurations shown in Figures 2-5 and 2-6 were developed. In both systems the orbiters are located forward,

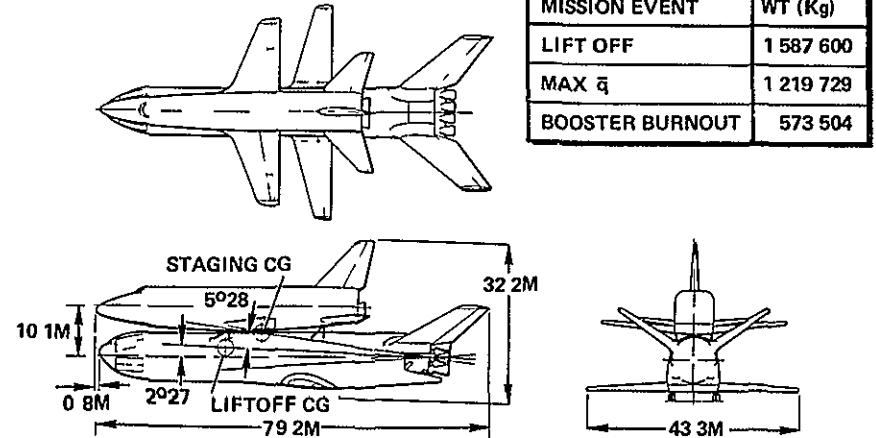
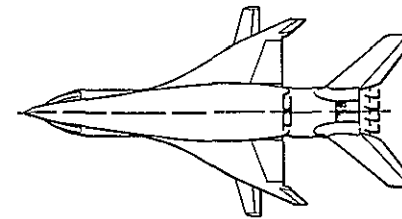


Figure 2 5 Mated Configuration, Low Cross Range Orbiter

MISSION EVENT	WT (Kg)
LIFT OFF	1 587 600
MAX $\bar{q}$	1 219 729
BOOSTER BURNOUT	573 504



MISSION EVENT	WT (Kg)
LIFT OFF	1 587,600
MAX $\bar{q}$	1 219 729
BOOSTER BURNOUT	573 504

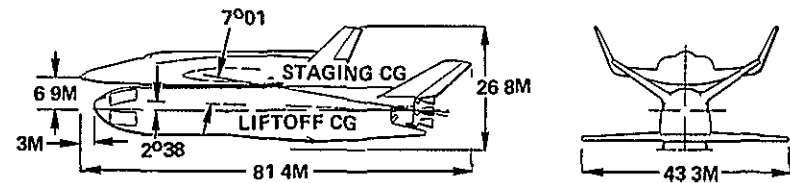


Figure 2 6 Mated Configuration, High Cross Range Orbiter

on the upper surface of the booster fuselage. This location provides an aerodynamically stable configuration. It also minimizes the main-engine gimbal angle required for the booster engine thrust vector to be aligned with the center of gravity (c.g.) of the integrated

system. As the figure indicates, approximately three degrees of gimbal is required because of the movement of the c.g. during boost for the straight-wing orbiter system. An additional two degrees is necessary on the delta-wing system. As the figures show, the booster size and weight are identical for both cross-range systems. The difference in overall length of the two integrated vehicles results from the overhang of the orbiters. Referring to the straight-wing orbiter, it will be seen that the overall length of the entire system is approximately 79.2 meters. The overall height of the stacked configuration, while resting on the booster landing gear, is 32.2 meters. The equivalent dimensions for the delta-wing orbiter are given in Figure 2-6.

With the integrated designs developed, the capability of the shuttle to undertake other missions was determined. That is to say, the performance of the vehicles at various altitudes and inclinations was computed. Typical of this are the data given in Figure 2-7, which

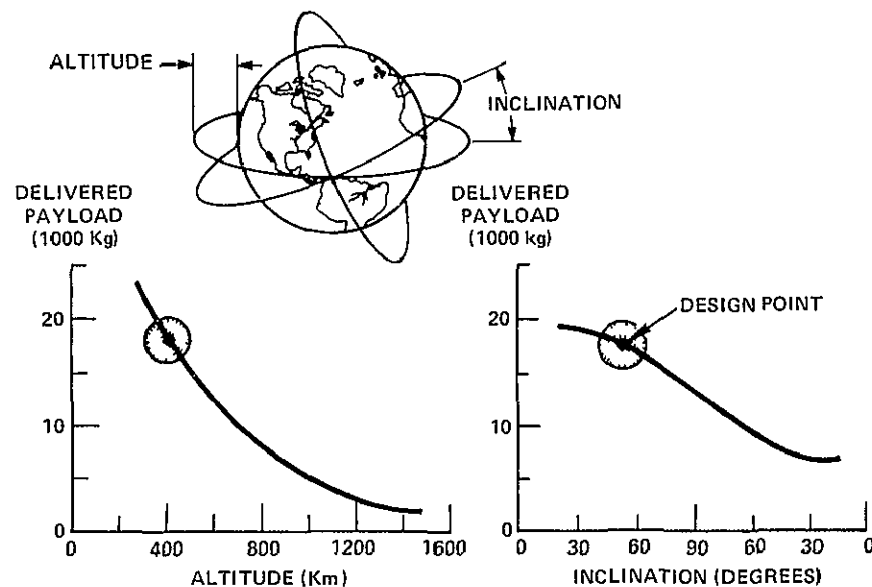


Figure 2-7 Payload and Mission Capability

depicts the payload capability of the straight-wing orbiter as a function of altitude and orbit inclination. As can be seen from the left-hand curve of Figure 2-7, approximately 25,000 kilograms of payload can be delivered to a 185-kilometer orbit. This, of course, means that, with the exception of the Saturn V, the shuttle would be able to carry more payload than any other launch system in the free world. As the curve illustrates, the payload capability reduces sharply with orbit altitude such that, for altitudes greater than 1500 kilometers, it will be necessary to use a separate propulsive stage or orbit-to-orbit tug. The propulsive stage, which could be an Agena or Centaur, and its payload, would be housed within the cargo bay of the shuttle. It would be carried to a 185-kilometer orbit by shuttle. After deployment from the cargo bay, it would be checked out and then ignited and boosted to the final operational mission trajectory. For example, this could be to a geosynchronous orbit or into a trans-Mars flight-path. The special requirements for conducting missions such as these, including the methods of loading the propulsion stage and its payload, checking the system out on the ground and in orbit and deploying it, will be investigated as part of the Phase B contract. The influence of carrying a tug and propellants for the tug within the shuttle will also be studied. Actual design of a space tug is being investigated for NASA under a separate contract awarded recently to Space Division. Details of the tug investigations will be covered in the paper to be presented later in this conference.

So far, we have primarily referred to optimizing the ascent portion of the vehicle flight to achieve maximum payload performance. However, the actual vehicle optimization must consider all phases of the mission. Specifically, the tradeoffs of vehicle boost loads, drag, boost and entry heating, in-orbit operations, etc., must be evaluated before the total system can be optimized. The trajectory or flight profile for the complete mission is illustrated in Figure 2-8, with added detail given in Figure 2-9. As shown, the vehicle is initially boosted from its vertical liftoff position to a staging altitude of 65.8 kilometers and velocity of 2846 meters per second, where the booster and orbiter separate. During boost

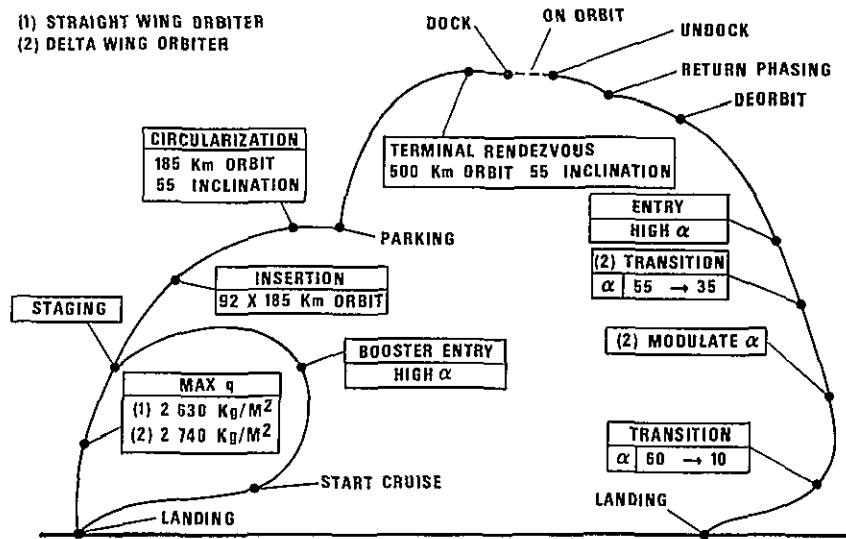


Figure 2 8 Flight Profile

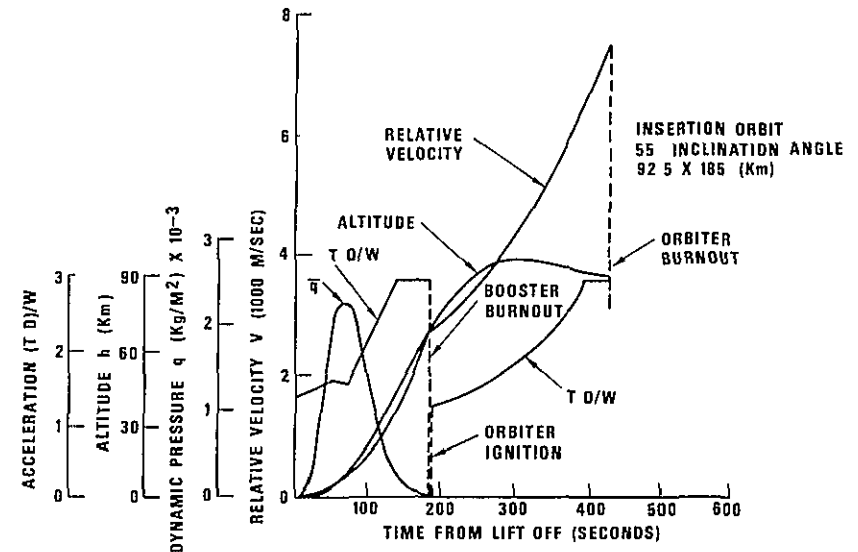


Figure 2 9 Ascent Trajectory Profile

through the atmosphere, a maximum aerodynamic pressure of about 2600 Kg/M<sup>2</sup> is experienced. This occurs approximately 65 seconds after liftoff at a Mach number of slightly greater than one and an altitude of 9.75 kilometers. During ascent, the engines on both stages will be throttled to reduce the axial acceleration experienced on the system to 3 g's. Referring to the left-hand side of Figure 2-9, it will be seen that the booster is rolled and banked during entry to reduce the down-range distance. At subsonic speeds, the turbojet engines on the booster are deployed and operated to fly the approximately 700 kilometers back to the launch site. From the point of separation, the orbiter accelerates to an elliptical orbit 92 by 185 kilometers at burnout of its main-rocket-engine system. Burnout actually occurs approximately 450 seconds after liftoff. The orbiter then coasts up to apogee, where its on-orbit maneuvering propulsion system is fired, and the vehicle orbit is circularized. It remains in a circular orbit of

185 kilometers until it is appropriately phased with the rendezvous point. After correct phasing is achieved, the on-orbit maneuvering propulsion system is used to change the altitude and inclination. This change requires a  $\Delta V = 170$  meters per second. From this point, the orbit operations are performed. After the orbit mission phase is completed,  $\Delta V = 130$  meters per second is used to decelerate the vehicle and apply an initial entry angle of  $-0.15$  degrees. After deorbit, the vehicles proceed through the atmospheric entry, through transition, jet engine deployment, and final landing.

This, then, is a summary of the integrated vehicles, their design features, sizing, and performance. We will now take each element of the system (orbiters, boosters, operations, and development program) and give more details.

### 3. SHUTTLE ORBITER

This section discusses in more detail specific features of each orbiter.

#### GENERAL CONFIGURATION

Figures 3-1, 3-2, and 3-3 illustrate the high and low aerodynamic cross-range orbiters that we started with in the Phase B investigations.

#### Low Cross-Range Orbiter

The straight-wing, low cross-range orbiter has the capability of placing approximately 20,400 kilograms of payload into the reference mission orbit. In computing this value, it is assumed that a nominal  $I_{sp}$  of 459 seconds is achieved with a high-pressure engine.

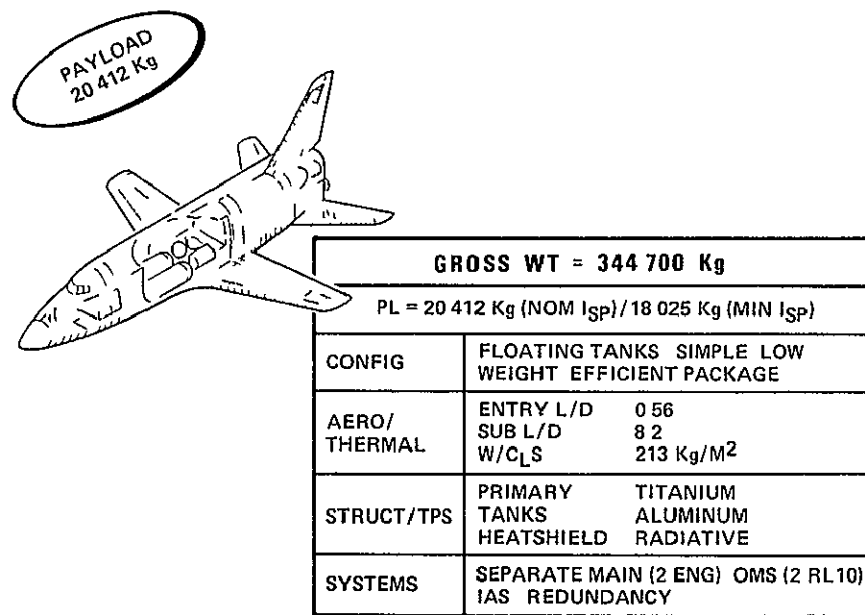


Figure 3 2 Straight Wing Orbiter, Low Cross Range

The nozzle expansion ratio of the engine selected for the baseline is  $\epsilon = 120.1$ . A payload degradation of 11 percent would result if the engines used on both stages actually delivered a specific impulse one percent under that quoted. This reduced payload is also noted on the figure. The low cross-range orbiter is configured to provide

1. A flat bottom, a large planform area and the ability to enter at high angle of attack to minimize heating (Unlike the high cross-range system, the low cross-range system does not require hypersonic trim capability at low angles of attack. The vehicle, therefore, maintains a high angle of attack until subsonic speed is achieved. Then it is pitched down for approach to the landing site.)

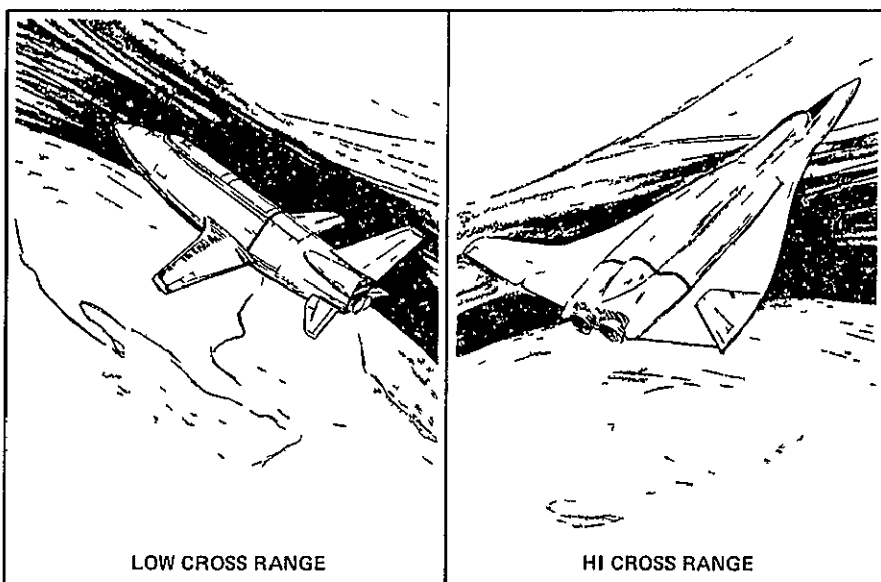


Figure 3 1 Shuttle Orbiters



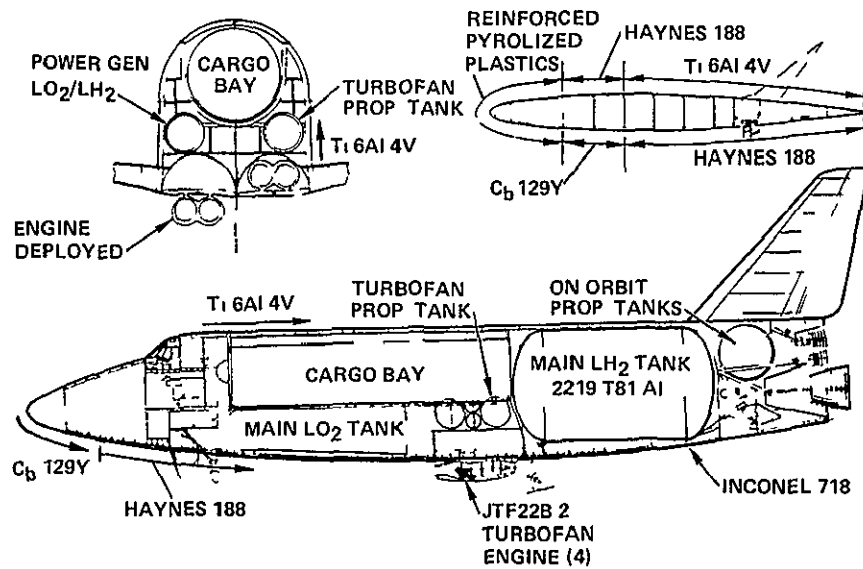


Figure 3-3 Orbiter Design Details, Straight Wing Orbiter

- 2 Efficient system packaging to minimize weight and to facilitate maintenance
- 3 Low-sweep, fixed wings for design simplicity, low weight, and good landing characteristics

The external shape and design characteristics are presented in Figures 3-2 and 3-3. The configuration is a derivative of a design conceived by a NASA-MSC team and investigated by Space Division during the previous Phase A study. The body shape and tank arrangement are directed toward design simplicity, ease of manufacture, maximum packaging efficiency, and minimum weight. A large leading-edge fillet at the intersection of wing and fuselage is used to reduce the interference flow between the wing leading edge and body during entry. An all-movable horizontal tail surface incorporates an elevator capable of the required response rates for the normal flight control mode. The independently hinged stabilizer is capable of low response rates to provide the necessary pitch trim. Because of the

independent hinging, it is possible to use the stabilizers for roll trim. Normal roll control is achieved by spoilers on the upper surface of the wing. This method of roll control was selected to eliminate a movable joint or slot on the lower surface of the wing. The problem of reduced effectiveness at high angles of attack may require either relocation of the spoilers or addition of small ailerons.

Internal features of the orbiter are shown in Figure 3-3. The basic load-carrying structure is titanium alloy with a radiative heat shield. The body is divided into three basic sections: (1) nose, (2) cargo bay and oxidizer tankage, and (3) fuel tank and main engine.

The nose section has provisions for the crew and passengers, nose landing gear, and vehicle equipment, including power supply and consumables. The crew and passenger compartments are arranged in two decks because of the short distance between the flight deck and the cargo bay (4.6 meters in diameter by 18.3 meters) and because of the deep body section. Station resupply missions normally will have a crew of two, plus two passengers for cargo handling. Provisions have been made for these four on the upper deck, with the crew and passengers sharing a common pressurized compartment. The area between the upper crew-passenger compartment and the cargo bay houses an air lock and the cargo deployment actuation system. Ten passengers are located on the lower deck. This approach was favored over using the cargo bay as the passenger compartment because it simplified the crew and life support system interfaces.

The oxidizer for the main propulsion system is carried in two floating aluminum tanks. The tanks are circular in section and slightly tapered. They are uninsulated and located just below the forward portion of the cargo bay. The wing carry-through structure consists of front and rear spars and provides sufficient volume for the four JTF22B-2 engines, which are installed in rotating pods. The engines are modified to use LH<sub>2</sub>. The volume between the stowed turbofans and the cargo bay is used to store LH<sub>2</sub> turbofan fuel.

The aft body section contains a floating LH<sub>2</sub> tank that is circular in section and internally insulated. Structural provisions are made for mounting independently hinged horizontal stabilizers and the vertical fin, on-orbit tankage support, and main-engine thrust structure. A single bulkhead supports the stabilizer spindle and actuator and the front spar of the vertical fin. A separate thrust structure is used for the main engines and the on-orbit engines. Orbit maneuvering propellant is contained in two spherical LO<sub>2</sub> tanks and two spherical LH<sub>2</sub> tanks.

The main engine bay has provision for installation of the two main engines and two orbit maneuvering engines. The main engines are LO<sub>2</sub>/LH<sub>2</sub>, high-chamber-pressure, bell-nozzle rockets with a sea level thrust rating of 181,436 kilograms. Structural and nozzle clearance is provided for a gimbaling travel of ±7 degrees in pitch and yaw, with the yaw clearance based on a return to null on one failed engine. This minimizes the base area by permitting the engines to be installed on a minimum center-to-center distance. The orbit maneuvering engines are mounted on a common-thrust structure with the main engines and provide ±4 degrees pitch and yaw gimbaling capability.

Booster attach fittings are located on a bulkhead just ahead of the turbofan engine pod and on the rear bulkhead that supports the horizontal stabilizer. This takes advantage of the existing main structure.

The low cross-range orbiter was designed to accomplish the entry and recovery mission profile shown in Figures 3.4 and 3.5. High angle-of-attack trim capability (60 degrees) from initial entry condition to subsonic speeds is required over a wide vehicle c.g. range. Low lift loading also is necessary to minimize entry heating, and aerodynamic control authority is essential to make the transition from high angle of attack to cruise conditions subsonically. Good subsonic flight characteristics and handling qualities are provided for safe landing within a 3000-meter runway.

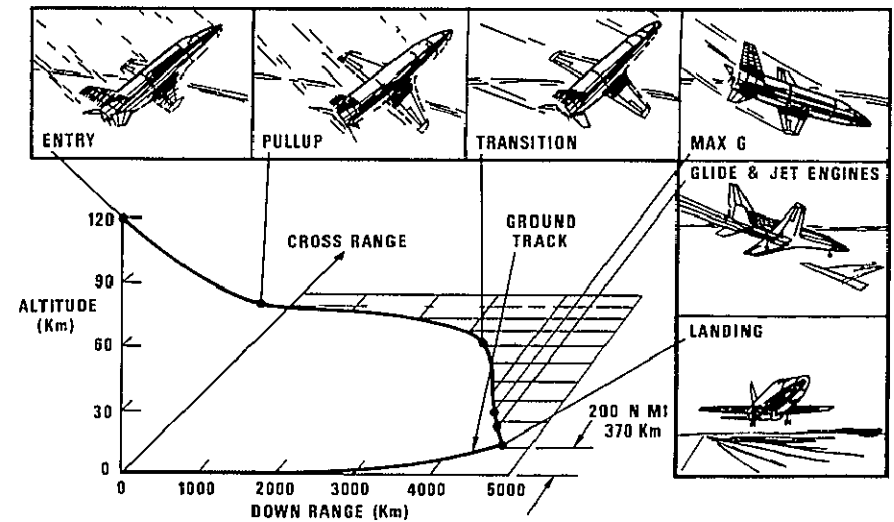


Figure 3.4 Entry Flight Profile for Low Cross Range

EVENT	V METER/ SEC	$\gamma$ (DEG)	$\alpha$ (DEG)	$\phi$ BANK (DEG)	t (SEC)	$\bar{q}$ Kg/M <sup>2</sup>	N (g s)
ENTRY	7 650	1 55	60	0	0	0	0
PULLUP	7 410	0 1	60	0 → 79	264	43	0 5
MAX g	2 040	3 4	60	20	816	138	1 75
TRANSITION	122	60 0	60 → 10	0	1000	118	1 00
BEGIN GLIDE & TURBOFAN IGNITION	150	0	10 → 5	0	1130	595	1 00
LANDING	149 KTS	3 0	12	0	1800	366	1 00

Figure 3.5 Entry Flight Profile for Low Cross Range

The external shape has been governed by stability and heating considerations. During entry at a high angle of attack, the flat bottom of the fuselage provides high lift, while the negative body camber aids in pitch trim and stability. The relatively sharp corners

promote separation around the sides of the body, resulting in low temperatures. The sloping sides aid in providing lateral and directional stability. Lateral range greater than 370 kilometers is achieved by programming a bank angle while maintaining angle of attack in the control mode shown in Figure 3-4. The configuration is longitudinally stable during entry and is self-trimming to the specified pitch angle (60 degrees) with a lift coefficient of 1.6 and a lift-to-drag ratio (L/D) of 0.56. Figure 3-6 defines the hypersonic aerodynamic characteristic of the orbiter. The data shown are based on analysis and verified by wind tunnel tests performed by ourselves and NASA. Damping and roll control is provided by the attitude control propulsion system. Subsonic characteristics displayed in Figures 3-7 and 3-8 show that the vehicle is stable at high (60 degree) and low angles of attack and that adequate control authority is available to perform the pitchdown maneuver to subsonic cruise. Center-of-gravity limits at hypersonic and subsonic speeds are displayed in Figures 3-8 and 3-9, respectively. The forward c.g. limit

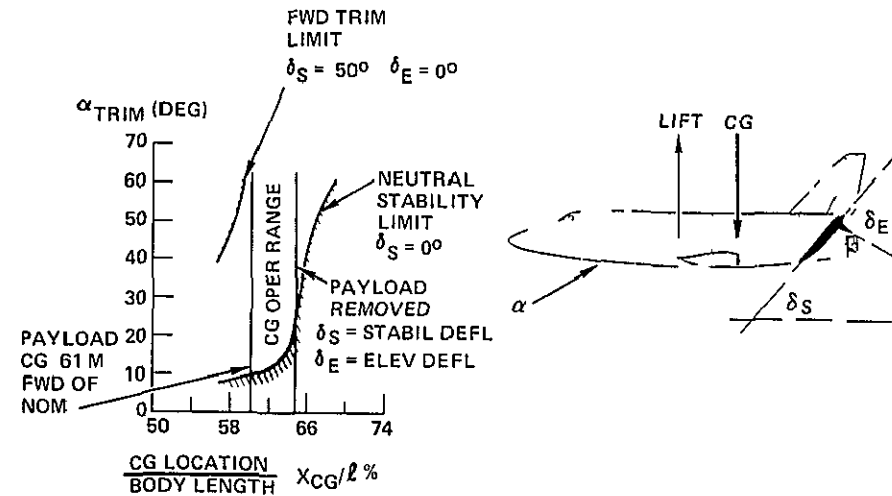


Figure 3 8 Cargo Center of Gravity Characteristics (Hypersonic)

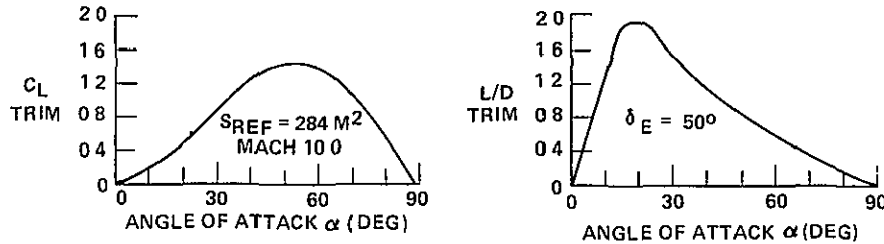


Figure 3 6 Hypersonic Straight Wing Orbiter

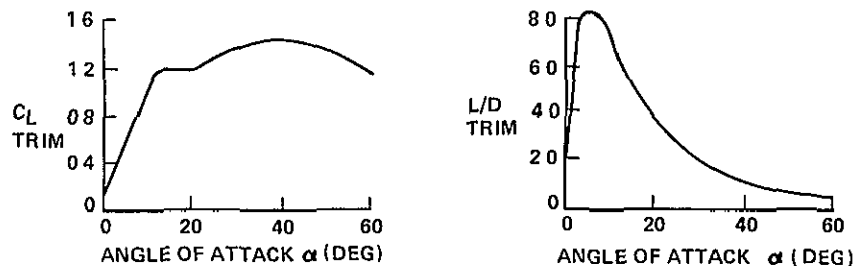


Figure 3 7 Subsonic Aerodynamic Characteristics, Low Cross Range Orbiter

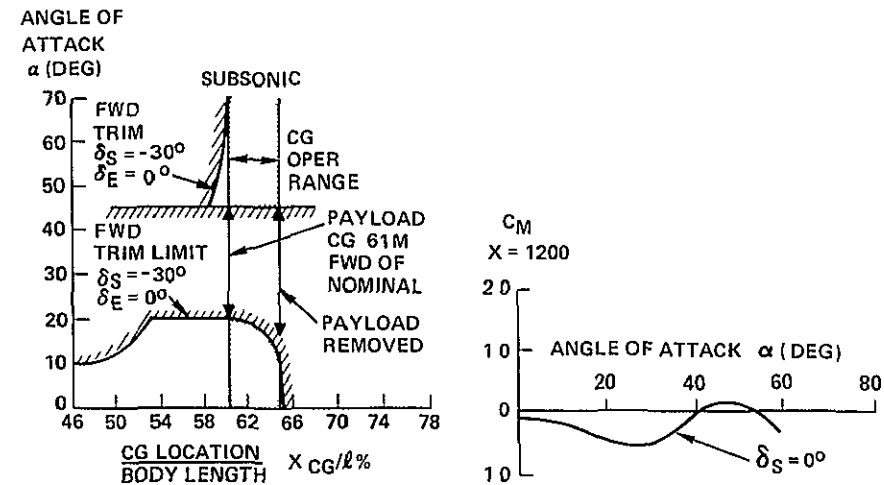


Figure 3 9 Cargo Center of Gravity Characteristics (Subsonic)

is defined by the nominal forward c.g. location, with payload in, plus 60 centimeters of tolerance. The aft c.g. location is defined with the payload removed. The all-movable tail provides maneuver and trim capability over the c.g. range.

Flight simulation studies have shown that the subsonic transition maneuver to a low angle of attack can be performed with aerodynamic control, with the pitchdown maneuver accomplished by a stabilizer command. Dynamic response was smooth and well damped. There was little overshoot, even though it was necessary to maneuver from one stable equilibrium point to another with nonlinear aerodynamic moments.

During subsonic cruise, the maximum trimmed L/D is 8.2 at an angle of attack of 7 degrees. The landing speed on a standard day is 149 knots (Figure 3-10).

The peak radiation equilibrium temperatures for the underside of the straight-wing orbiter entering at a 60-degree angle occur at approximately the pullout condition. It has been observed that wing leading-edge blending and sweep are beneficial in reducing interference heating on the wing and fuselage at high angles of attack.

RUNWAY LENGTH 3 048M  
TURBOJET APPROACH  
LANDING SPEED 149 KTS  
AUTO LANDING AIDS

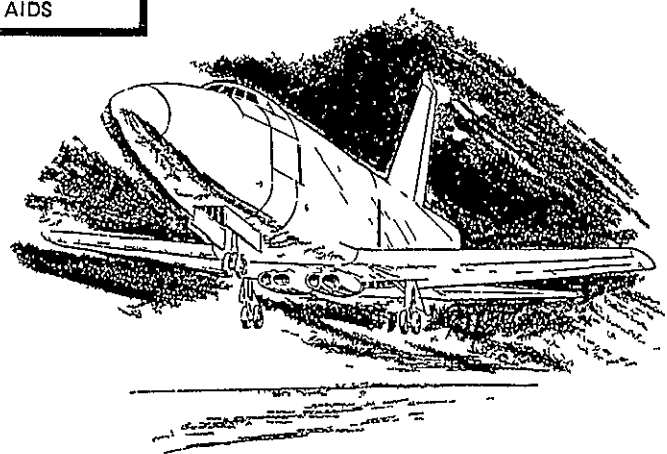


Figure 3 10 Orbiter Landing

Radiation equilibrium temperature distributions for the vehicle during ascent and entry are presented in Figure 3-11. Design temperatures over the upper surface of the vehicle occur during boost and over the remainder of the vehicle during entry. Temperatures over a large area of the vehicle are less than 1000°C, with higher temperatures on the nose and wing leading edge. The maximum temperature on the leading edge of the vertical stabilizer reaches 470°C during boost because of interference effects. The wing leading edge reaches 1690°C because of the interaction of the body and wing shock.

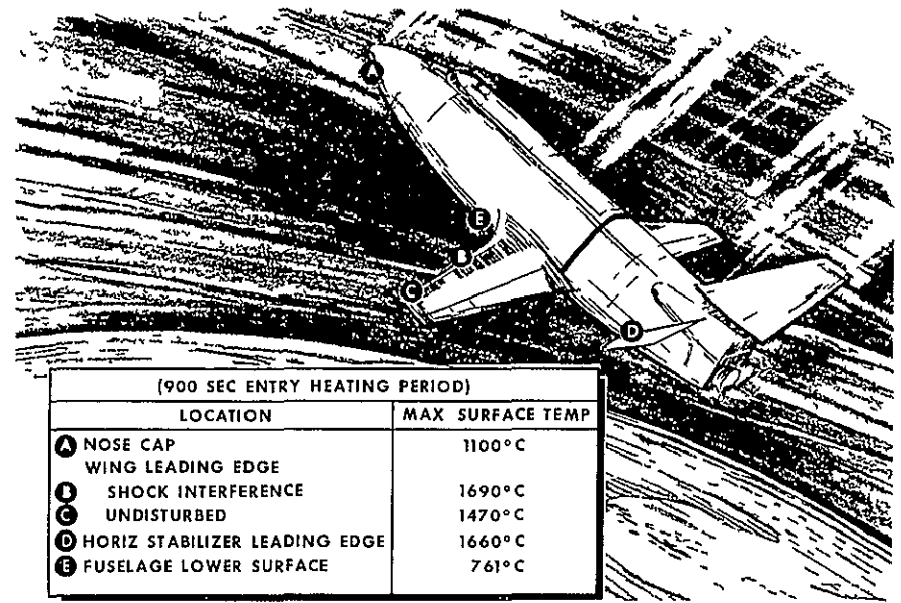


Figure 3 11 Straight Wing Orbiter Entry

Figure 3-12 provides additional temperature data. It also shows a condensed summary of heat shield material selections. Over a large area of the vehicle, the temperatures are less than 1000°C, allowing use of materials that are in a more advanced state of development than those for the delta wing.

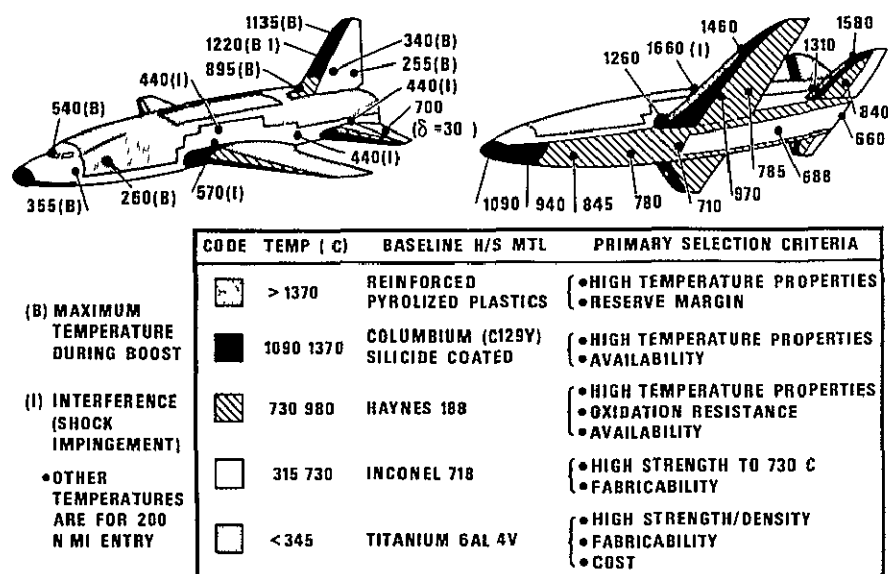


Figure 3-12 Maximum Temperatures and Materials

### High Cross-Range Orbiter

The baseline, quasi-delta-shaped, high cross-range orbiter has a payload capability to the reference mission orbit of approximately 9000 kilograms. This is based on the engine performance assumptions defined earlier. It is configured to provide the following:

- 1 Large planform area and capability for entry at high angles of attack to minimize heating
- 2 Aerodynamic shape with good hypersonic lift-to-drag characteristics
- 3 Thermal protection system (TPS) designed for 1500-nautical-mile cross-range thermal environment
- 4 Efficient system packaging to minimize weight and facilitate maintenance

- 5 Aerodynamic shape for good subsonic flight and landing characteristics

The external shape and design characteristics of the orbiter vehicle are presented in Figure 3-13. Internal features are shown in Figure 3-14. Vehicle basic load-carrying structure is titanium alloy with a radiative heat shield. The body is divided into three major sections: (1) the nose and crew and passenger compartment, (2) the cargo area, and (3) the main engine bay.

The nose section has sufficient volume for the LH<sub>2</sub> tank, crew and passenger compartment, and nose landing gear. The shaping provides the necessary aerodynamic characteristics, resulting in the crew compartment being located aft of the nose. Thus, the projected lateral area is minimized, and a reasonable fin size is maintained for directional stability. A floating aluminum LH<sub>2</sub> tank is used. It is a double-cell pressure vessel shaped for maximum volume usage.

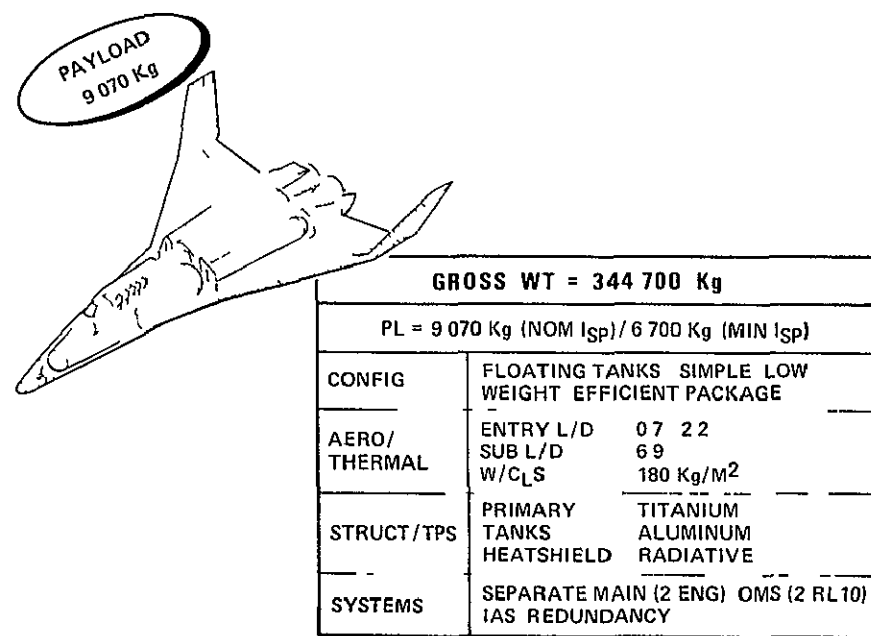


Figure 3-13 Delta Wing Orbiter, High Cross Wing

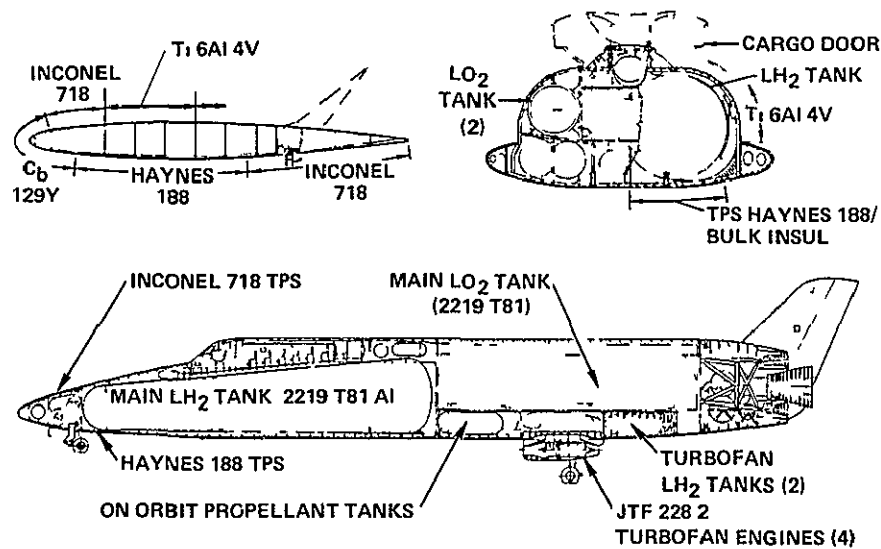


Figure 3-14 Orbiter Design Details

The crew and passengers are accommodated in a single pressurized compartment, with an air lock provided for intra-vehicular activity (IVA) access to the cargo bay and space station. The flight compartment has side-by-side seating. This makes it practical for sharing certain controls, windows, and displays and for multiple use of access space.

The cargo bay is designed with top loading doors. The main LO<sub>2</sub> tanks are located on both sides of the cargo bay to provide a relatively stable c.g. location, with only a slight aft travel during burn of the main propellants. These uninsulated aluminum tanks are of a simple cylindrical shape and are supported from the body structure in a manner that minimizes induced body loads into the tanks. The area below the cargo bay and LO<sub>2</sub> tanks is used for the wing carry-through structure and installation of air-breathing engines, landing gear, and orbit maneuvering propellant.

The air-breathing engines are identical to those described earlier. As with the straight-wing orbiter, the engines are paired in two

deployable nacelles located in the underside of the body near the c.g. Thus, elimination of the air-breathing engines through modification of the go-around requirement would not significantly affect the vehicle c.g.

The landing gear consists of two dual-wheeled main landing gears with a dual-wheeled, steerable, nose landing gear. The preliminary analysis used to establish the baseline landing gear resulted in the selection of standard Type VII tires. The landing gear extension and retraction system and landing gear doors are electrically controlled and hydraulically operated.

Booster attach fittings, located on the bulkheads at each end of the cargo bay, are slightly recessed inside the mold line of the thermal protection system. At separation, the recesses are covered with self-closing doors to assure a smooth exterior surface and to minimize local heating.

The baseline high cross-range orbiter's aerodynamic configuration was designed to satisfy criteria based on the entry flight profile shown in Figures 3-15 and 3-16. At the same time, the design provides low drag and aerodynamic stability during the full flight regime and good subsonic handling and landing characteristics. Aerodynamic heating must be minimized during the initial entry phase of the flight, and an adequate hypersonic L/D is necessary to provide the 2770-kilometer cross range. To achieve the low entry heating and cross-range capability, it is necessary to provide for a low planform loading and the ability to trim over a wide angle-of-attack range. With this wide trim capability, the orbiter's baseline entry mode is to enter at a high angle of attack (55 degrees) and to pitch down (35 degrees) after peak heating. Referring to Figure 3-15, it will be observed that the transition to the low-angle-of-attack, maximum-L/D attitude occurs when approximately half the cross-range distance has been achieved. The vehicle is then further banked to achieve cross range. Transition to a low angle of attack occurs at supersonic speed, followed by subsonic powered approach to the landing site.

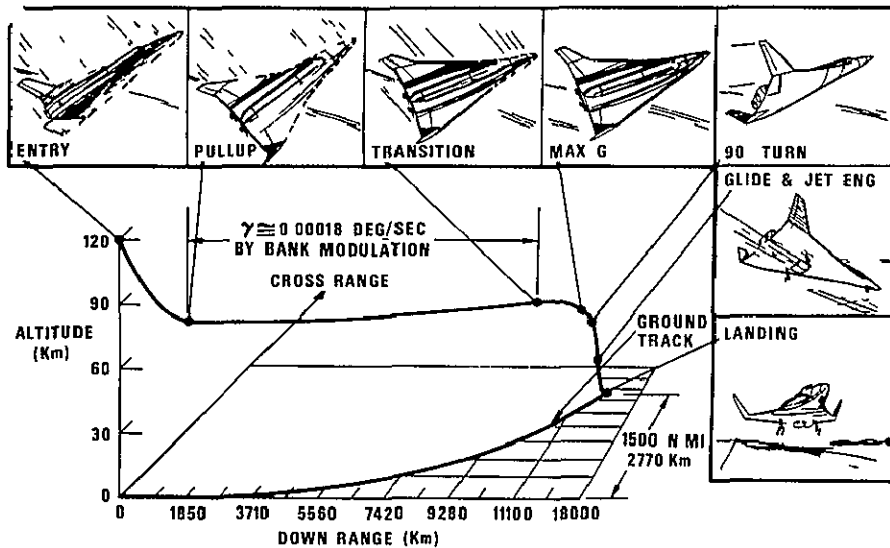


Figure 3-15 Entry Flight Profile for High Cross Range, Delta Wing Orbiter

EVENT	V METER/ SEC	$\gamma$ (DEG)	$\alpha$ (DEG)	$\phi$ BANK (DEG)	t (SEC)	$\bar{q}$ Kg/M <sup>2</sup>	N (g s)
ENTRY	7 650	1 55	55	0	0	0	0
PULLUP	7 500	0 04	55 → 35	0 → 81	261	39	0 2
BEGIN TRANSITION	3 750	0 3	35	20	1625	180	0 94
MAX g	1 640	1 7	20	20	1984	205	1 21
90 DEG TURN	625	7 9	10	20 → 0	2142	293	1 1
TURBOFAN IGNITION	182	10 0	8	0	2350	317	1 0
LANDING	119 KTS	3 0	15	0	2800	234	1 0

Figure 3-16 Entry Flight Profile for High Cross Range, Delta Wing Orbiter

The delta-wing orbiter planform and aerodynamic fineness ratio provide high L/D at hypersonic speeds and an acceptable trim range over the entire flight regime. Roll modulation for range control during entry is accomplished through the attitude control propulsion

system. Aerodynamic characteristics of the vehicle are presented in Figures 3-17 and 3-18. They show that the vehicle provides a hypersonic L/D of 1.4 when trimmed at  $\alpha = 35$  degrees and  $L/D \approx 2.2$  at  $\alpha = 20^\circ$ . The maximum subsonic L/D is 6.9. As shown in Figure 3-19, pitch control by elevons is sufficient for aerodynamic trim throughout an angle-of-attack range from 0 to 60 degrees, with an operational c.g. range of 60 centimeters either side of a nominal position to provide flexibility in payload c.g. and for uncertainties in consumables. The vehicle is designed to remain stable at all speeds and pitch angles. At hypersonic speeds, the unstable region at low

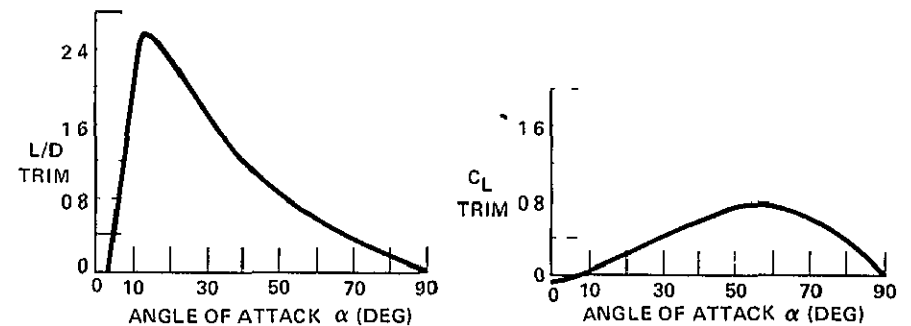


Figure 3-17 Hypersonic Aerodynamic Characteristics, Delta Wing Orbiter

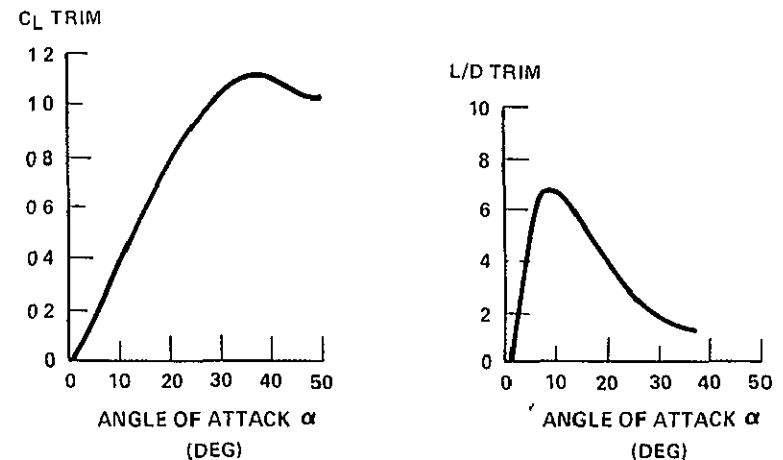


Figure 3-18 Subsonic Aerodynamic Characteristics, Delta Wing Orbiter

### HYPERSONIC

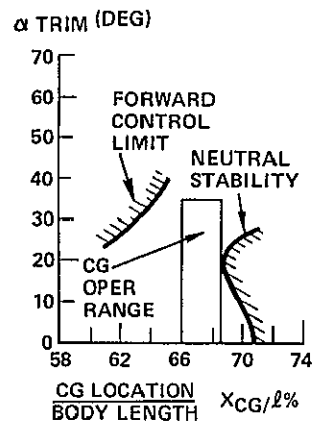


Figure 3 19 Cargo Center of Gravity Variations

angles of attack has been minimized by high forebody fineness ratio and by reducing body camber effects. This design also results in relatively low drag during ascent, where booster-orbiter drag influences total payload to orbit. Directional stability is provided by twin vertical tails mounted at the wing tips and sized to provide stability throughout the speed range. Two variables (wing dihedral and vertical tail cant) are used to establish the proper level of effective dihedral. Control is through conventional rudders and elevons, with control interlinkage where necessary to eliminate aerodynamic coupling.

With the vehicle trimmed at a 15-degree angle of attack, its landing speed on a standard day is 119 knots, with an approximate total landing distance of 1150 meters on a dry runway. Additional data on the aerodynamic and landing parameters, such as approach speed and go-around climb rate, are given in Figures 3-20 and 3-21.

Radiation equilibrium temperature distribution over the vehicle during ascent and entry is presented in Figure 3-22. Design temperatures for the upper surface of the vehicle occur during boost. The remainder of the vehicle experiences its maximum temperature

### SUBSONIC

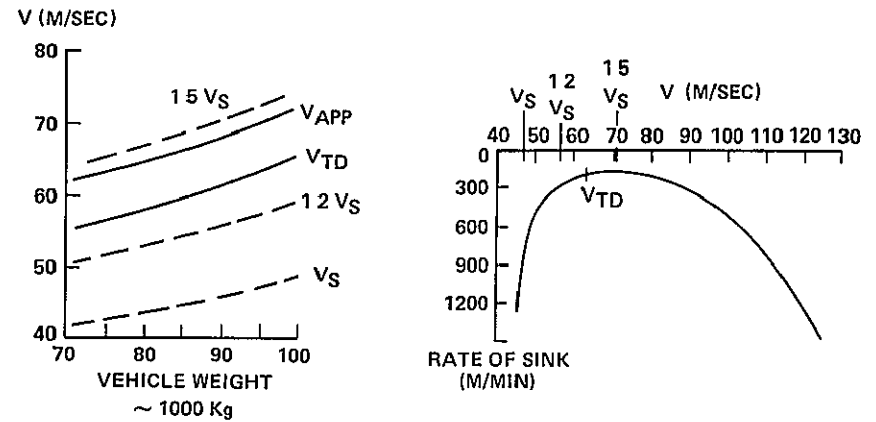
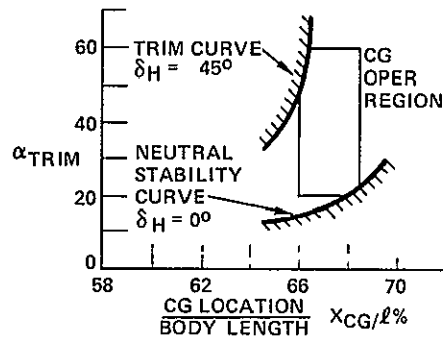


Figure 3 20 Landing Characteristics

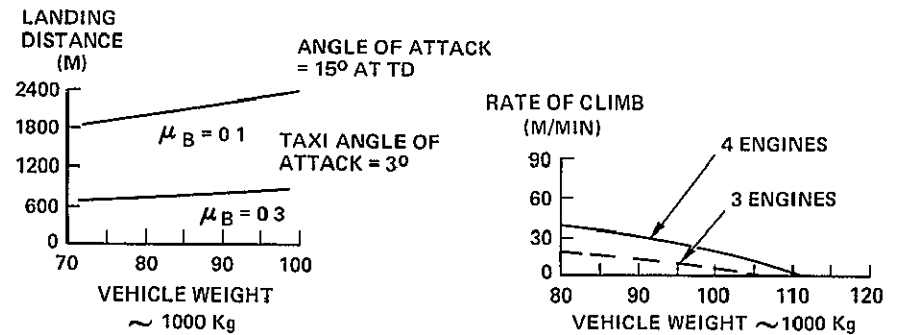


Figure 3 21 Landing Characteristics

during the high cross-range entry. Entry temperatures are generally less than 1000°C over a large area of the vehicle, however, the nose and leading edges experience temperatures up to approximately 1400°C. These temperatures reflect the modulated entry profiles already discussed.

Referring to Figure 3-23, it can be seen that load-carrying structural material, because of its attractive strength-to-density properties, coupled with satisfactory creep characteristics in thermal environments up to 340°C, is titanium. The fuselage, wing, and thrust structure use Ti-6Al-4V alloy. The main propellant tanks are



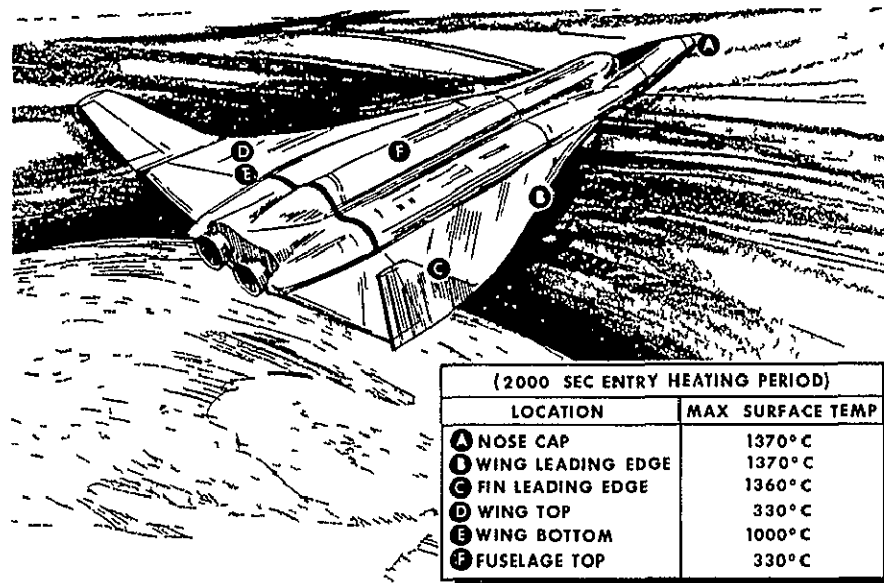
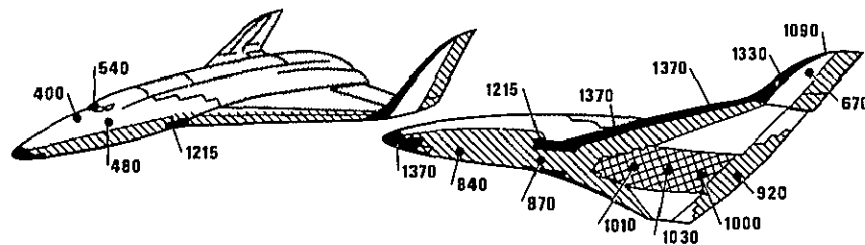


Figure 3-22 Delta Wing Orbiter Entry

constructed of 2219-T81 aluminum alloy. It was chosen for its compatibility with cryogenics, acceptable strength, good fracture toughness, and weldability. Extensive experience with this material has been gained on the Saturn program. Figure 3-21 is a condensed summary of heat shield materials. They were chosen primarily on the basis of vehicle surface-temperature profiles. Major portions of the surface are Haynes 188 and Inconel 718, with lesser amounts of TD NiCr and coated columbium. The major portion of the upper surface of the orbiter fuselage and the wing will be titanium hot structure.

It is well recognized by engineers working on the shuttle vehicle design that developing a lightweight, low cost, thermal protection system with multi-reuse capability is a key factor. We define the thermal protection system as the heat shield, insulation and structure from the external surface through to the inside of the propellant tanks or the cargo bay or the passenger cabin. Illustrated in Figure 3-24 is a typical cross section of the thermal protection



CODE	TEMP (C)	BASILINE H/S MTL	PRIMARY SELECTION CRITERIA
■	1090 1370	COLUMBIUM (C129Y) SILICIDE COATED	<ul style="list-style-type: none"> <li>• HIGH TEMPERATURE PROPERTIES</li> <li>• AVAILABILITY</li> </ul>
⊠	980 1090	TD NiCr	<ul style="list-style-type: none"> <li>• NO OXIDATION COATING REQUIRED</li> </ul>
▨	730 980	HAYNES 188	<ul style="list-style-type: none"> <li>• HIGH TEMPERATURE PROPERTIES</li> <li>• OXIDATION RESISTANCE</li> <li>• AVAILABILITY</li> </ul>
□	315 730	INCONEL 718	<ul style="list-style-type: none"> <li>• HIGH STRENGTH TO 730 C</li> <li>• FABRICABILITY</li> </ul>
□	345	TITANIUM 6AL 4V	<ul style="list-style-type: none"> <li>• HIGH STRENGTH/DENSITY</li> <li>• FABRICABILITY</li> <li>• COST</li> </ul>

Figure 3-23 Maximum Temperatures and Materials

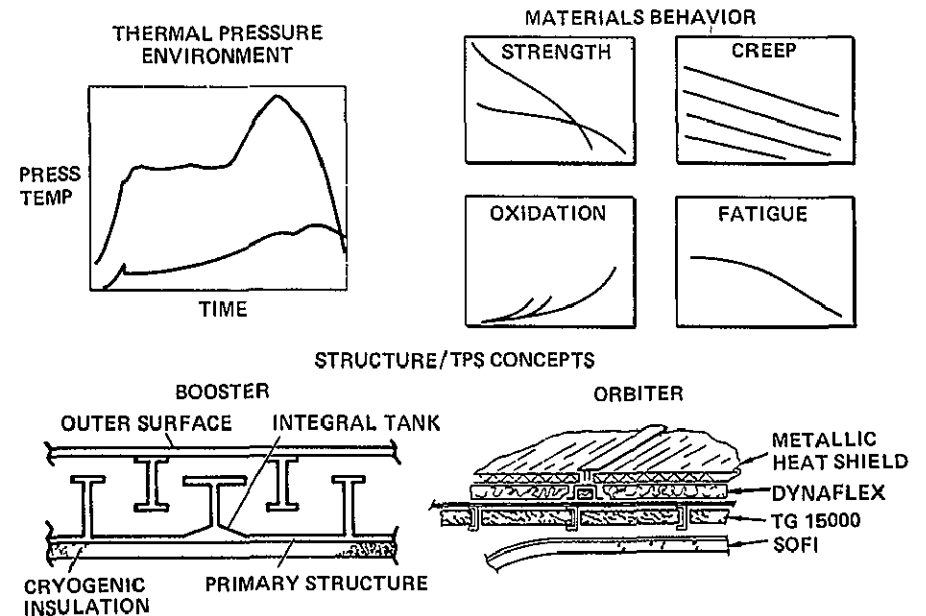
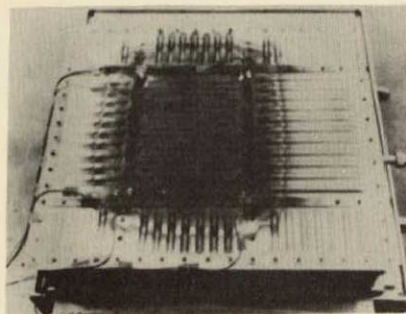


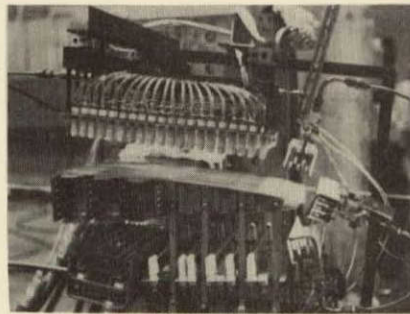
Figure 3-24 Thermal Protection System Key Technology Factors

system. Referring to the orbiter drawing, it shows a metallic heat shield and dynaflex insulation supported on the primary load-carrying structure. Between the primary load-carrying structure and the propellant tank is additional insulation. The governing parameter is the total temperature rise that occurs at the spray-on foam insulation (SOFI) bond line of the hydrogen tank. A limiting value of approximately 220°C exists at this point. Above that value the integrity of the bond breaks down. Also shown in Figure 3-24 are the other major parameters that must be accounted for in selecting the thermal protection system. Not the least of them is the accurate prediction of the thermal environment and the computation of the temperature distribution within the structure. Through the X-15, Apollo and other programs, sophisticated analytical tools have been developed for performing these estimates. They will require further refinement and test program verification during shuttle development.

Space Division and Convair have both been investigating heat shield and high-temperature structural materials and designs for the past several years. In addition, tests on TD Ni chrome materials and coated columbium have been performed, with the entry environment of the shuttle orbiter simulated. Photographs of typical specimens are illustrated in Figure 3-25.



TD NiCr HEAT SHIELD



COLUMBIUM LEADING EDGE

## PRIMARY ORBITER SUBSYSTEMS

### Structure and Primary Orbiter System

The material covered so far in this section has been configuration dependent. To the first-order approximation, the overall requirements and design characteristics of the systems are the same for both the low and high cross-range orbiters. Therefore, the structures, propulsion systems, and avionics subsystems for the delta wing will be discussed as they are typical for both orbiters.

### Vehicle Structures

An overall summary of the primary structure and materials for the orbiters has already been presented. The primary loading conditions that govern the strength requirements of the load-carrying structure are illustrated in Figure 3-26. As this figure indicates, the

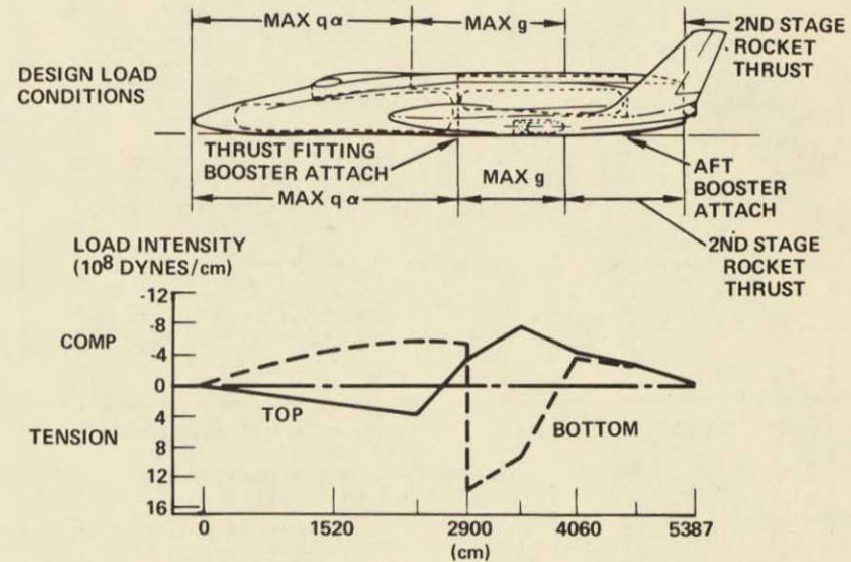


Figure 3-26. Delta-Wing Orbiter Design Conditions and Load Intensity



highest loads experienced over a large portion of the fuselage structure occur during boost flight. Specifically, the upper and lower surfaces of the forward fuselage are designed by the maximum aerodynamic pressure ( $\max q\alpha$ ) and control moments that are experienced in reacting steady-state wind shears and wind gusts in the integrated launch configuration. The loading level per unit length of cross section is also shown in this figure.

In conjunction with NASA, the space shuttle contractors will design and test a representative large-scale section of the booster and orbiter. Examples of the type of structure under consideration for design and test are shown in Figure 3-27. It illustrates the wing root-fuselage joint for the orbiter. Also shown is a propellant-tank fuselage cross section of the booster.

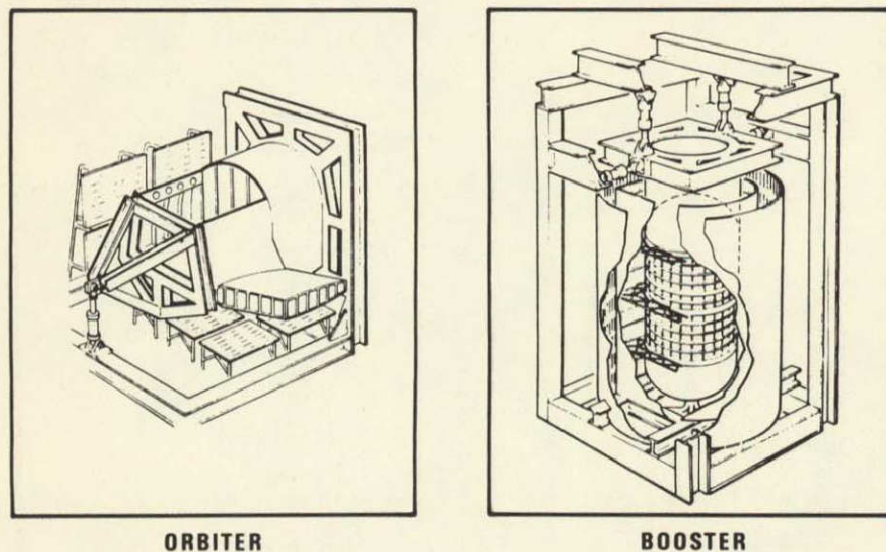


Figure 3-27. Large Structure Tests, Major Structural Subassemblies

### Rocket Engine Systems

During a normal mission, the orbiter will be required to (1) boost itself into orbit; (2) perform on-orbit maneuvers and

operations, (3) deorbit; and (4) control its attitude and make small course corrections. To accomplish this, it is provided with separate main rocket engine systems, on-orbit systems, and attitude control systems (Figure 3-28). The general locations of the engines and their propellant tanks are also shown in this figure.

The orbiter main propulsion system (Figure 3-29) employs two turbopump-fed rocket engines burning a  $\text{LO}_2/\text{LH}_2$  propellant combination at a nominal mixture ratio of 6:1. The engine power head assembly is identical to that used in the booster. A  $\epsilon = 120:1$  expansion ratio nozzle assembly (two-position type) is used to achieve high performance. A redundant, self-checking engine control unit (ECU) controls and monitors engine operation, including throttling over a thrust range of 50 to 115 percent of rated thrust. Thrust vector control over a range of  $\pm 7$  degrees is obtained with a self-contained gimbal actuation system mounted on the engine. Engine-mounted pressure volume compensated (PVC) flexible lines are employed at the engine/vehicle propellant duct interfaces. Use of

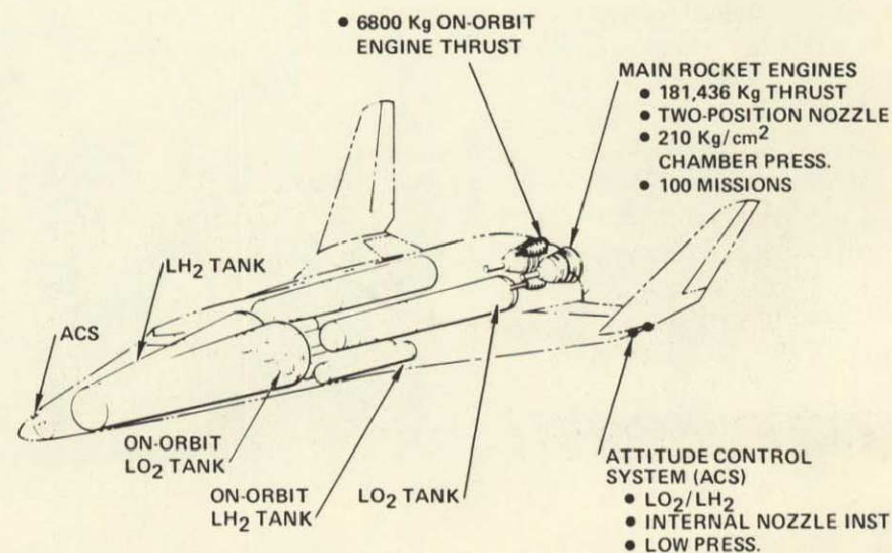
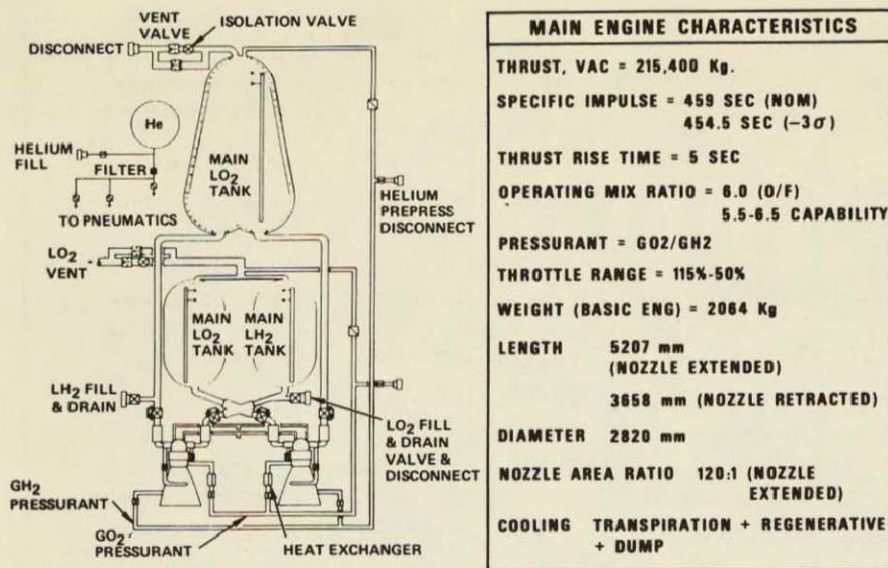


Figure 3-28. Rocket Engine Systems





MAIN ENGINE CHARACTERISTICS	
THRUST, VAC	= 215,400 Kg.
SPECIFIC IMPULSE	= 459 SEC (NOM) 454.5 SEC (-3σ)
THRUST RISE TIME	= 5 SEC
OPERATING MIX RATIO	= 6.0 (O/F) 5.5-6.5 CAPABILITY
PRESSURANT	= GO <sub>2</sub> /GH <sub>2</sub>
THROTTLE RANGE	= 115%-50%
WEIGHT (BASIC ENG)	= 2064 Kg
LENGTH	5207 mm (NOZZLE EXTENDED) 3658 mm (NOZZLE RETRACTED)
DIAMETER	2820 mm
NOZZLE AREA RATIO	120:1 (NOZZLE EXTENDED)
COOLING	TRANSPIRATION + REGENERATIVE + DUMP

Figure 3-29. Orbiter Main Propulsion System

common engines and related equipment in the two stages will substantially reduce development costs and simplify the operational phase of the program.

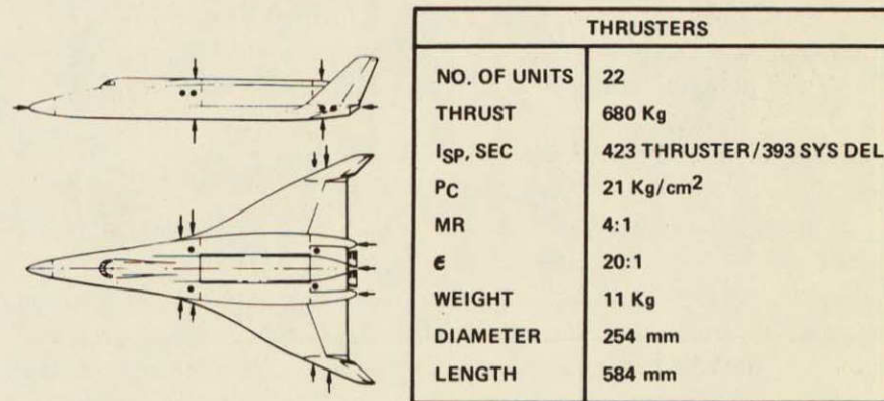
The propellant tanks are pressurized with GH<sub>2</sub> tapped from the engine preburner inlet and GO<sub>2</sub> extracted from the turbine discharge heat exchanger of the LO<sub>2</sub> turbopump. Tank pressure is controlled by redundant flow control regulators. Ground-supplied helium is used for prelaunch pressurization prior to engine ignition.

The LH<sub>2</sub> tank is insulated with closed-cell polyurethane foam applied to the tank inner wall. A fiberglass reinforcement layer protects the surface of the foam from damage and inhibits permeation of the foam by the LH<sub>2</sub>. The LO<sub>2</sub> tank is uninsulated; a dry GN<sub>2</sub> purge is used to inhibit ice formation on the tank during prelaunch servicing. Propellant feedline ducts are routed to allow convective preconditioning of the main propulsion engines before liftoff. Normally open isolation valves with position latches are

installed in each LO<sub>2</sub> and LH<sub>2</sub> feedline to provide emergency cutoff of propellant flow in the event of extreme leakage or propellant line rupture.

Point sensors and capacitance probes monitor liquid level and measure on-board propellant weight during prelaunch servicing. Propellant residuals are minimized by propellant loading bias; depletion sensing and shutdown will be accomplished by the engine subsystem. Provisions are made for propellant utilization because of the direct exchange between residual propellant weight and payload capability in the orbiter.

The orbiter attitude control propulsion system (ACS) provides capability for small translational maneuvers and three-axis attitude control. As shown in Figure 3-30, the baseline engine arrangement employs 22 thrusters, each operating at a vacuum thrust of 680 kilograms to provide minimum angular accelerations of 0.5°/sec<sup>2</sup> and translational rates of 0.03 m/sec<sup>2</sup> for each vehicle axis with one engine inoperative. Fail-safe attitude control at 67 percent of the



● SIMILAR ACS ENGINE LOCATIONS FOR BOTH STRAIGHT WING & DELTA WING ORBITER

Figure 3-30. Orbiter Attitude Control Propulsion System



minimum design rate is possible after loss of any two thrusters. Translation at the minimum acceleration rate is possible after loss of either one or two thrusters.

The thruster configuration selected for the baseline system burns a gaseous hydrogen/oxygen propellant combination at a chamber pressure of 21 kg/cm<sup>2</sup>. A nozzle expansion ratio of 20:1 was selected to limit nozzle exit plane diameter and thereby minimize the area of vehicle outer skin penetrated by the thruster nozzle. The selected baseline thruster uses augmented spark ignition. Shielding will be employed if required to minimize electromagnetic interference effects. In addition to providing adequate attitude and translation rates for the orbiter, the selected 680 kilograms thrust level provides the desired attitude control system (ACS) control authority for the booster; therefore, a common thruster configuration may be used with an associated reduction in hardware development and production costs.

The orbit maneuvering system provides the capability for orbiter maneuvers, including circularization, orbit transfer, rendezvous, and deorbit. Our baseline system (Figure 3-31) employs two rocket engines using LO<sub>2</sub> and LH<sub>2</sub> propellants stored in tankage completely independent of the main propulsion system.

### Integrated Avionics and Electromechanical Subsystem

Through the integrated avionics and electromechanical subsystem (IAS), all elements and subsystems of the vehicle are integrated, controlled, and monitored. Since the requirements between the orbiter and the booster vehicles are quite similar, a high degree of commonality is possible in the avionics equipment, and the following descriptions are therefore equally applicable to both vehicles.

Figure 3-32 represents a simplified block diagram of the IAS showing the major functional elements that are all controlled

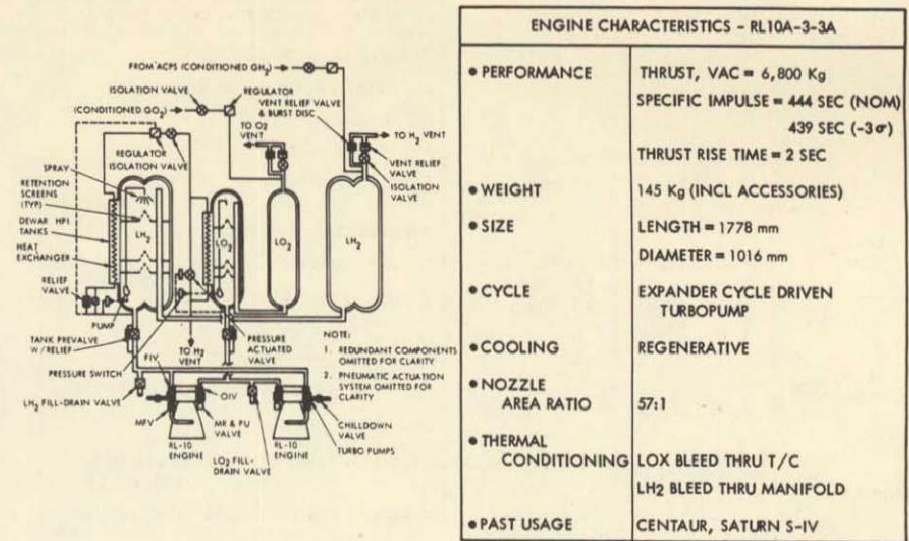


Figure 3-31. On-Orbit Maneuvering System Schematic

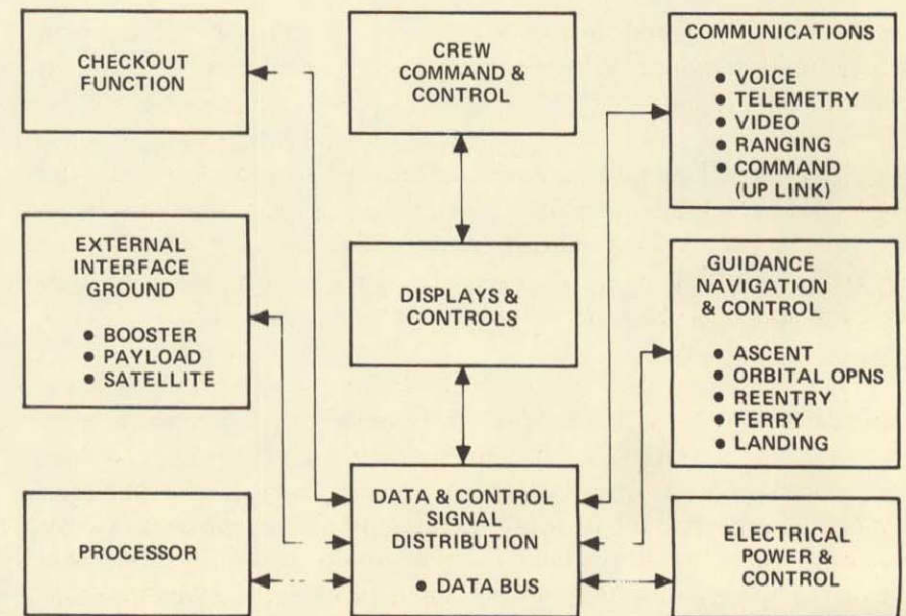


Figure 3-32. Integrated Electronics



through a central data management system. Characteristics of the IAS are enumerated on Figure 3-33. A brief description of the IAS elements follows.

- PROVIDE ON-BOARD CHECKOUT, COMMAND & CONTROL & SAFING PROVISIONS
- INTEGRATED GN&C
- CONVENTIONAL COMM, NAV & LANDING AIDS
- CENTRALIZED & SELECTED DEDICATED COMPUTERS
- DATA BUS & STANDARD INTERFACE UNITS
- MULTIPURPOSE DISPLAYS & CONTROLS
- FAIL OPERATIONAL / FAIL OPERATIONAL / FAIL SAFE OPERATION
- ACCESS TO EACH LINE REPLACEABLE UNIT (LRU) INDEPENDENTLY
- COMMON MODULAR SOFTWARE

Figure 3-33. Integrated Avionics Characteristics

### Data Bus and Computers

A common multiplexed data bus transmits all commands, responses, and data, thus integrating all functional elements of the vehicle. The current preliminary computer configuration is primarily centralized with dedicated processors for flight control and main rocket engine systems. Standard interface units are used to couple subsystem elements to the common data bus. They include data acquisition and stimulus capability to support checkout and redundancy management.

### Guidance, Navigation, and Flight Control

These functions use a strap-down-type inertial reference that is aligned optically. Flight control is accomplished through a digital system. Control of the vehicles throughout all boost, orbital, and atmospheric flight phases presents a difficult flight-control problem in which we must use the knowledge gained through operations of the Saturn and Apollo vehicles, as well as commercial aircraft practices.

### Communications

This element of the IAS provides voice, data, ranging, and navigational aids capabilities, as shown in Figure 3-34. The voice, data, and ranging requirements will apply the techniques and probably much of the equipment that has been space-flight proved in Apollo. For the atmospheric flight phase, equipment developed for commercial and military aircraft is directly applicable. This subsystem, therefore, requires little basic development but rather an effective means of integrating its functions into the vehicle system.

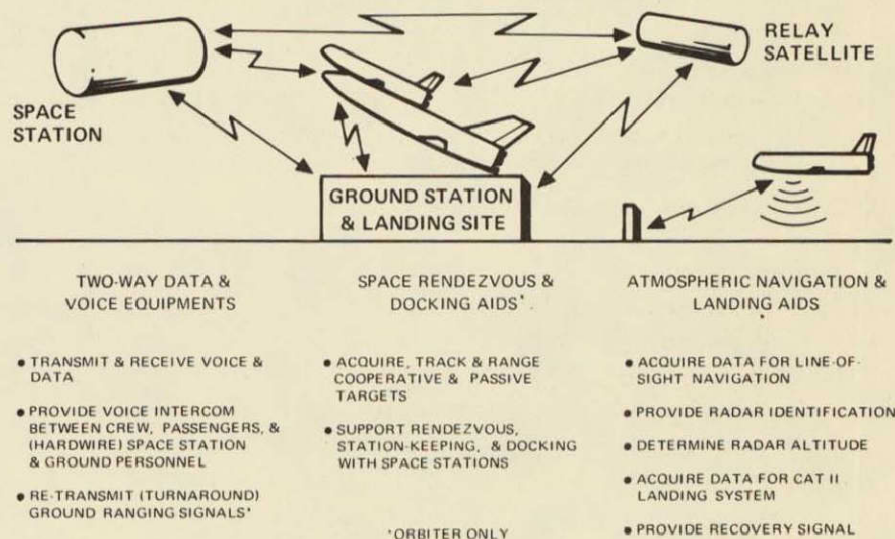


Figure 3-34. Communications

### Crew Command and Control

The shuttle cockpit is configured basically like an aircraft cockpit (Figure 3-35). However, since the orbiter vehicle must function either as a spacecraft or an aircraft, the cockpit incorporates controls and displays to satisfy all mission phases. On the Apollo spacecraft, the principal flight displays were represented by individual instruments, as shown on Figure 3-36. If this approach is used



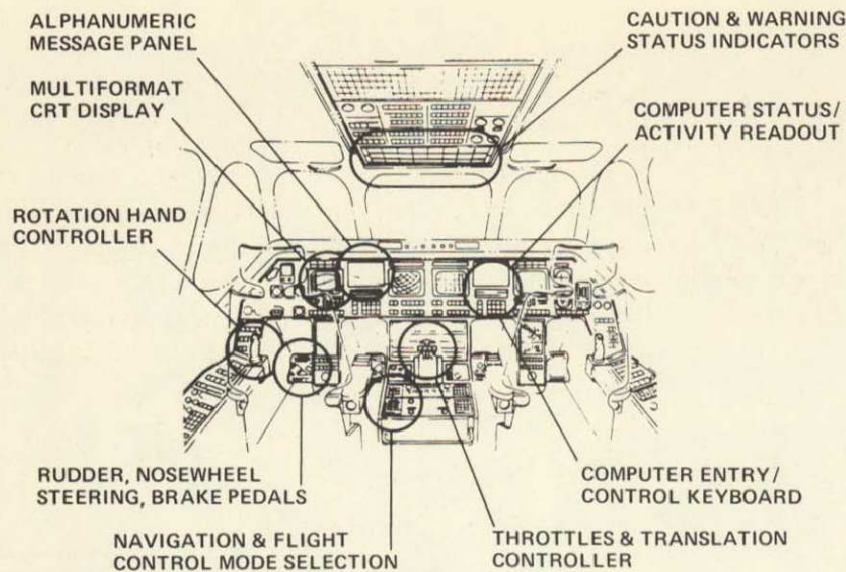


Figure 3-35. Shuttle Orbiter Cockpit

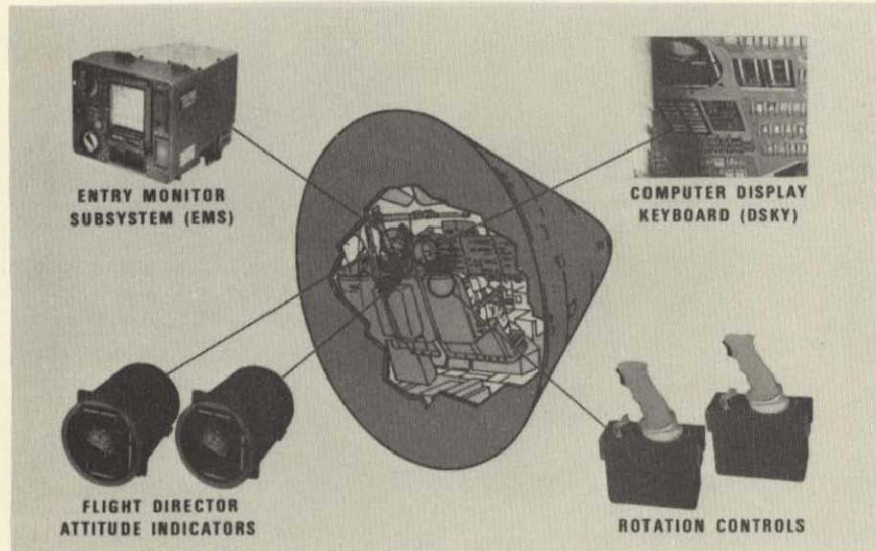


Figure 3-36. Apollo Crew Station and Equipment

on shuttle, the cockpit would be larger and more complex and might require more than the two-man crew now planned. Therefore, a solution is to use fewer instruments having greater flexibility. Multi-format cathode-ray tube (CRT) displays can present on a single instrument the information that required a number of instruments in the past. Examples of the types of formats that will be used in two different flight phases are shown in Figures 3-37 and 3-38. The same CRT presents a display for ascent guidance during the boost phase and later presents a space attitude display for flight control during on-orbit phases. On Apollo, the computer was used only for navigation and guidance, and the display keyboard unit (DSKY) was limited to that task. Since the shuttle computers do many additional things, more flexibility is required but the same approach is used.

Solid-state alphanumeric readouts and all-electronic keyboards are planned. To command the vehicle attitude in space, the Apollo-type and proved three-axis rotation hand controller is used. During atmospheric flight, only two axes pitch and roll, are controlled with the hand controller. Conventional aircraft-type pedals control yaw. A single translation controller similar to the Apollo type is mounted on the pedestal near the throttles for linear motion control in space.

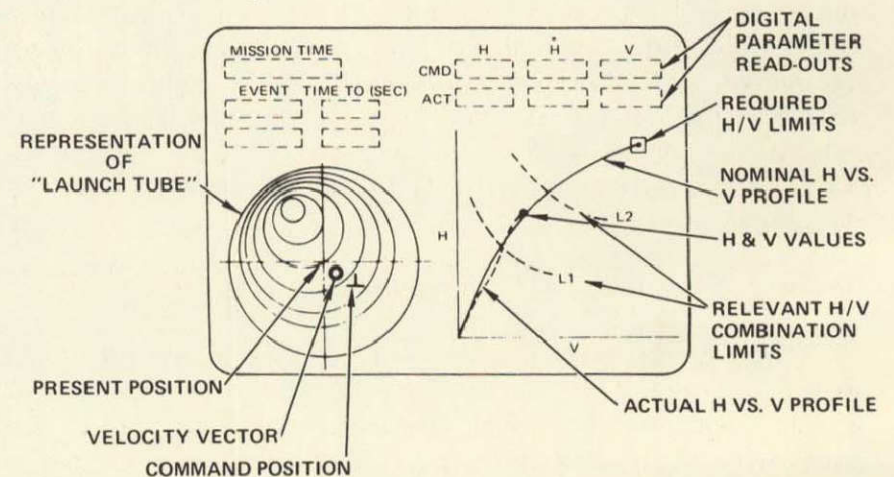


Figure 3-37. Boost and Ascent Display



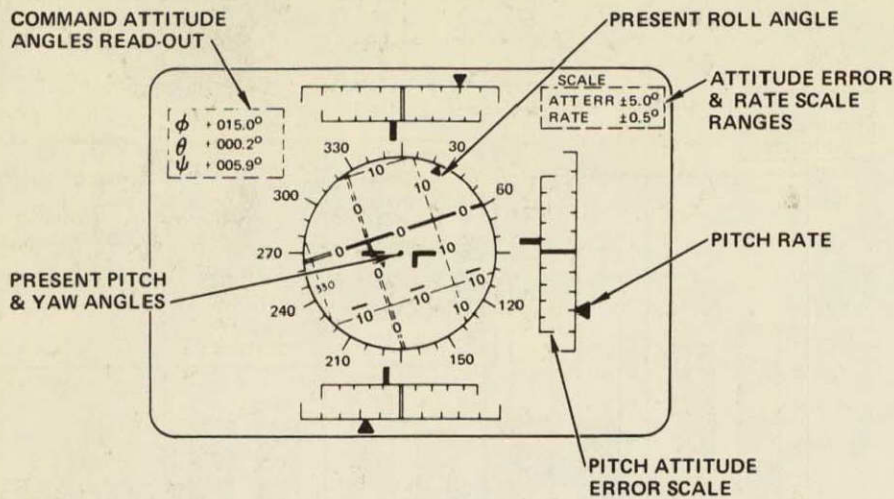


Figure 3-38. Space Attitude Display

### Checkout

For a drastic reduction in ground equipment, number of ground personnel required, and turnaround time, the shuttle vehicles use on-board checkout. How the central data management system is applied in accomplishing the checkout function is shown in Figure 3-39. The example is the main rocket engines. Using appropriate sensors and transducers for the important engine parameters, the computer processes these data and compares the results to the expected or normal case. Through judicious use of primarily operational parameters, the broad requirements of checkout are satisfied. These include demonstration of operational readiness, caution, and warning displays for critical functions, fault isolation, and switching techniques, in addition to long-term trend analyses.

### Electrical Power and Control

The power sources include fuel cells, APU's, and batteries. Appropriate conversion and distribution equipment is controlled through the common data bus.

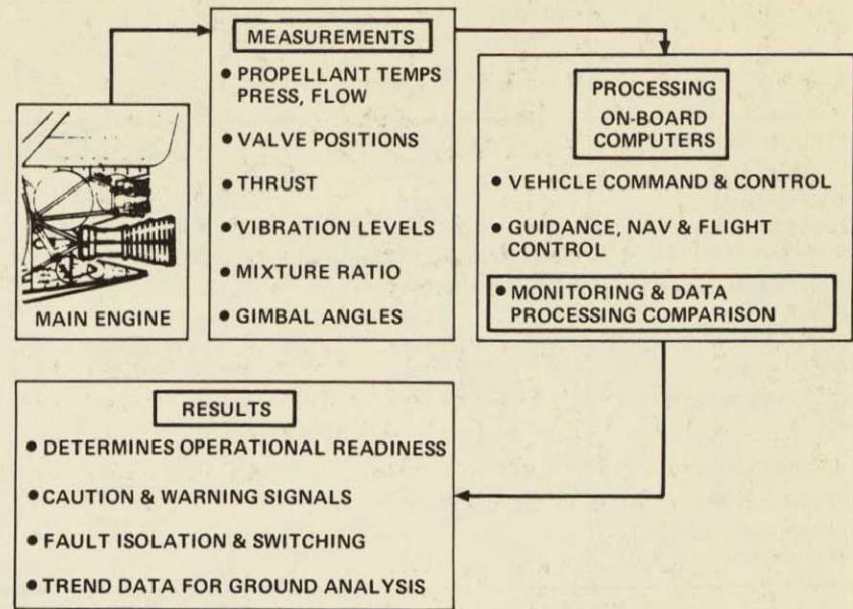


Figure 3-39. On-Board Checkout

### ORBITER COMPARISONS

It is appropriate to conclude the discussion with a comparison of the two systems. It has been noted that the payload performance characteristics of each orbiter differ by 2:1 in favor of the straight-wing design. This higher payload results principally from less thermal protection being required to meet the low cross-range requirement. Other benefits are gained because a simpler packaging of the propulsion and other systems is possible. Additional details of the weight breakdown and stage mass fraction of the vehicles are shown in Figure 3-40. The values are for the gross liftoff weight limit of 1,587,000 kilograms. These same data are illustrated graphically in Figures 3-41 and 3-42. These figures indicate clearly the magnitude of the penalty for thermally protecting vehicles to achieve a high cross range.




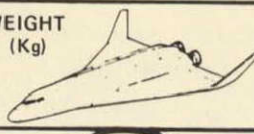
	WEIGHT (Kg)	WEIGHT (Kg)
		
STRUCTURE & TPS	43,636	56,382
LANDING & DOCKING	4,899	4,581
PROPULSION	19,187	20,140
ORIENTATION, CONTROL & SEPARATION	4,218	2,495
SUBSYSTEMS	5,035	5,126
PERSONNEL	318	318
PAYLOAD	20,412	9,070
MAIN PROPELLANT	242,041	241,224
OTHER PROPELLANT	7,394	7,757
LIFTOFF WEIGHT	344,736	344,736
ENTRY WEIGHT	98,250	98,749
LANDING WEIGHT	97,297	97,751
STAGE MASS FRACTION	.74	.712

Figure 3-40. Baseline Vehicle Mass Characteristics, Gross Liftoff Mass = 1,587,000 Kilograms

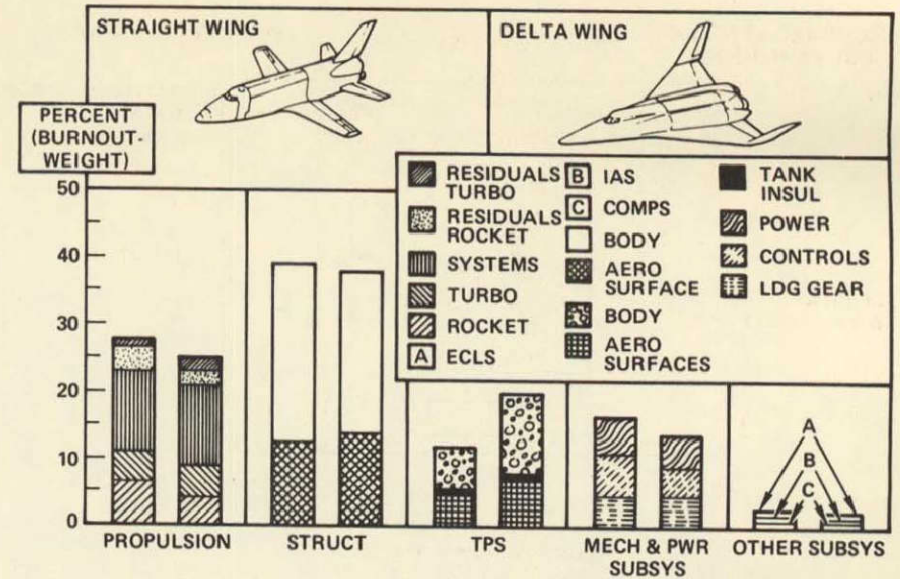


Figure 3-42. Structural and Subsystem Weight Distribution

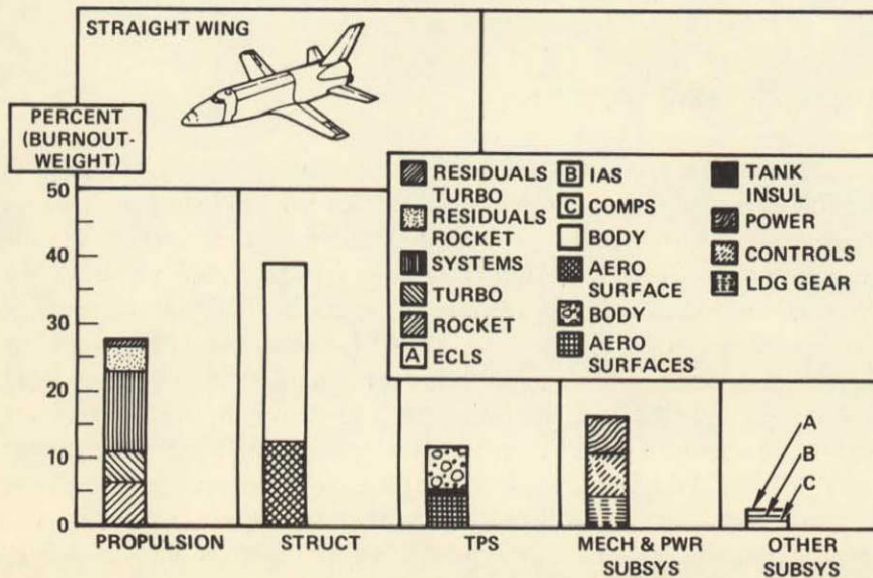


Figure 3-41. Structural and Subsystem Weight Distribution

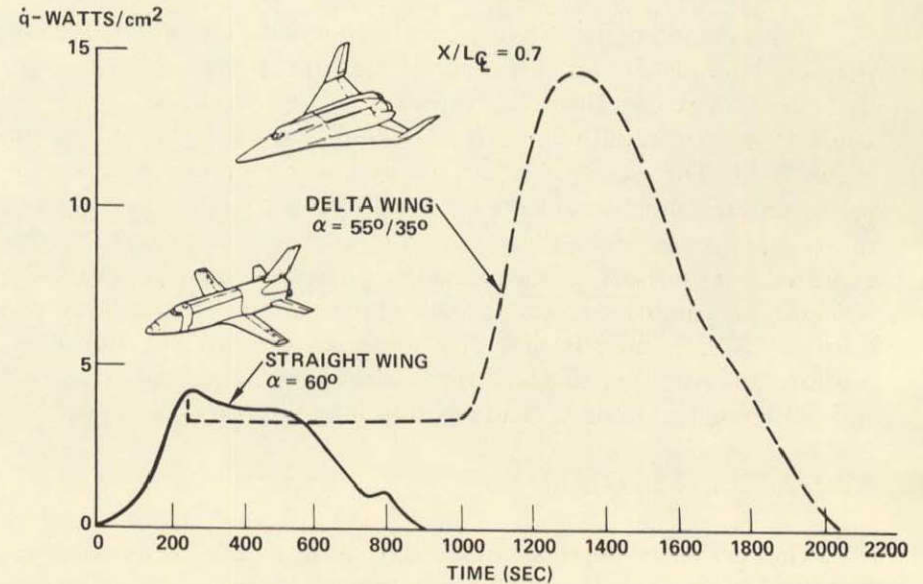


Figure 3-43. Comparison of Orbiter Fuselage Heating Histories, High and Low Cross-Range Entry

A further illustration of this point is shown in Figure 3-43. This presents the heating rate histories of both orbiters. These heating histories were computed for the entry trajectories presented in the General Configuration section. The integral under this heating-rate-

time curve provides a direct measure of the total heat load experienced by a vehicle of this design. It shows that the heat load for the high and low cross-range vehicles vary by a factor greater than 5.



## 4. SHUTTLE BOOSTER

### BOOSTER MISSION PROFILE

The booster illustrated in Figure 4-1 will be briefly discussed according to the outline in Figure 4-2. The object of the booster, of course, is to accelerate the orbiter to the appropriate staging conditions. The booster flight profile is indicated in Figure 4-3. Features of the booster include (1) vertical launch, (2) a maximum dynamic pressure of slightly more than 2600 kilograms per square meter (occurring at an altitude of slightly under 10 kilometers) and (3) separation of the orbiter at an altitude of slightly more than 65 kilometers 3.2 minutes after launch and at a velocity of 2850 meters per second. After separation, the booster coasts to its apogee of 75 kilometers and then enters at a high angle of attack (55 degrees) and with a bank angle of approximately 40 degrees. The bank angle is modulated to limit the maximum load factor to 4 g's. The bank

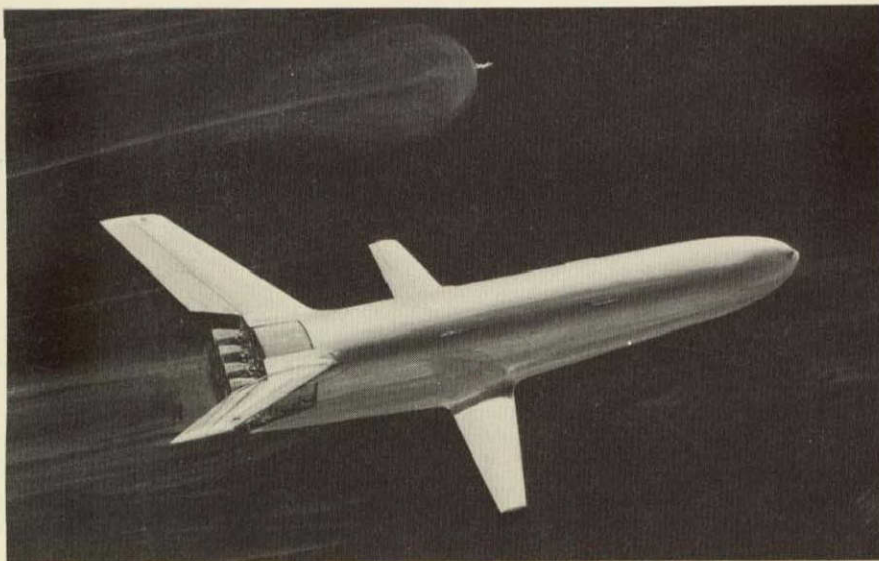


Figure 4-1. Baseline Booster After Staging

### GENERAL DESCRIPTION OF BASELINE

#### AERODYNAMIC CHARACTERISTICS

#### SEPARATION AND ABORT

#### STRUCTURE AND TPS

#### PROPULSION SYSTEMS

#### OTHER SUBSYSTEMS

Figure 4-2. Outline of Booster Briefing

maneuver minimizes the down-range travel and thus the fuel required for cruising back for a landing at the launch site.

After the booster has slowed during the entry maneuver to subsonic speed, the air-breathing flyback engines are deployed and started, and the booster cruises back as a large subsonic aircraft and makes a normal horizontal landing at a runway near the launch site. Landing occurs at a velocity of 155 knots approximately 111 minutes after liftoff.

As noted in Figure 4-4, the booster operates as a rocket-powered launch vehicle for approximately three minutes, as an unpowered hypersonic glider for approximately 10 minutes, and as a subsonic aircraft for approximately an hour and a half. Landing is followed by a two-week turnaround operation on the ground.

The booster is designed to be an efficient rocket-powered vehicle during the three-minute boost phase. During entry, cross-range capability is not required for the booster. The configuration selected has acceptable hypersonic characteristics, but the lift-drag ratio (4D) at high velocities has been purposely compromised in the selection of its design features to assure efficient operating character-



istics during the hour and one-half that the vehicle is operating as a subsonic aircraft.

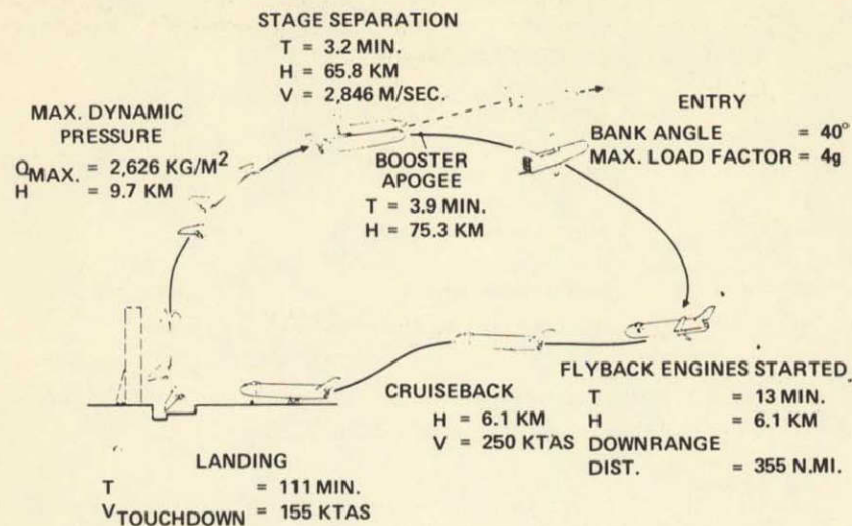


Figure 4-3. Booster Flight Profile

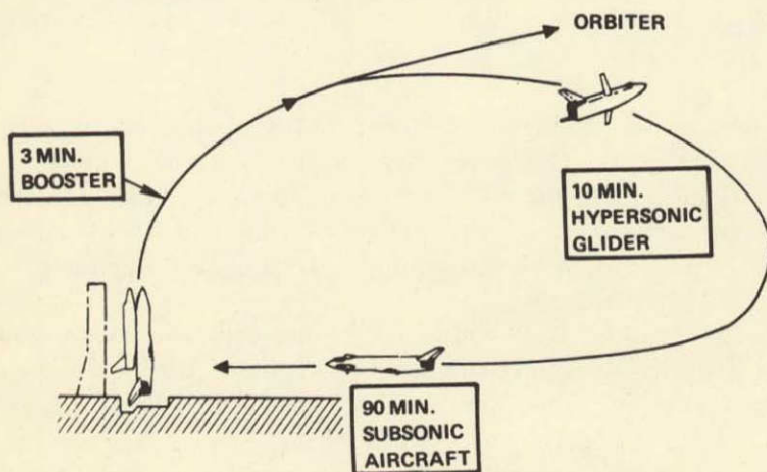


Figure 4-4. Booster Flight Modes

## BOOSTER CHARACTERISTICS

Design of the hypersonic vehicle is influenced by the requirement to assure rapid and low-cost refurbishment during the turnaround cycle. The basic characteristics of the baseline booster are listed in Figure 4-5. Note that the tail area is slightly larger than that of the wing: 219 square meters for the tail and 186 square meters for the wing. The total platform area of more than 1000 square meters is largely fuselage underbody. This, of course, provides most of the lift during the hypersonic glide phase. The baseline configuration has a fixed straight wing and a vee tail. The straight wing was chosen for simplicity and low weight, taking into consideration that the hypersonic characteristics need not be optimized and that the low hypersonic L/D of 0.5 is satisfactory since cross range is not a criterion. The fixed-wing configuration yields an L/D of 6.7. This ratio assures satisfactory cruise capability. The lift loading of 430 kilograms per square meter is moderate to minimize aerodynamic heating.

Pertinent characteristics of the baseline booster are noted in Figure 4-6. The air-breathing engines for the cruise phase are stowed during the boost and hypersonic flight phase and then are deployed for cruising back to the launch site. These engines are mounted

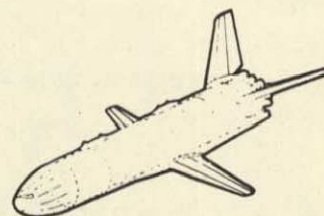
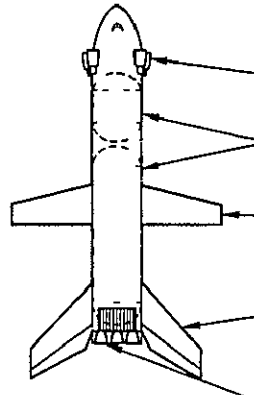


Figure 4-5. Baseline Booster Configuration

AREAS (M <sup>2</sup> )	WING	185.8
	TAIL	219.1
	TOTAL PLATFORM	1,008.0
L/D	HYPERSONIC	0.5
	SUBSONIC	6.7
STAGING	VELOCITY (M/SEC.)	2,874
	ALTITUDE (KM)	65.8
LIFT LOADING	W/SC <sub>L</sub> (KG/M <sup>2</sup> )	432.1
LANDING SPEED	V(KTAS)	155



CHARACTERISTIC	RATIONALE
AIR BREATHING ENGINES STOWED FORWARD	BALANCE MINIMUM WEIGHT
SEPARATE CYLINDRICAL TANKS	MINIMUM DEVELOPMENT COST & OPERATIONAL RISK
FIXED STRAIGHT WING	SIMPLICITY CRUISE LANDING PERFORMANCE & MAXIMUM PAYLOAD
VEE TAIL	ORBITER PLUME IMPINGEMENT MINIMUM WEIGHT
12 ENGINES	MISSION COMPLETED EVEN WITH TWO ENGINES FAILED

Figure 4 6 Characteristics of Baseline Booster

forward to bring the center of gravity of the vehicle forward and help compensate for the large weight of the rocket engines at the aft end. The liquid oxygen and liquid hydrogen tanks are cylindrical, load-carrying structures and they are separate tanks with no common bulkheads. Twelve rocket engines are provided for the boost phase. The choice of 12 engines will be discussed later.

The vee tail was selected partly because of the consideration of plume impingement of the orbiter engines during the staging sequence. Basic dimensions of the booster are indicated in Figure 4-7. The overall length is slightly under 80 meters, the wing span is slightly over 43 meters, and the fuselage diameter is approximately 9 and 1/2 meters. The gross liftoff weight of the booster is approximately 1.2 million kilograms.

A size comparison of the booster with the Boeing 747 and the Boeing 707 is presented in Figure 4-8. The relative dimensions and other characteristics of these three systems are presented in Figure 4-9. Note that the major differences are that the booster has a much higher maximum speed than either of the commercial

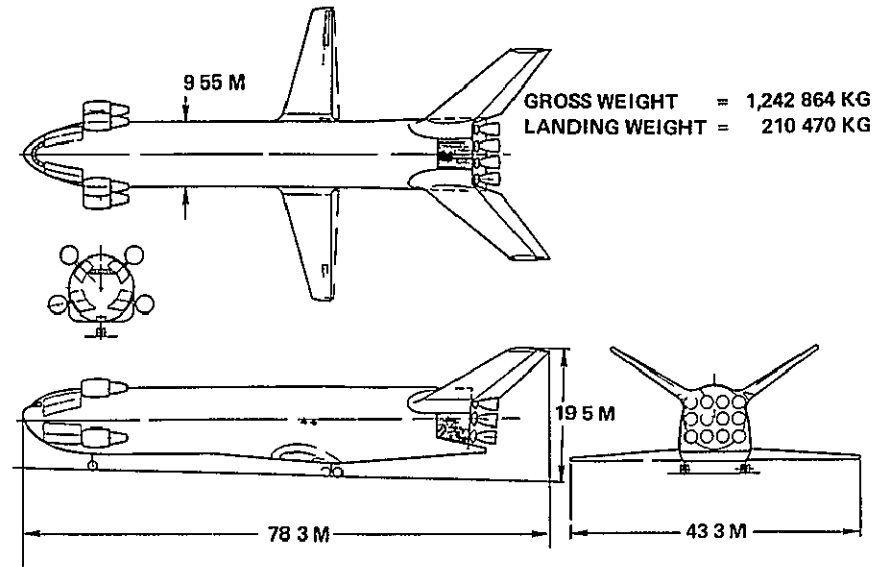


Figure 4 7 Baseline Booster

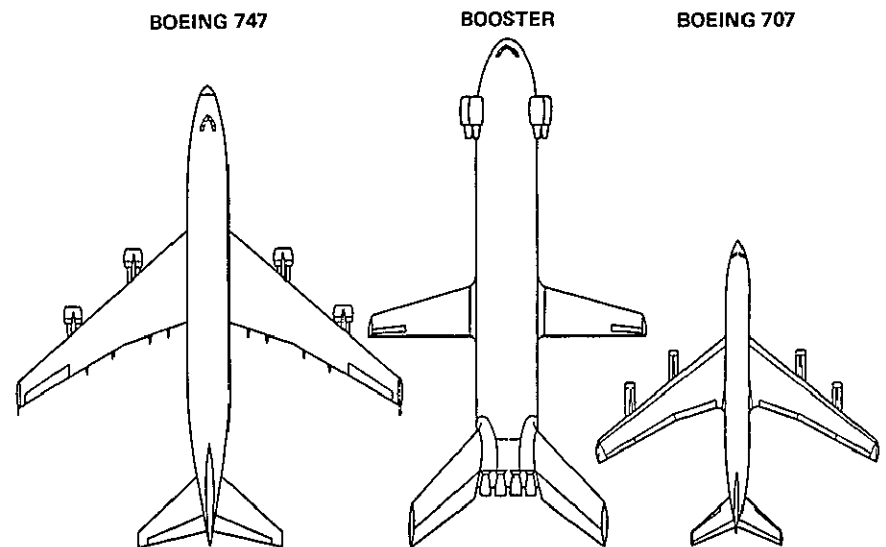


Figure 4 8 Booster Size Comparison

transports, a much higher payload (the orbiter gross weight), and a much higher gross weight. The wing span for the booster is almost identical with the wing span for the Boeing 707, and the total height for the booster is almost identical to that of the Boeing 747. The booster is approximately 8 meters longer than the Boeing 747.

Note that the landing weight of the booster is actually less than the maximum landing weight of the Boeing 747, which is operating commercially.

A comparison of the weight characteristics of the booster with those of the straight-wing orbiter and the delta-wing orbiter is presented in Figure 4-10. The gross weight of the booster is approximately four times that of either of the orbiters, while the empty weight is slightly over two times that of the orbiters. Major empty weight differences are in the structural and thermal protection area and in the propulsion systems. The propellant mass fractions for these three vehicles are booster, 0.81, straight wing, 0.74, and orbiter, 0.71.

	BOEING 747	BOOSTER	BOEING 707
<b>VELOCITIES (KTAS)</b>			
MAXIMUM SPEED	556	554	541
LANDING SPEED	140	155	140
<b>DIMENSIONS (M)</b>			
SPAN	59.6	43.3	43.4
LENGTH	70.5	78.3	46.6
HEIGHT	19.4	19.5	12.7
<b>WEIGHTS (KG)</b>			
PAYLOAD	28,123	344,736	12,792
EMPTY WEIGHT	165,564	201,897	61,236
LANDING WEIGHT	255,830	210,606	93,895
GROSS WEIGHT	351,540	1,242,864	141,523

Figure 4-9 Booster Comparison Data

	BOOSTER	STRAIGHT WING ORBITER	DELTA WING ORBITER
STRUCTURE & THERMAL PROTECTION	120,159	43,636	56,382
LANDING (& DOCKING) SYSTEM	8,800	4,899	4,581
PROPULSION SYSTEM	61,236	19,187	20,140
ORIENTATION CONTROL & SEPARATION	7,258	4,218	2,495
OTHER SUBSYSTEMS	4,445	5,035	5,126
PERSONNEL	227	318	318
PAYLOAD		18,008	6,713
MAIN PROPELLANT	1,013,206	242,041	241,224
OTHER PROPELLANT	27,533	7,394	7,757
LIFTOFF WEIGHT	1,242,864	344,736	344,736
ENTRY WEIGHT	217,320	98,250	98,749
LANDING WEIGHT	210,606	97,297	97,751

Figure 4-10 Baseline Vehicle Weight Characteristics (kg) Gross Liftoff Weight 1,587,000 kg

### AERODYNAMIC CHARACTERISTICS

The combination of the large, flat undersurface of the fuselage with the fixed straight wing and the large vee tail leads to favorable aerodynamic stability trends, as indicated in Figure 4-11. The normal force coefficients for the booster fuselage by itself, for the wing by itself, and for the vee tail by itself as a function of Mach number are shown in the diagram at the upper right-hand corner of the chart. Note that the body normal force coefficient is essentially independent of the Mach number. The force coefficient for the tail increases moderately and that for the wing increases quite dramatically as the Mach number decreases toward the transonic regime. When these three elements are combined, the overall effect (as indicated in the diagram in the lower left-hand corner of Figure 4-11) is a decreasing trim angle of attack (noted by circles in the diagram) with decreasing Mach number. The trim angles of attack are determined by considering the location of the center of pressure and the center of gravity.

Another way of indicating the variation of the trim angle of attack with Mach number is presented in the diagram in the lower

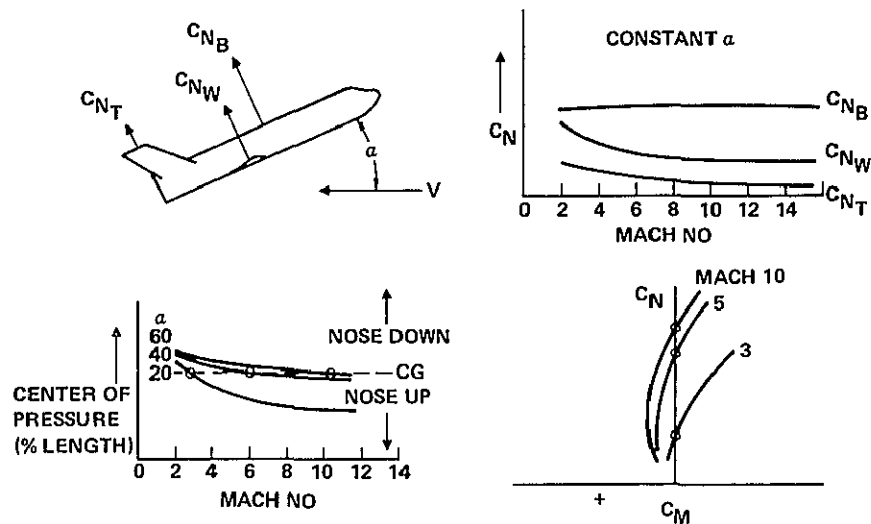


Figure 4-11 Booster Stability Trends

right-hand corner of Figure 4-11, which shows the normal force coefficient versus the moment coefficient for trim conditions, the moment coefficient must be zero. Therefore, as indicated, the trim normal force coefficient (and angle of attack) decreases with decreasing Mach number.

The resultant variation in trim angle of attack with Mach number is portrayed in Figure 4-12. The upper dashed control boundary is for the maximum ruddervator travel of 40 degrees up. The lower dashed control boundary is for the maximum down ruddervator travel of 20 degrees. Stable operating conditions lie between these boundaries. Note that for the case of no ruddervator deflection, the trim angle of attack decreases from approximately 55 degrees at Mach 10, in a smooth manner, to zero degrees at approximately Mach 1. The natural reduction in trim angle of attack as the Mach number decreases during the entry phase has a very favorable weight impact. Potentially high buffet loads associated with penetrating the transonic regime at a high angle of attack are avoided. Ruddervator area and control power requirements are also minimized.

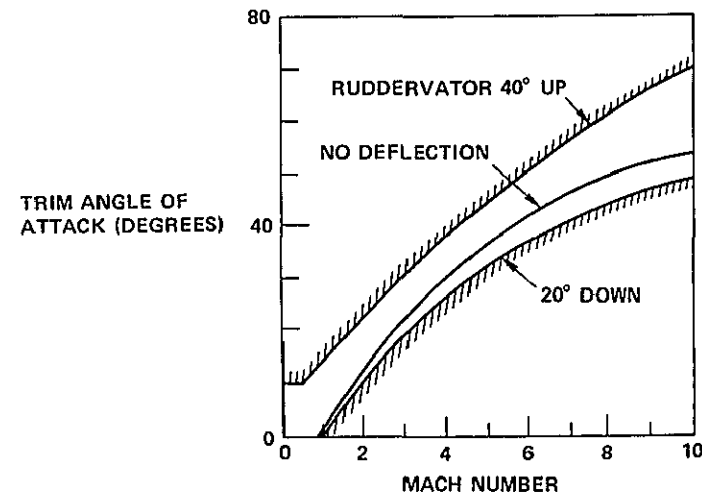
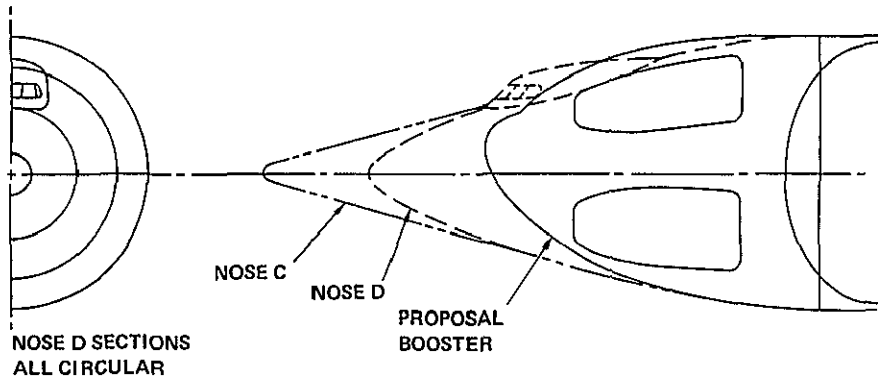


Figure 4-12 Variation of Trim Angle of Attack

The payload capability for the mated booster/orbiter system is quite sensitive to drag loss during the boost phase. As a result of recent investigation, the nose of the booster has been sharpened from that of the proposal booster. This change in nose shape has resulted in a net payload change of 57 kilograms (Figure 4-13). Still sharper noses, such as nose C, are being investigated. The tradeoff that must be examined, of course, is the reduction in boost-phase drag loss as compared to the weight increase associated with further streamlining. This study of nose shape is typical of the many studies which are underway to improve the capability of the baseline booster further.

## SEPARATION AND ABORT

Selection of the baseline separation concept was based on many criteria. These included (1) the exclusion of droppable hardware (which would preclude the attainment of all azimuth launch capability), (2) the exclusion of pyrotechnics and of expendable components such as solid rocket staging motors, and (3) the inherent capability to provide positive separation, not only at normal staging conditions, but also under abort conditions.

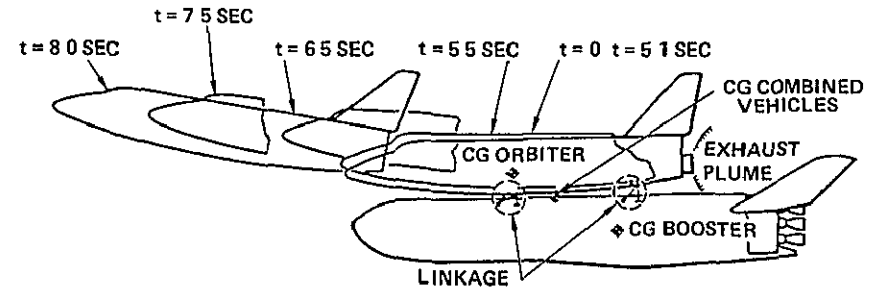


NOSE SHAPE	PAYLOAD CHANGE (KG)
PROPOSAL BOOSTER	0
WITH NOSE D	+56 7
WITH NOSE C	+226 8
WITH HEMISPHERE NOSE	1088 6

Figure 4-13 Variations to Baseline Booster Nose

The separation concept selected for the baseline is shown in Figure 4-14. The orbiter main rocket engines are ignited to provide separation force. The auxiliary propulsion systems, in both booster and orbiter, provide attitude control during the separation phase. Mechanical linkages attached to the booster ensure the maintenance of appropriate separation clearances.

Separation sequencing is shown in Figure 4-15. The sequencing is initiated when a low-level sensor in either the liquid oxygen or liquid hydrogen propellant tank in the booster is uncovered near the end of the boost-phase operation. Uncovering the low-level sensor activates a run-out clock, which, in proper time sequencing, sends out the discretes to ignite the rocket orbiter engines, to command shutdown of the booster rocket engines, and to initiate linkage rotation. The exact time sequencing can only be determined after definitive experimental data are obtained on the thrust transients associated with booster shutdown and orbiter engine startup and altitude. This staging system, as noted, offers the inherent capability to operate under conditions of abort.



ORBITER MAIN ENGINES PROVIDE SEPARATION FORCE  
AUXILIARY PROPULSION SYSTEMS PROVIDE ATTITUDE CONTROL  
MECHANICAL LINKAGES ENSURE SEPARATION CLEARANCES

Figure 4-14 Baseline Separation Concept

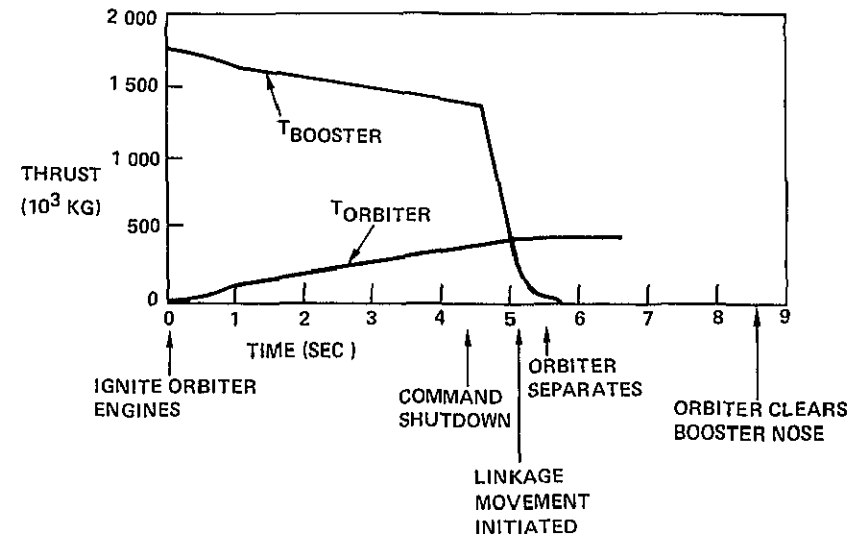


Figure 4-15 Baseline Separation Sequencing



Intact abort is a desired feature and is indicated in Figure 4-16. The concept is that, if major malfunctions occur prior to staging, the mated vehicle combination will continue to an altitude where the dynamic pressure is sufficiently low to permit separation of the orbiter and booster. After this abort separation, the booster will continue to operate at least some of the rocket engines to burn off all the rocket engine propellants. It will then make a normal entry and cruise, using its air-breathing engines, back to the landing strip at the launch site. After abort separation, the orbiter will also burn off its rocket propellants and, during this operation, will adjust its trajectories to assure that at the completion of its entry phase it is within range of an acceptable landing site.

### STRUCTURAL AND THERMAL PROTECTION SYSTEMS

A simple inboard profile of the booster is presented in Figure 4-17. The major characteristics selected and the rationale for their selection are presented in Figure 4-18. The main propellant tanks are separate, cylindrical, load-carrying structures fabricated of

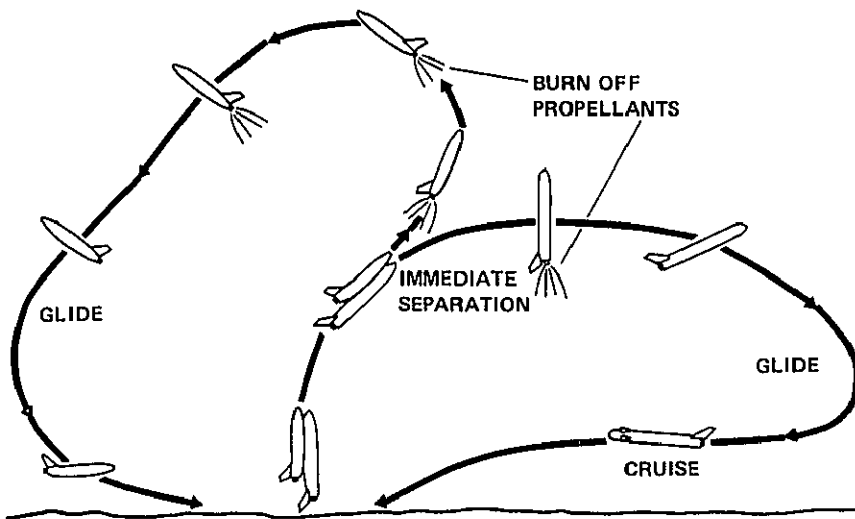


Figure 4-16 Intact Abort

2219 aluminum. Such tanks lead to high volumetric efficiency and low structural weight.

The liquid oxidizer tank is located forward to assist in keeping the center of gravity forward near the aerodynamic center of pressure. No penetrations are made of either liquid oxygen or liquid hydrogen propellant tanks for purposes of structural attachment. The air-breathing engines are deployable and mounted forward. This provides a benign environment for the air-breathing engines during the boost and entry phase, assists in balance by moving the center of gravity forward, and assures excellent inlet performance for the engines in their deployed (operating) condition.

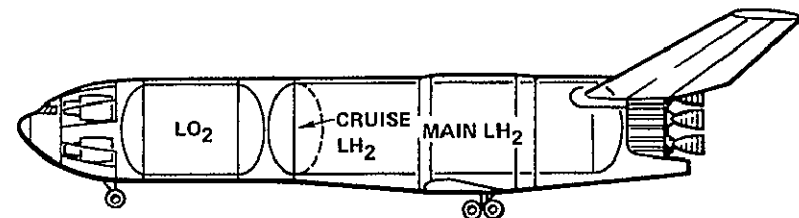


Figure 4-17 Booster Design and Packaging Considerations

#### MAIN PROPELLANT TANKS

CYLINDRICAL  
LOAD CARRYING  
SEPARATE  
LO<sub>2</sub> TANK FORWARD  
NO STRUCTURAL PENETRATIONS

VOLUMETRIC EFFICIENCY  
LOW WEIGHT  
MINIMUM OPERATIONS RISK  
AND COST

#### AIRBREATHING ENGINES

FORWARD  
DEPLOYABLE

BALANCE  
ENVIRONMENT  
INLET PERFORMANCE

Figure 4-18 Booster Design and Packaging Considerations

Some other packaging arrangements considered are shown in Figure 4-19. Common bulkheads were eliminated to assure a reliable structure compatible with low-cost fabrication and with easy accessibility for inspection and repair. Floating tanks were eliminated in favor of integral load-carrying tanks. This is feasible for the booster since it does not have large cutouts such as the orbiter requires for the cargo bay. The aft location of the liquid oxidizer tank was eliminated because that position resulted in an unfavorable aft location of the center of gravity.

Structural design conditions are portrayed in Figure 4-20. The forward portion of the fuselage is designed by the condition of 3 g's at booster burnout. The cylindrical portion of the oxidizer tank and the interstage structure is designed by the max  $q\alpha$  condition. The cylindrical portion of the liquid hydrogen tank is primarily designed by the 3-g condition at booster burnout, but at an aft station the maximum ground-wind condition dominates. The lower portion of the aft fuselage is designed by thrust plus max  $q\alpha$ . The corresponding load intensities (plus for tension and minus for compression) are shown in the lower diagram of Figure 4-20. Peak values in both tension and compression are approximately 900 kilograms per centimeter.

To avoid penetration of the main propellant tanks, four major ring structural assemblies are used (Figure 4-21). A ring assembly just forward of the liquid oxygen tank takes out structural loads associated with the nose landing gear, with operation of the attitude control propulsion system thrusters, and with deployment and operation of the air-breathing cruise engines. The second major structural assembly is in the intertank region, where, at the top of the fuselage, the loads associated with the forward orbiter attachment are taken out. The main structural ring assembly is located at approximately the middle of the liquid hydrogen tank. At this station the structural loads associated with the wing, main landing gear, and with the aft attachment of the orbiter are taken out. The rear barrel assembly aft of the liquid hydrogen tank takes out structural loads associated with the vee tail and the axial thrust of the main rocket engines.

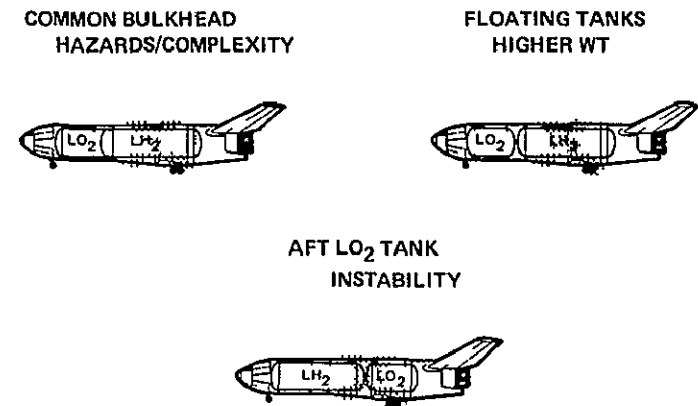


Figure 4-19 Alternate Design Approaches

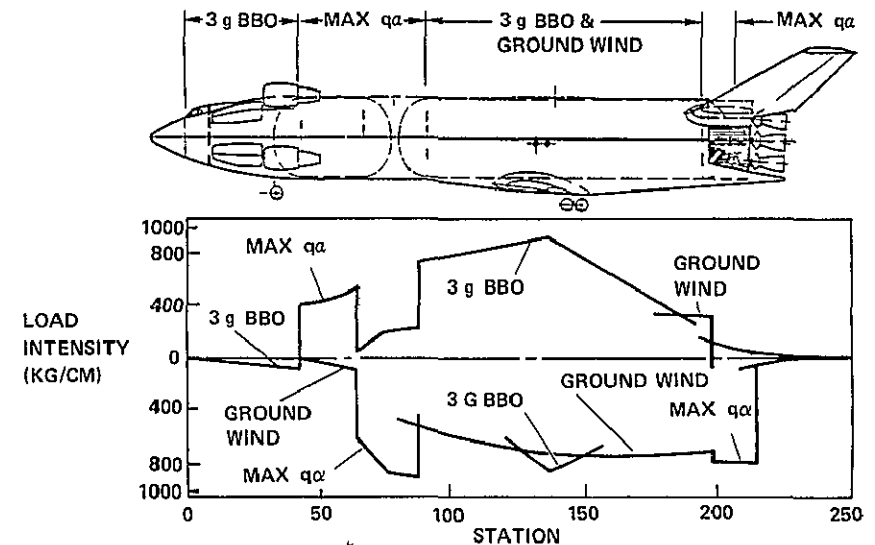


Figure 4-20 Booster Design Conditions and Load Intensities

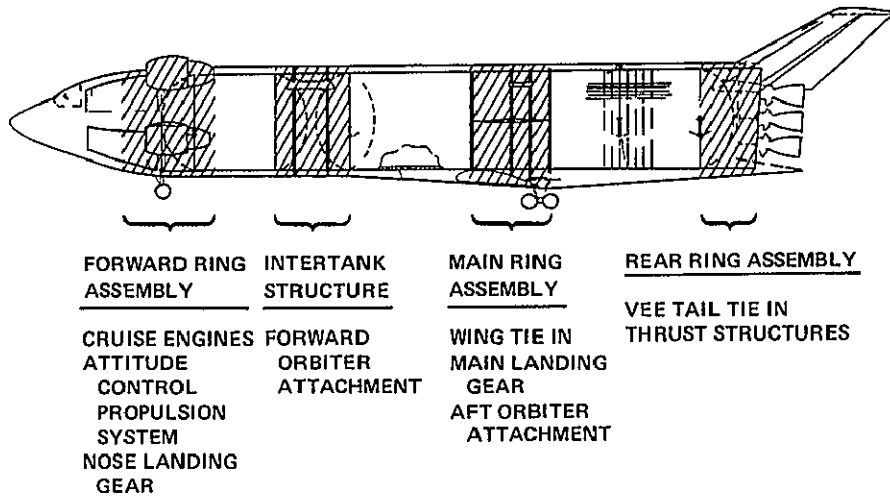


Figure 4 21 Booster Structural Features

The cold load-carrying structure is protected from the boost and entry heating environment by a thermal protection system. In addition, certain of the structural elements are of the hot structure variety. Selection of the external material is dependent on the thermal environment experienced during the boost and entry phase. This is determined by detailed thermodynamic analysis and will be confirmed by wind tunnel tests.

Figure 4-22 presents a comparison of the booster entry trajectory with the flight corridor that has been experimentally explored during flights of the X-15 research aircraft. Maximum heating during booster entry occurs just to the right of where the booster entry trajectory penetrates the right boundary of the corridor explored by the X-15. However, it is close enough so that good extrapolation of X-15 flight test data is possible, and this extrapolation of experimental data correlates well with theoretical analysis. Figure 4-23 shows the calculated variation of the temperature of a thermal protection system panel located under the liquid oxygen propellant tank 12.2 meters from the nose of the booster. The temperature of the aluminum liquid oxygen tank is also shown as a function of time.

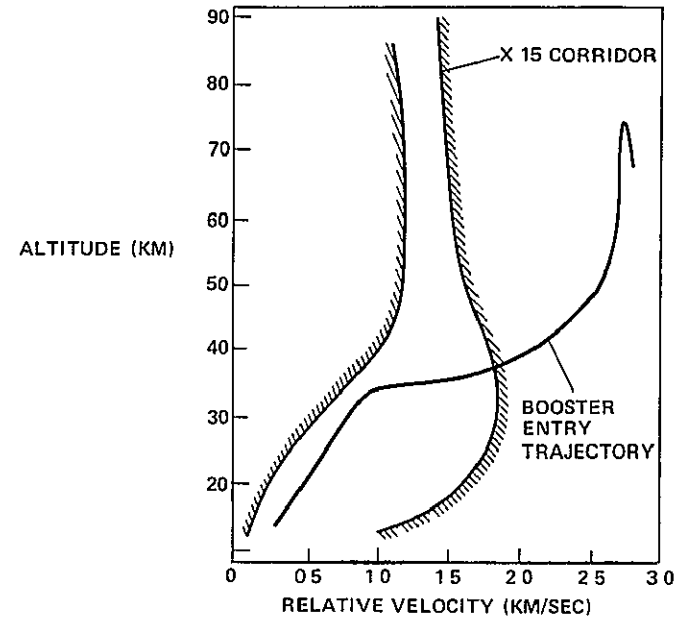


Figure 4 22 Entry Corridor Comparison

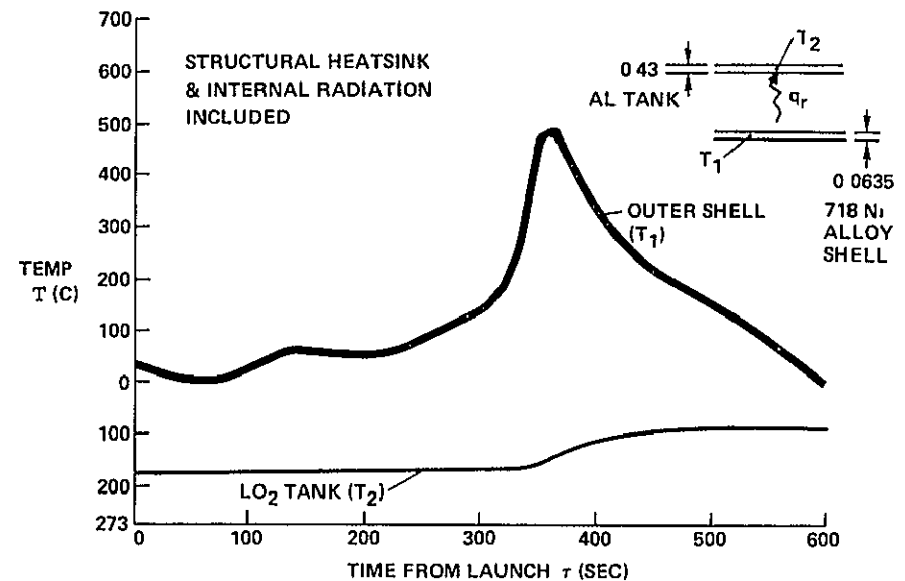


Figure 4 23 Booster Temperature, Oxygen Tank Area Lower Surface 12.2 Meters From Nose

The outer shell experiences a peak temperature of approximately 500°C, and this peak temperature is reached at approximately six minutes after launch, during the entry phase. The outer shell is separated from the aluminum liquid oxygen propellant tank by a space purged with dry nitrogen. Thus, the aluminum LO<sub>2</sub> tank is protected from convection heating, and its modest temperature increase (Figure 4-23) is that resulting from radiation from the inside surface of the thermal protection system panel.

Similar data are presented in Figure 4-24 at a point on the lower surface on the booster 27.4 meters from the nose in the liquid hydrogen propellant tank region. The outer shell temperatures are quite similar to the previous case. The temperature of the aluminum liquid hydrogen tank is somewhat higher than that of the aluminum liquid oxygen propellant tank (Figure 4-22) since the hydrogen tank, unlike the LO<sub>2</sub> tank, has internal insulation and is thus not subjected to the internal cryogenic temperature of the liquid hydrogen.

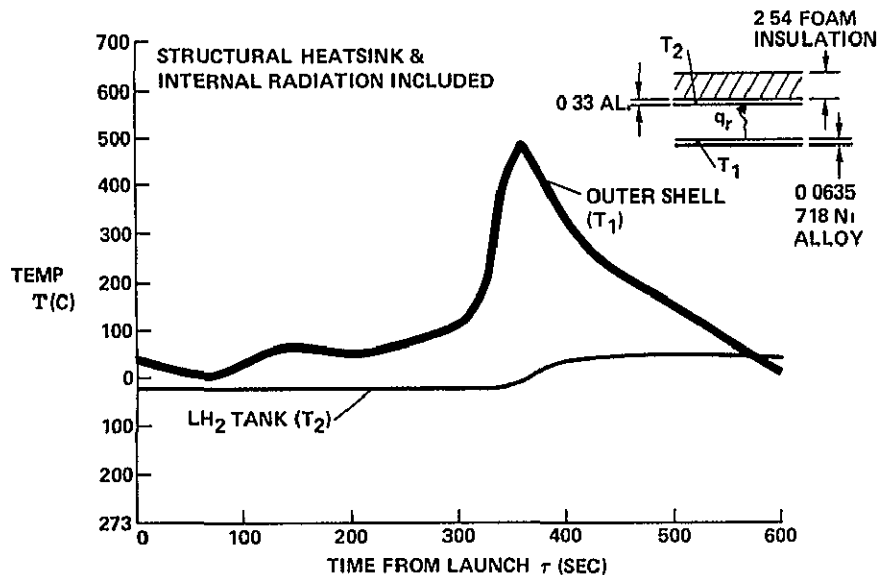


Figure 4-24 Booster Temperature, Hydrogen Tank Area Lower Surface 27.4 Meters From Nose

The maximum temperatures experienced during either the boost or the entry phase and selected materials for the thermal protection system and hot structure are summarized in Figure 4-25. The upper surface of the fuselage has moderate temperatures of less than 300°C. Thus titanium 6Al-4V, which has an excellent strength-to-weight ratio, can be used. Major portions of the underside of the fuselage are subjected to temperatures in the range of 400 to 700°C. For these areas Inconel 718 has been chosen. The lower surface of the stabilizer, which is subjected to high heating rates during entry, experiences temperatures up to 850°C, and in this region René 41 has been selected. The leading edge of the wing in the inboard region and in certain other small areas of shock impingement heating will experience temperatures as high as 1300°C. For these relatively small areas, coated columbium has been selected. The temperature distribution shown and choice of materials will probably change slightly as more definitive experimental data are obtained in wind tunnel tests and more definitive material characteristics are obtained from material and structural tests.

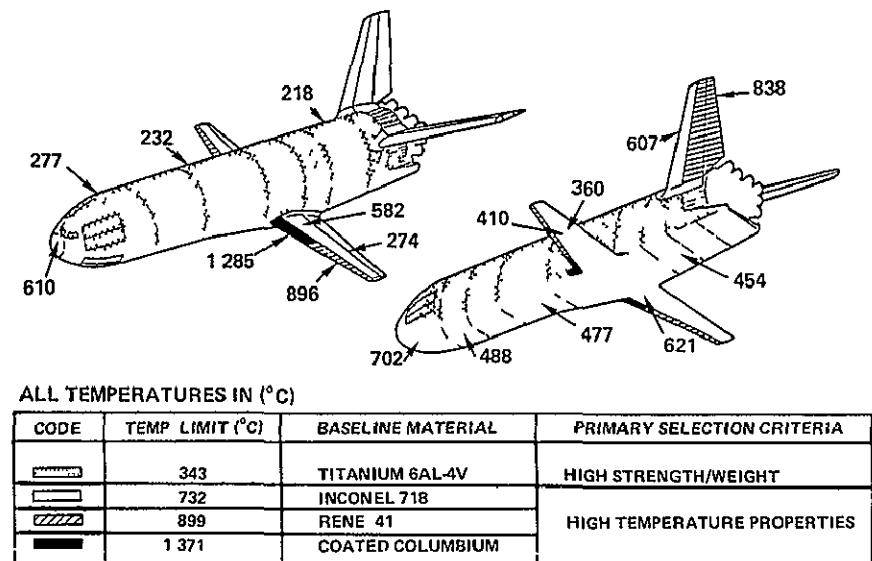


Figure 4-25 Booster Maximum Temperatures and Materials Distribution

The variation of acoustic levels at liftoff versus distance from the rocket nozzle exit plane is presented in Figure 4-26. Overall sound pressure levels of approximately 175 db are experienced near the nozzle exit plane. As a consequence, careful attention to fatigue associated with repeated exposure to such acoustic levels must be a prime consideration in design of the vee tail and selection of structural materials.

### BOOSTER PROPULSION SYSTEMS

Three propulsion systems provide thrust for the booster during its flight (Figure 4-27). Twelve liquid oxygen and liquid hydrogen propellant rocket engines developing 2,170,000 kilograms of total thrust at launch accelerate the booster and orbiter to staging conditions. When the acceleration reaches a level of 3 g's, the rocket engine thrust is throttled to maintain acceleration at 3 g's. After separation, the booster is pitched to an angle of attack of 55 degrees and banked 40 degrees to reduce its down-range flight. Thrust from the attitude control system provides reactant torque for these

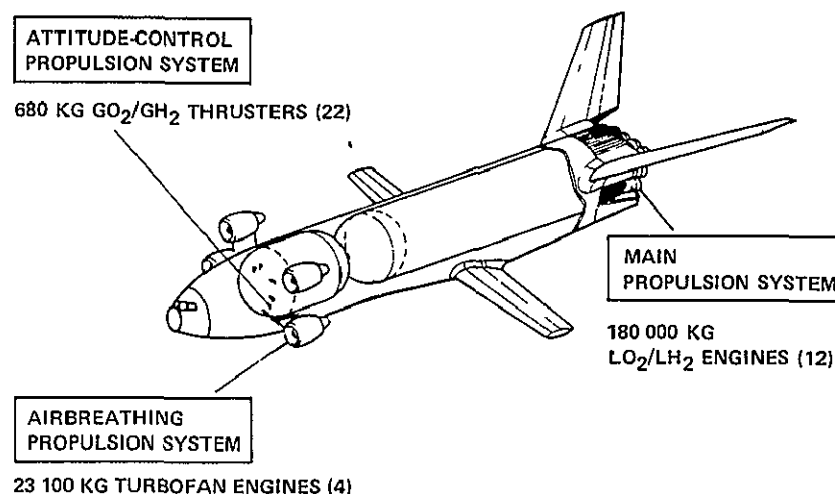


Figure 4-27 Booster Propulsion Systems

maneuvers and vehicle stabilization during entry until aerodynamic surfaces are effective. Four air-breathing engines are deployed when the booster is subsonic, and these provide thrust for the cruise return flight of approximately 350 nautical miles to the launch site. The engines are also used for ferry flights of the booster from one location to another. Each system will now be discussed in more detail.

### Main Propulsion System

The main propulsion system (Figure 4-28) is the primary propulsion system of the booster. The other two propulsion systems provide for the safe recovery of the booster after it has accelerated the orbiter to staging conditions.

The propellant tanks for the main propulsion system serve as the primary structural member of the booster body. The oxygen tank is located forward of the hydrogen tank to provide balance (center-of-gravity location) for vehicle stability in case of loss of rocket power.

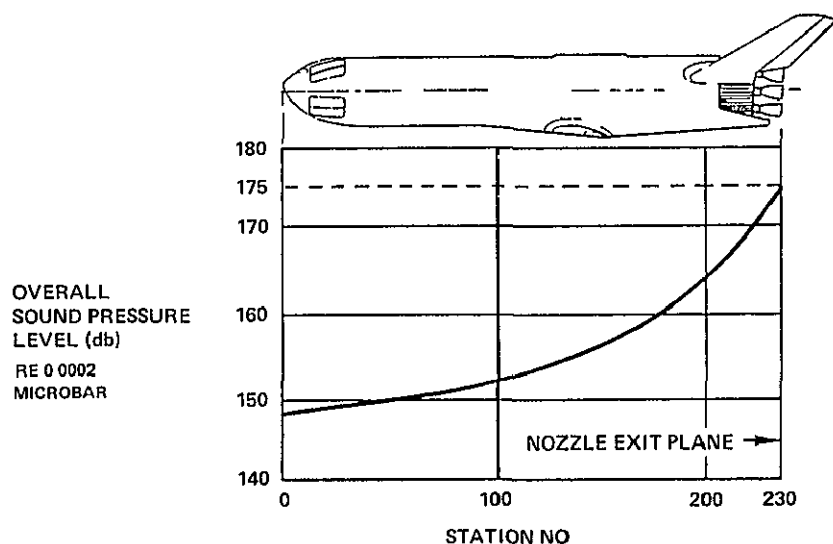


Figure 4-26 Acoustic Levels at Liftoff

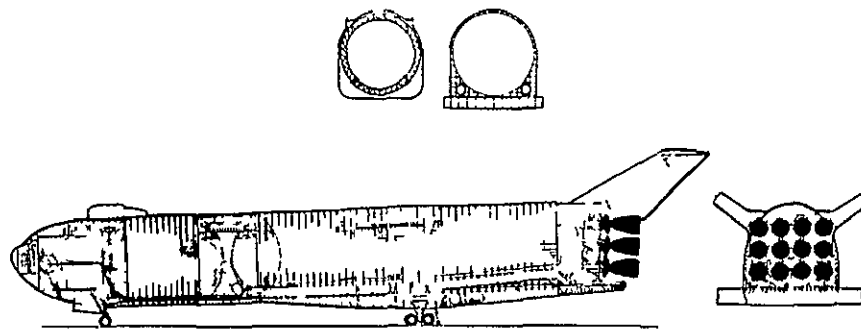


Figure 4-28 Main Propulsion System

The main propulsion system includes 12 high-performance  $\text{LO}_2/\text{LH}_2$  engines. The capability to complete the mission even after loss of one engine is required to meet the system reliability criteria. This capability is provided by operating the remaining engines at 9 percent overthrust. Even with two engine failures, the primary mission can be accomplished by operating the remaining engines at 15 percent overthrust.

Design features of the propulsion system (Figure 4-29) have been selected to minimize maintenance and servicing requirements, while obtaining high reliability and safety. This is achieved by the elimination of nonessential components and subsystems, or by redundancy. Use of flex joints or bellows, which may be subject to fatigue failures, is minimized. Where required, tension-carrying flex joints with external double-wall multiple bellows are used.  $\text{LH}_2$  ducts are vacuum-jacketed throughout. An active propellant utilization system is not used, since repeated flight experience with each operational booster will allow elimination of significant systematic residual errors, and sensitivity of payload capabilities to remaining errors is slight. Tank pressurization is obtained by gasified propellants supplied from the engine (278 K,  $\text{H}_2$ , and 444 K,  $\text{O}_2$ ). This reduces maintenance through elimination of a separate helium pressurization system.

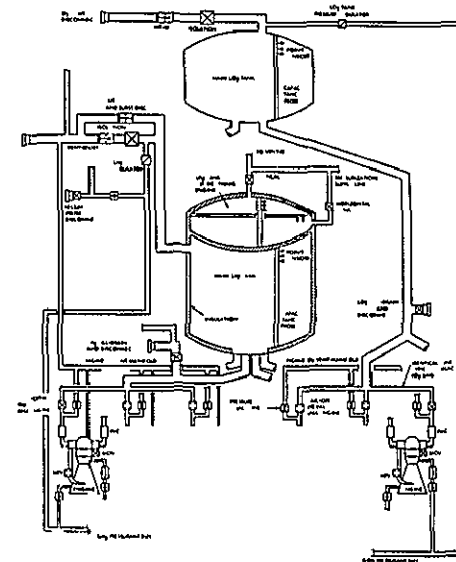


Figure 4-29 Booster Main Propulsion System

$\text{LO}_2$  is supplied to the engine through two manifolds, each branching to feed six engines. The  $\text{LH}_2$  is supplied to the engine through four manifolds, each branching to feed three engines. Branch points are located to provide equal-length flow paths to each engine, minimizing residuals and giving equal pressure losses and transients at each engine. Thermally driven natural circulation, obtained by connecting the liquid oxygen manifolds at the engine interface with recirculation ducts, eliminates geysering and preconditions the engine feed ducts. This form of recirculation requires no active subsystems and has been proved on the Saturn 1C, Atlas, and Titan I.

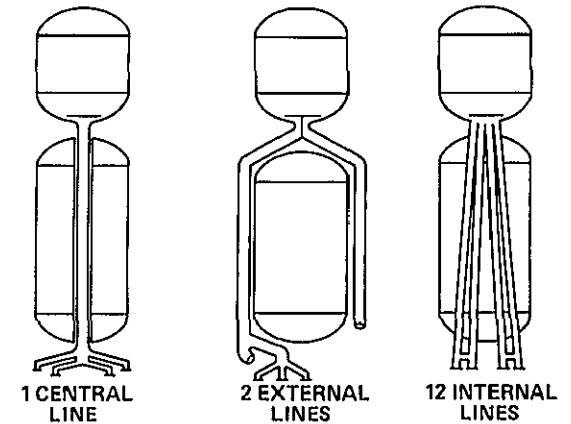
As shown in Figure 4-30, the number of main rocket engines on the booster optimizes at 12 for the 180,000-kilogram-thrust engines. This relates to a thrust-to-weight ratio of 1.37 at liftoff for the booster. As the number of engines is increased or decreased by one, there is a corresponding reduction of payload capability of 7 and 11 percent, respectively.

NO OF BOOSTER ENGINES	11	12	13
PARAMETER			
RELATIVE PAYLOAD CAPABILITY	89%	100%	93%
OVERTHRUST REQUIRED WITH 1 ENGINE OUT	10%	9%	8%
OVERTHRUST REQUIRED WITH 2 ENGINES OUT	17%	15%	13%

Figure 4 30 Number of Booster Engines

Reliability and cost analyses have shown that it is most cost effective to continue the flight if one engine becomes inoperative. To provide this capability, the remaining engines overthrust to compensate for lost thrust resulting from one engine out. This engine capability is provided at the engine nominal mixture ratio with little or no reduction in engine life. If two engines fail, the mission can be completed by overthrusting the ten operating engines by 15 percent. Operation at 15-percent overthrust will probably result in a modest reduction in engine life, but such operation would only occur in the rare case in which two engines fail.

Several liquid oxygen feed duct options were investigated to select the baseline configuration of two external lines (Figure 4-31). Their geometry is important to the booster propulsion system since they contain 67,000 kilograms of liquid oxygen (8 percent of the total) and reach an internal pressure of 17 kilograms per square centimeter during flight as a result of acceleration effects.



HARDWARE WEIGHT	HEAVY	LIGHTEST	HEAVY
RESIDUALS	HIGH	LEAST	HIGH
REFURBISHMENT OR REPAIR	DIFFICULT	EASIEST	DIFFICULT
PROPELLANT CONDITIONING	DIFFICULT	CIRCULATION	EASY
THRUST SECTION COMPLEXITY	COMPLEX LINE ROUTING	COMPLEX LINE ROUTING	SIMPLEST
DEVELOPMENT CONFIDENCE	LOWEST	HIGHEST	LOW

Figure 4 31 LO<sub>2</sub> Feed Duct Geometry Options

Weight favors the external duct configuration, as only a single wall duct is required versus a dual wall duct for an internal line to insulate the oxygen from the hydrogen. Additionally, with the external ducts, both propellant tanks are shorter, and oxygen volume in the ducts is greater. Also, there is no corresponding reduction in available hydrogen tank volume.

Residuals occur as a result of unequal usage in the event of an engine out or different flowrates. The least effect will be felt with the arrangement having the shortest line length from the branch point, i.e., the dual external line.

If leaks occur with the internal duct configuration, the duct must be removed from the tunnel for repair. For external ducts, leak potential is halved, since there are no tunnels, and liquid oxygen duct leaks may be repaired in place without duct removal.

The use of dual external lines also provides a natural recirculation to prevent geysering and to maintain subcooled LO<sub>2</sub> at the thrust section for unlimited hold durations. With internal lines, heat transfer to the LH<sub>2</sub> may suppress recirculation to an unsteady flow condition that may not be predictable. A subsystem such as helium injection would therefore be needed to force circulation.

### Booster Attitude Control Propulsion System

The booster attitude control propulsion system provides pitch, yaw, and roll control during the phase of booster flight between booster and orbiter separation and transition to aerodynamic controls at approximately six minutes after separation. During this phase, when aerodynamic controls are ineffective, the system provides the required control torques to correct separation disturbances, maneuver the vehicle to the desired pitch and bank attitude for atmospheric entry and turn to the flyback heading, and maintain desired vehicle attitude during the entry phase.

The booster system uses high-chamber-pressure, 21 kg/cm<sup>2</sup>, engines operating with gaseous hydrogen and oxygen propellants supplied through vaporization of stored liquids in a gas generator and heat exchanger conditioning loop. The baseline system (Figure 4-32) is a low development risk system. It can be developed and proved independently of the booster vehicle and can use minimum technology risk components.

The system is configured to provide operational capability after component failure with no reduction in performance. Even after three component failures, safe capability is provided, although with reduced performance. Components are sized to accommodate the maximum system impulse over the range of missions assigned.

As illustrated, engines and system components are located forward of the main LO<sub>2</sub> tank to maximize engine moment arms, minimize system weight and complexity, and aid vehicle balance considerations.

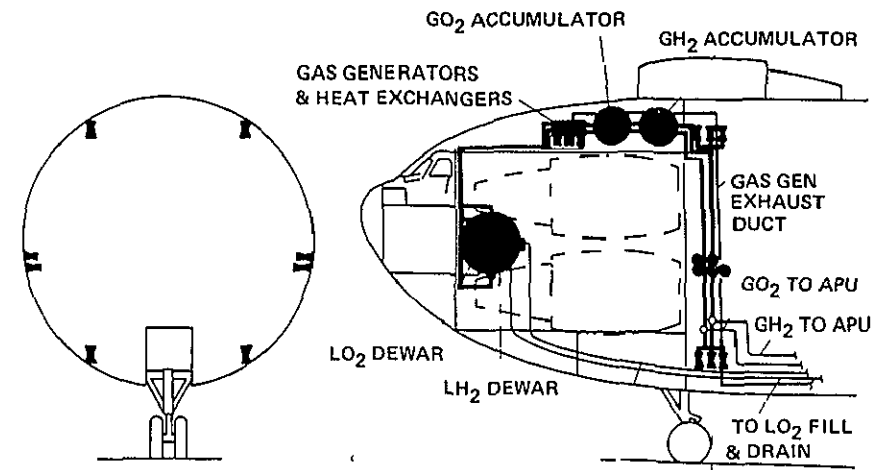


Figure 4-32 Attitude Control Propulsion System

Twenty-two engines, at 680 kilograms of thrust each, supply 0.5-degree per second squared of rotational acceleration rates and minimum cross coupling with one engine in any axis inoperative. Engines are located to avoid penetration of the vehicle thermal protection system in areas of maximum entry heating. As propellants are used by the thrusters and by the gas generators, decay of accumulator pressure is sensed and makeup liquid propellants are supplied to the heat exchanger for thermal conditioning and accumulator charge. The proper feed temperature to the attitude control engines is obtained by modulating the gas generator flowrate to maintain constant propellant discharge temperature from the heat exchanger.

Propellant feed for the vehicle auxiliary power units is tapped off downstream of the accumulators. Operation of the propellant supply and conditioning loop for auxiliary power supply begins at launch minus five minutes and continues until termination of operation shortly after booster landing.

The hot-gas generator exhaust gases are ducted to the base of the vehicle, where they are vented during in-flight operation. During



operation prior to launch, the exhaust products are ducted away from the vehicle through a disposal system connected to the in-flight vent port

For maximum commonality and minimum development cost, attitude control engines, propellant conditioning loop components, and system valving and regulators will be common between booster and orbiter, where possible

A chamber pressure of 21 kilograms per square centimeter and a nozzle expansion ratio of 20:1 were selected to limit engine size and exit plane area and minimize system weight. An insulation jacket around the engine nozzle and combustion chamber allows buried installation in the booster. Dump-cooled extensions to the basic thrust chamber provide for engine installation, with the exit plane flush with the vehicle skin surface and resulting exit plane scarfing angles of approximately 32 degrees for the pitch and roll engines. The engine uses a dual spark ignition system. Engine design accommodates both steady-state and pulse-mode firing operation. The requirement for extended operating life and cyclic capability is a major challenge for design of the attitude control engines. The basic characteristics of the engine are summarized in Figure 4-33

of one engine, three engines will provide thrust for cruise at Mach 0.35, at maximum continuous thrust setting. With two engines failed, the vehicle will cruise at maximum continuous thrust at Mach 0.28 with the two remaining engines operating. LH<sub>2</sub> is used for booster cruise. Its greater energy per pound, relative to JP-type fuel, results in an increase of 9,000 pounds in payload to orbit.

### Air-Breathing Propulsion System

Cruise, go-around, and ferry propulsion are provided in the baseline configuration by four hydrogen-fueled General Electric CF6-50C high-bypass-ratio (BPR) turbofans (Figure 4-34). These engines, committed to production for the DC-10 Series 30 transport, have the highest thrust rating and the best thrust-to-weight ratio (T/W) of any programmed high BPR turbofans in the 18,000- to 23,000-kilogram-thrust class. The superior cruise specific fuel consumption results in the lowest system weight. Other candidate engines, however, are being considered.

The four-engine installation permits safe cruise flight after entry even if two of the engines fail to deploy or operate. With the failure

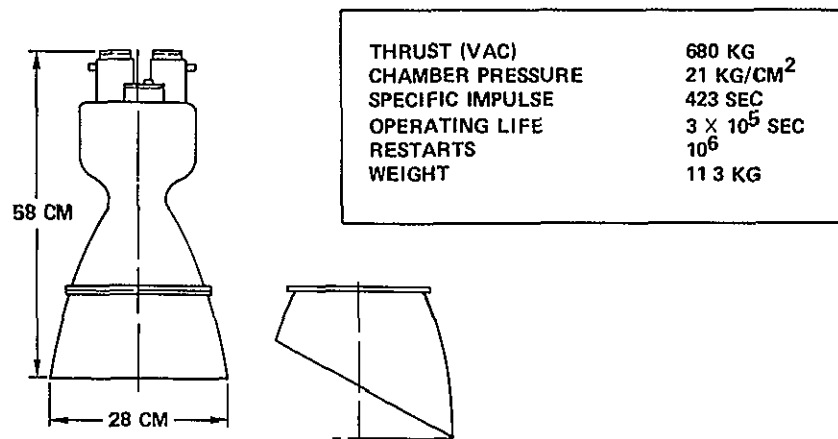


Figure 4-33 Attitude Control Propulsion System Engine Characteristics Summary

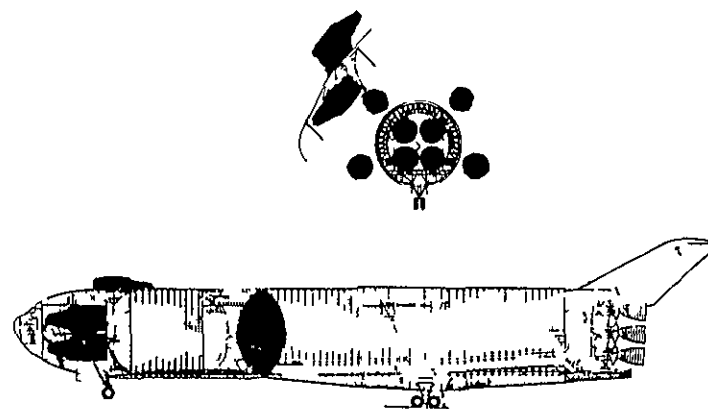


Figure 4-34 Air Breathing Propulsion System

The podded turbofans are stowed in an unpressurized compartment forward of the main liquid oxygen tank. After entry, they are deployed hydraulically about individual pivots. Short concentric inlets and concentric noncoplanar exhaust nozzles provide optimum cruise performance. The DC-10 wing-mounted pods are similarly arranged. The pod and pylon concept places the engines in a desirable flow field for operation. It also enhances ground turn-around, service, and maintenance. Double-breech cartridge starters are used for maximum air-start reliability.

The LH<sub>2</sub> fuel is contained in a separate cruise fuel tank, formed by an added bulkhead in the forward portion of the main LH<sub>2</sub> tank. Submerged boost pumps supply liquid to the engine. After the startup, gaseous hydrogen, bled from the heat exchangers at the engines, is used for tank pressurization.

An existing air-breathing engine is preferred over a new development to save \$200 to \$500 million in nonrecurring costs and 12 to 20 months in development time, at a relatively small engine and fuel weight penalty (Figure 4-35). Not only are the development costs an order of magnitude higher for a new engine, but the maintenance costs would be appreciable because of engine use on the shuttle alone, and not on any airlines.

	EXISTING	NEW
NON RECURRING COST THRU QUALIFICATION	~\$30M	\$200-500M
GO AHEAD THRU QUALIFICATION	36 MONTHS	48-56 MONTHS
AVAILABLE FOR FIRST HORIZONTAL FLIGHT TEST	YES	DOUBTFUL
CYCLE OPTIMIZATION	GOOD	BETTER
COMMONALITY WITH ORBITER	UNLIKELY	UNLIKELY

Figure 4-35 Existing Versus New Air Breathing Engines

Four engines available from three different companies are prime candidates for the booster turbofans. The ensuing competition will help to reduce engine development and procurement costs. These engine options are shown in Figure 4-36.

The GE CF6-50C turbofan was selected for the baseline booster because it is lighter and has a higher thrust level than competing engines committed to production. The higher-thrust engines permit the booster to lose two engines and still return to the launch site.

## OTHER SUBSYSTEMS

### Integrated Avionics Subsystem

A major objective in the definition and design of the integrated avionics subsystem (IAS) is cost savings to be achieved by commonality between the orbiter and booster avionics. The subsystem (discussed in greater detail in the orbiter section) is diagrammed in

MANUFACTURER	GENERAL ELECTRIC		P&W	ROLLS ROYCE
PRODUCTION MODEL	TF39-1	CF6-50C	JT9D-15	RB211-56*
APPLICATION	C-5A	DC-10-30	B747	L-1011
**SLS RATING (KILOGRAMS)	18,617	23,103	20,610	23,718
DRY WEIGHT (KG)	3,187	3,708	3,797	4,590
CRUISE SFC (H <sub>2</sub> ) KG/HR/KG	0.175	0.185	0.180	0.180

\*PRODUCTION CONTINGENT UPON SALE OF STRETCHED L-1011. NOT YET COMMITTED.

\*\*SEA LEVEL STATIC.

Figure 4-36 Candidate High Bypass Ratio Turbofans

Figure 4-37 Because of the orbiter's more sophisticated mission requirements, the integrated avionics design is driven by the orbiter requirements, with hardware and software eliminated for the booster only. Since the requirements for the booster are less stringent than those for the orbiter, some of the hardware and software required for the orbiter IAS can be eliminated in the booster application. In particular, the entire rendezvous and docking avionics subsystem can be eliminated (Figure 4-37).

### Crew Compartment

The crew compartment, designed for a crew of two, is shown in Figure 4-38. The overall compartment configuration, arrangement, seats, flight controls, avionics, and displays are essentially identical to the orbiter. Differences in console exist because of elimination of translation controls.

Displays, readouts, and backup flight instruments are located on the forward panel. Subsystem controls are located on the consoles and overhead panels. Hand controllers for flight control are located on each seat arm rest. The booster can be flown from either seat and by a single crewman. External visibility is comparable to that of commercial aircraft.

Ingress and egress are provided by two overhead hatches and from a hatch that leads to the bottom of the vehicle.

Crew procedures and operations are the same as for the orbiter to minimize training requirements and to provide flexibility in crew selection.

The environmental control life support system (Figure 4-39) provides a shirt-sleeve environment, controls cabin temperature, humidity and pressure, removes CO<sub>2</sub>, and provides cooling for electrical and avionic equipment. The oxygen and nitrogen atmosphere is controlled to 0.7 kilogram per square centimeter absolute with 0.217 kilograms per square centimeter oxygen partial pressure.

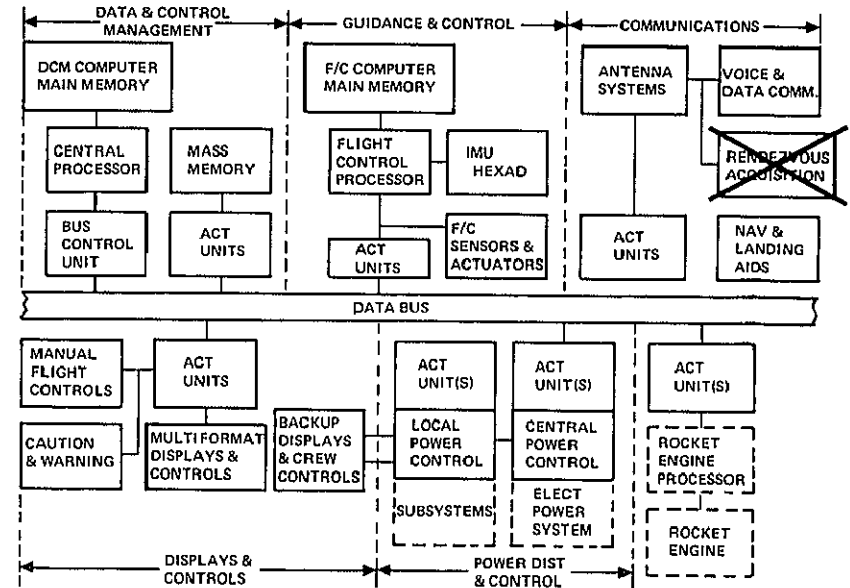


Figure 4-37 IAS Block Diagram

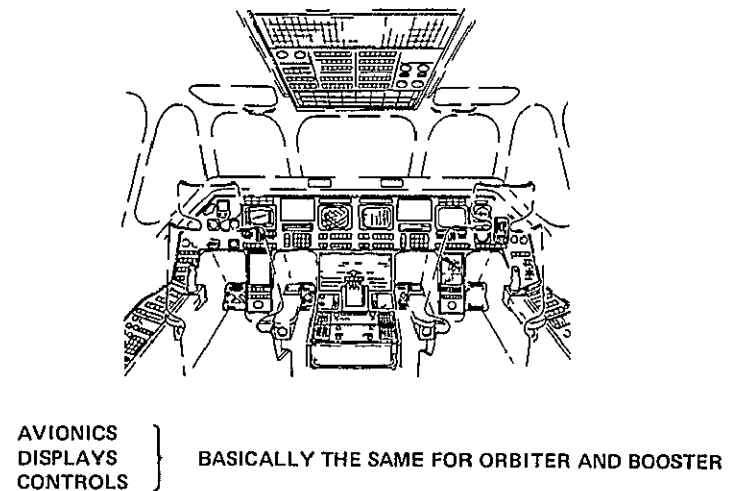


Figure 4-38 Crew Compartment

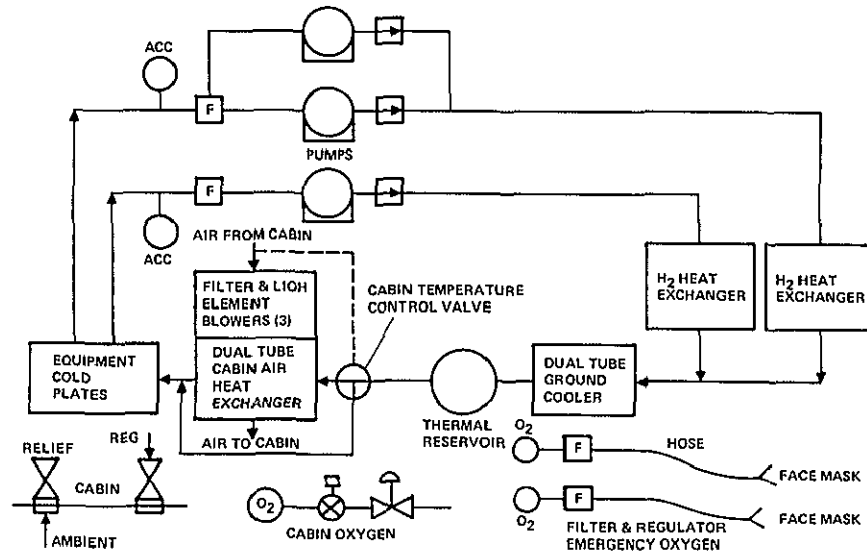


Figure 4-39 Environmental Control and Life Support Baseline

A fluid loop with redundant pumps transports heat from the cabin heat exchanger and equipment cold plates and rejects it to a hydrogen heat exchanger. A small quantity of oxygen is stored for replenishing the atmosphere to maintain the required oxygen partial pressure level and to provide emergency oxygen for use with a face mask. The orbiter system is common to that of the booster except for the requirements that are unique to orbiter operations such as food, water and waste management, the need for a space heat sink, and long-duration operation.

### Power Subsystem

The power subsystem has four identical auxiliary power units (APUs), as shown in Figure 4-40. Each unit drives a hydraulic pump and a generator, provides all power for the electrical and avionics systems, aerodynamic flight controls, cruise engine deployment, and landing gear operation. APU's operate continuously from prelaunch to landing. Gaseous  $O_2/H_2$  reactants were selected because of lower fuel consumption and to provide commonality with the propulsion

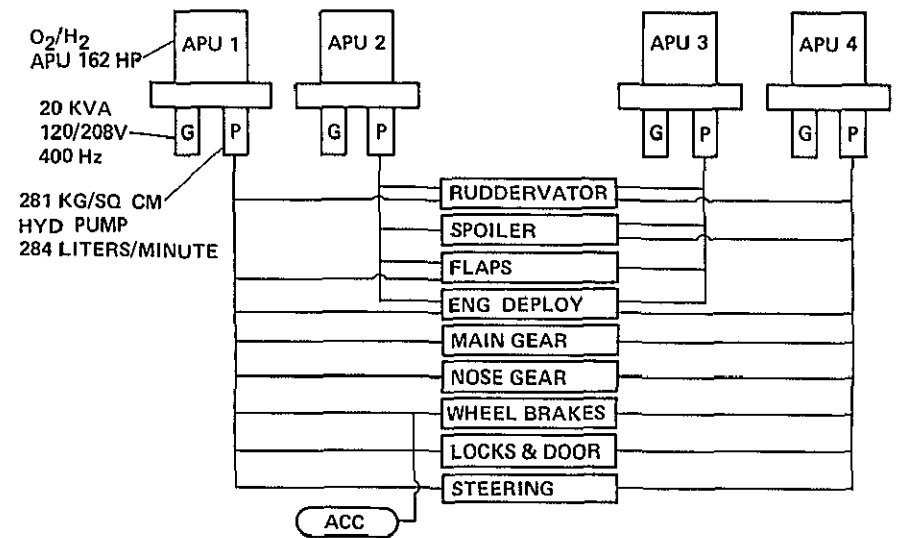


Figure 4-40 Power System Baseline

propellants. The four hydraulic systems are physically separated and functionally isolated from each other to preclude multiple system loss in event of failure. The flight control system is fly-by wire. The redundant servoactuators incorporate automatic fault isolation capability. The redundancy shown provides for safe operation after two failures for the mechanical systems and safe operation after three failures for the electrical system, consistent with the avionics system criteria. The APU, hydraulic pumps, and generators are identical to those used on the orbiter. Conventional state-of-the-art components and design concepts are used in the hydraulic and electrical systems.

### Landing Gear

The landing gear is a tricycle type. Each main gear consists of a conventional air-oil telescoping shock strut, folding side brace, four wheels, brakes, and anti-skid system. The system retracts inboard (Figure 4-41). The outboard door is linked to the strut, and the inboard door is hydraulically actuated. The nose gear (Figure 4-42) consists of a conventional air-oil telescoping shock strut, folding drag



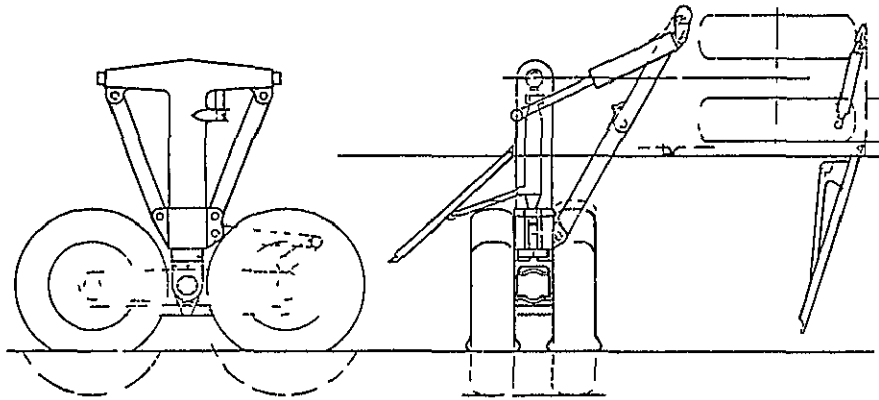


Figure 4 41 Main Landing Gear

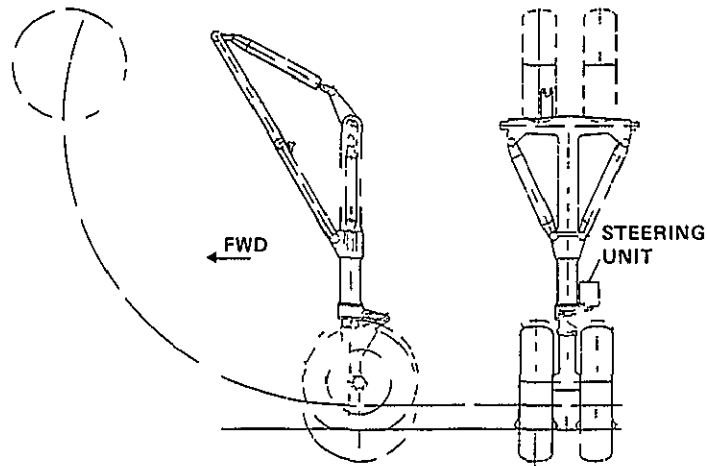


Figure 4 42 Nose Landing Gear

brace, dual wheels, and steering. Doors are mechanically actuated by operation of the gear. The landing system utilizes conventional state-of-the-art equipment and is similar to that used on large commercial and military aircraft. Landing gear characteristics are summarized in Figure 4-43.

AIR OIL TELESCOPING STRUT

MECHANICAL DOWN AND UP LOCKS

TYPE VII TIRES (142 CM X 41 CM)

18.3 KG/CM<sup>2</sup> MAIN GEAR

7.7 KG/CM<sup>2</sup> NOSE GEAR

MAIN GEAR ANTI SKID BRAKE SYSTEM

NOSE GEAR STEERING

Figure 4 43 Landing Gear

## 5. OPERATIONS

Operations from the post-landing operation through flight are discussed in this section. As shown in (Figure 5-1), the time for the total operation from landing to liftoff is 14 days. This includes post-landing operations, maintenance and refurbishment operations, prelaunch operations, and launch operations. The booster flight operation lasts under two hours. The baseline orbiter can stay in orbit approximately seven days before returning to the launch site. Thus, although the booster has an operational cycle of 14 days, the cycle for the orbiter is 21 days.

American Airlines is a key member of the North American Rockwell and Convair team. The airline's extensive experience in operating and maintaining commercial aircraft is being applied in the early phase of shuttle definition and design to assure that low-cost operations can be achieved. American Airlines is preparing detailed time lines and manpower loading tables for shuttle maintenance and refurbishment and for other ground operations. American Airlines personnel are working with members of the North American Rockwell and Convair design teams to assure that appropriate design features are included that will facilitate low-cost operations.

The baseline operations facilities are described in this section, followed by a more detailed discussion of each operational phase.

### BASELINE OPERATIONS SITE

The baseline operations location selected is the Kennedy Spaceflight Center (KSC), Florida. This baseline (Figure 5-2) is simply a point of departure for the many trade studies (with respect to final selection of the operation site) that will be conducted during Phase B. Final selection of the operations site will be made by NASA. The KSC baseline would use existing Saturn and Apollo facilities with minimal modification. A new runway 3050 meters long would be required. The Vertical Assembly Building (VAB) would be modified as shown to provide both the high bay and low

bay required for booster and orbiter maintenance and refurbishment. A safing area would be required to deplete and clean the propellant tanks after landing. This area would be located between the runway and the maintenance building. Either Saturn/Apollo Pad A or B

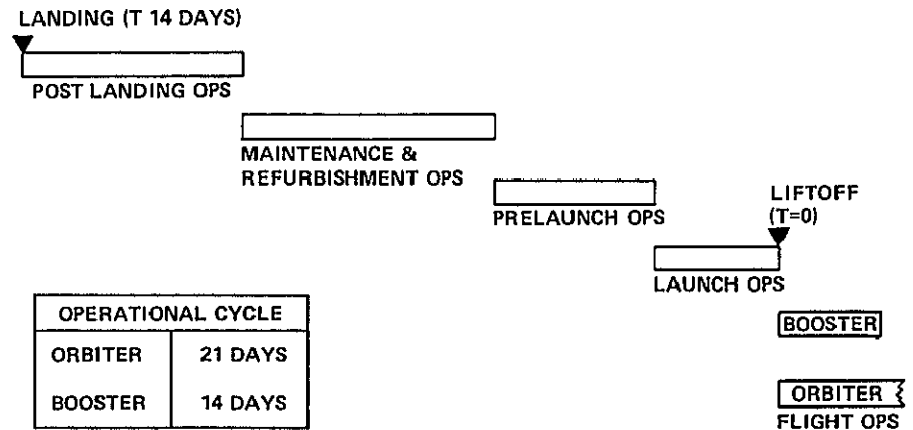


Figure 5-1 Ground and Flight Operations

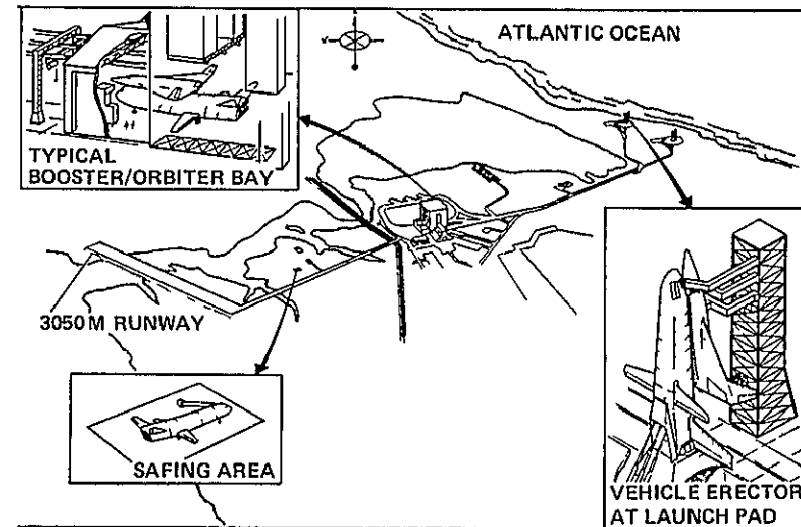


Figure 5-2 Baseline Operations Facilities

would be modified to facilitate erection of the mated booster and orbiter. Fuel and oxidizer would be loaded and checkout completed at the pad. Existing liquid hydrogen flow rate capacity at the pads is not adequate for the shuttle and will therefore require modification.

One of the features of the NR/Convair design is the piggyback arrangement shown (Figure 5-3). This arrangement allows for the orbiter (unfueled) and payload to be installed on the booster and then towed to the pad on the booster landing gear, thereby eliminating the expense and complexity of a crawler-type vehicle. This capability does not create a design load in the booster landing gear since the gear is designed by landing loads.

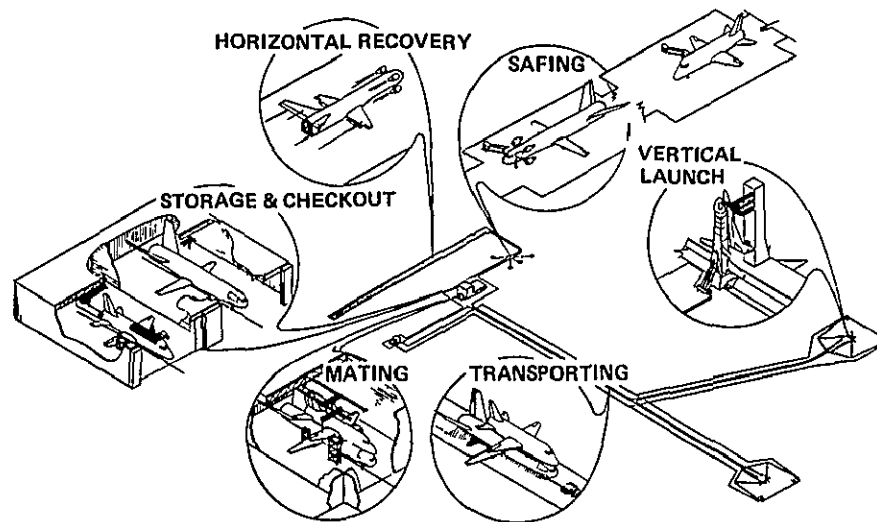


Figure 5-3 Ground Operations

## POST-LANDING OPERATIONS

An artist's concept of the booster landing is shown in (Figure 5-4). (This event is related to the first bar in Figure 5-1.) After the landing, the vehicle will taxi off the strip and will be towed (or taxi) to the safing area (Figure 5-5).

The post-landing operations for the booster take a little less than five hours from touchdown to delivery to the maintenance and refurbishment area. A time line of this activity is shown in Figure 5-6, which indicates that portions of the longest functions of safing, data analysis, and inspection will be done in parallel to permit completion of the operations in less than one work shift.

A similar breakdown for the orbiter is shown in Figure 5-7. This operation takes approximately seven hours, two hours longer than for the booster. The two additional hours are required because of passenger and cargo unloading and because of the increased amount of integrated avionics on board the orbiter as compared to the booster.

## MAINTENANCE AND REFURBISHMENT

Shifting now to the second bar in Figure 5-1, the maintenance and refurbishment cycle begins with the launch preparation shown in Figure 5-8. The booster and orbiter time lines for the maintenance and refurbishment cycle are shown in Figure 5-9. These time lines are based on one shift per day, five days a week. On this basis, fewer than seven working days are required for the maintenance and refurbishment phase.

## PRELAUNCH OPERATIONS

After the maintenance and refurbishment cycle, prelaunch operations (third bar of Figure 5-1) are conducted. The payload is installed in the orbiter, and the orbiter is mated to the booster in the horizontal position. This mated configuration is then towed to the launch site on the landing gear of the booster (Figure 5-10). Being able to transport the mated configuration on the booster's landing gear is one of the features of the piggyback arrangement proposed by NR/Convair for Phase B. It eliminates the need for a crawler. However, vertical mating and alternative methods of transport including the crawler will be analyzed during Phase B. Once the mated configuration reaches the launch site, it is erected into the vertical position (Figure 5-11). It is important to note that the

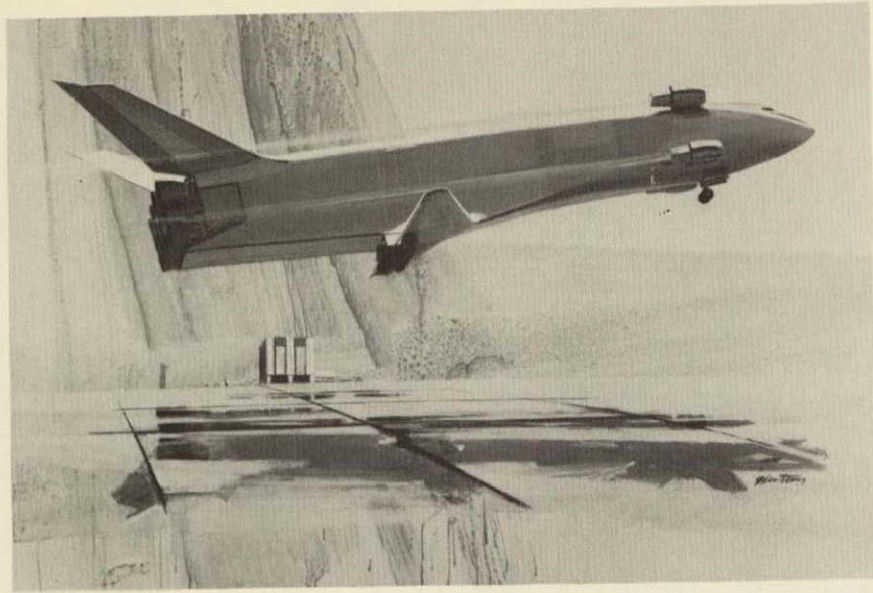


Figure 5-4. Booster Landing

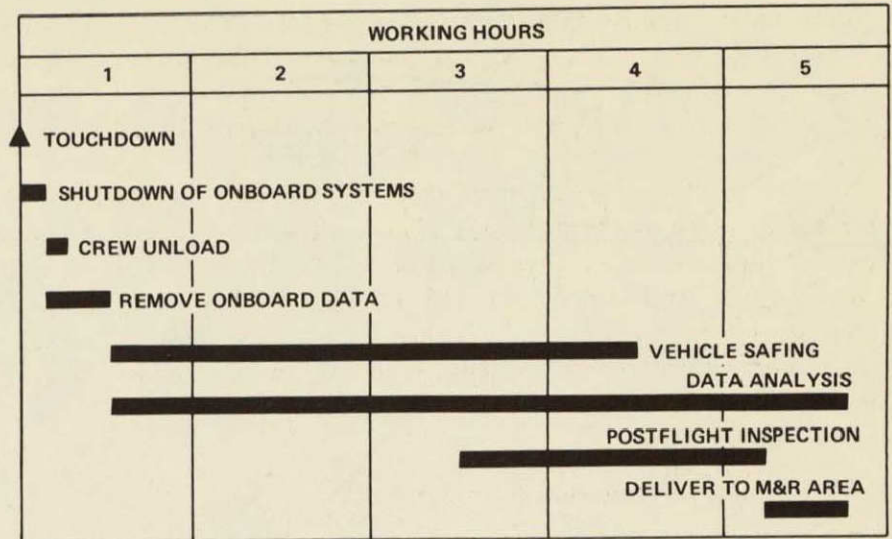


Figure 5-6. Post-Landing Operations Time Line (Booster)

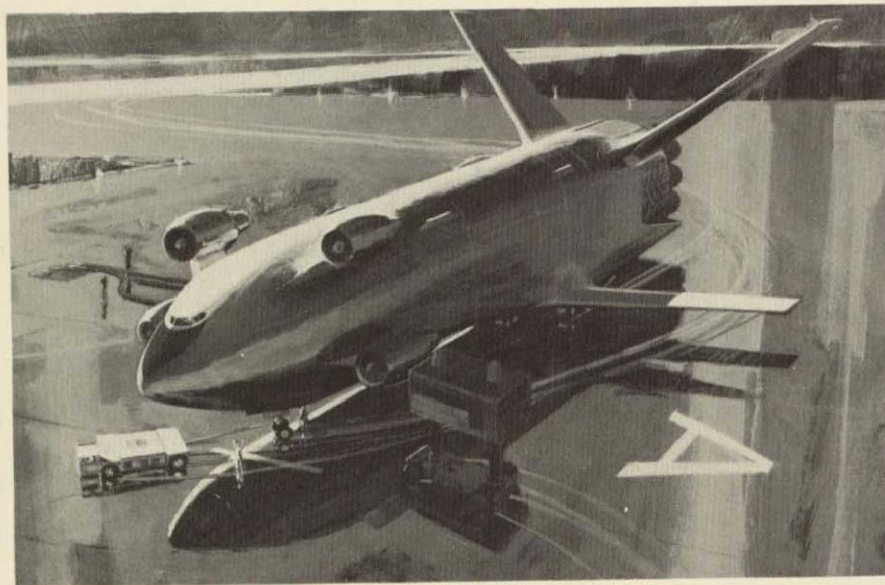


Figure 5-5. Booster in Safing Area

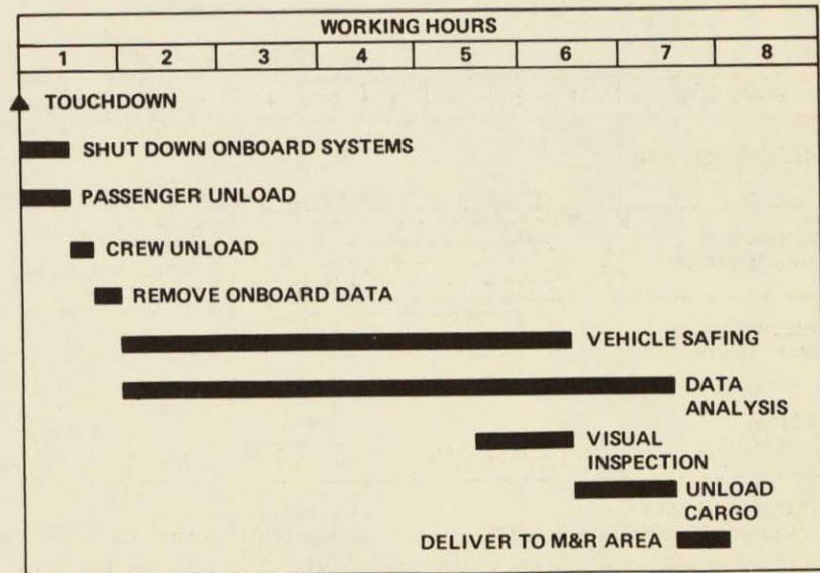


Figure 5-7. Post-Landing Operations Time Line (Orbiter)



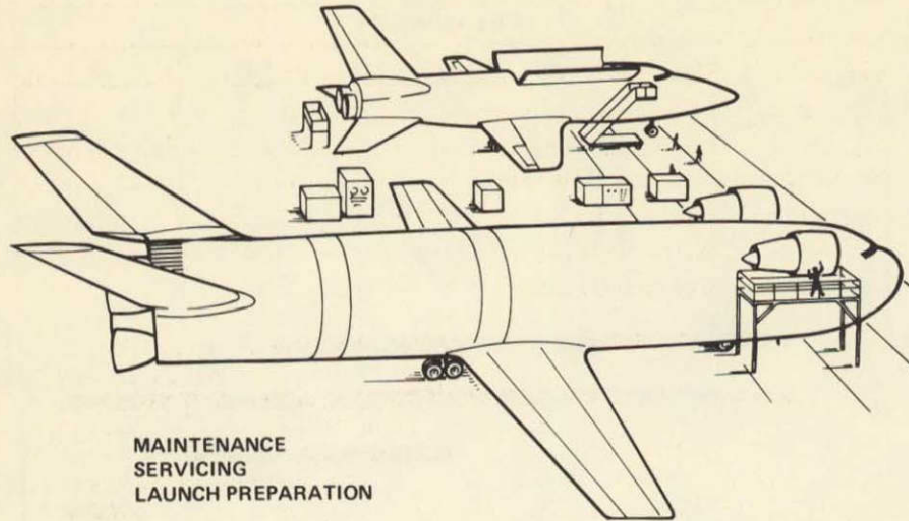


Figure 5-8. Launch Preparation

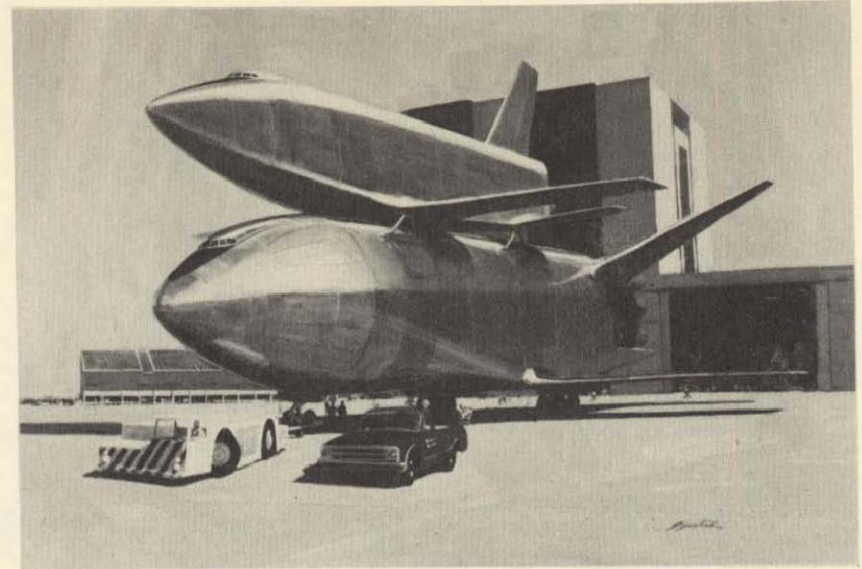


Figure 5-10. Towing Shuttle to Launch Site

FUNCTION	WORKING DAYS									
	1	2	3	4	5	6	7	8	9	10
PREPARE FOR M&R	<div style="display: flex; align-items: center;"> <div style="width: 100px; height: 10px; border: 1px solid black; margin-right: 5px;"></div> <div style="width: 100px; height: 10px; border: 1px dashed black; margin-right: 5px;"></div> </div>									
SCHEDULED MAINTENANCE	<div style="display: flex; align-items: center;"> <div style="width: 100px; height: 10px; border: 1px solid black; margin-right: 5px;"></div> <div style="width: 100px; height: 10px; border: 1px dashed black; margin-right: 5px;"></div> <div style="margin-left: 20px;"> <p>NOTE</p> <div style="display: flex; align-items: center;"> <div style="width: 20px; height: 10px; border: 1px solid black; margin-right: 5px;"></div> ORBITER                     <div style="width: 20px; height: 10px; border: 1px dashed black; margin-left: 10px; margin-right: 5px;"></div> BOOSTER                 </div> </div> </div>									
UNSCHEDULED MAINTENANCE	<div style="display: flex; align-items: center;"> <div style="width: 100px; height: 10px; border: 1px solid black; margin-right: 5px;"></div> <div style="width: 100px; height: 10px; border: 1px dashed black; margin-right: 5px;"></div> </div>									
SYSTEM CHECKOUT	<div style="display: flex; align-items: center;"> <div style="width: 100px; height: 10px; border: 1px solid black; margin-right: 5px;"></div> <div style="width: 100px; height: 10px; border: 1px dashed black; margin-right: 5px;"></div> </div>									
SECURE FOR ASSY & PRELAUNCH OPS	<div style="display: flex; align-items: center;"> <div style="width: 100px; height: 10px; border: 1px solid black; margin-right: 5px;"></div> <div style="width: 100px; height: 10px; border: 1px dashed black; margin-right: 5px;"></div> </div>									

Figure 5-9. Maintenance and Refurbishment Time Line

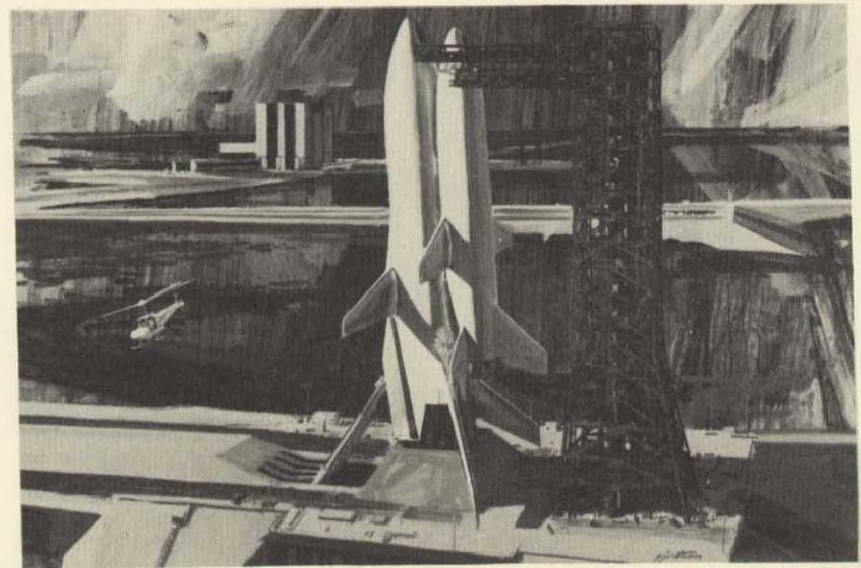


Figure 5-11. Space Shuttle in Vertical Launch Position

payload is accessible through all phases of this operation. Again the baseline configuration shown is for the KSC, but the structure shown would be that required for any launch site.

The prelaunch operations time line is shown in Figure 5-12. These operations require 18 working hours and can thus be accomplished in less than 3 eight-hour shifts.

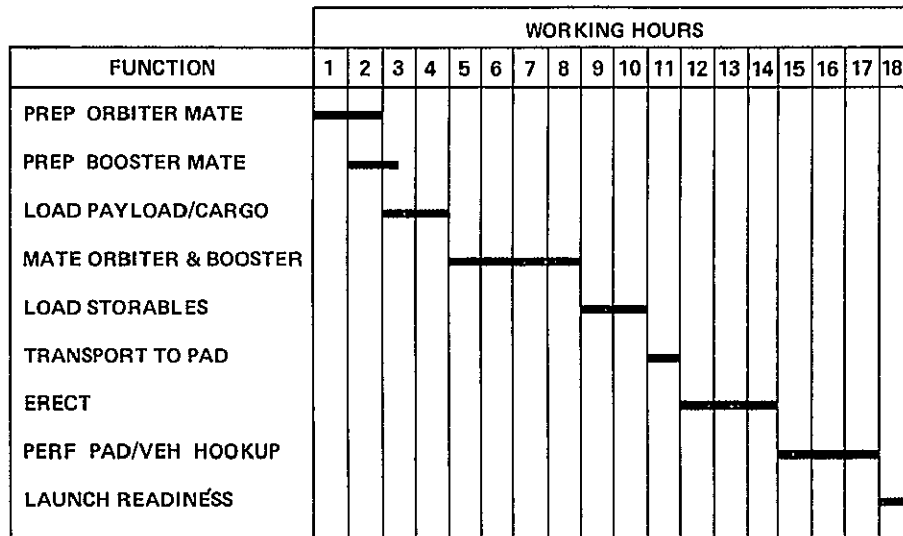


Figure 5-12 Prelaunch Operations Time Line

## LAUNCH OPERATIONS

The fourth bar on Figure 5-1 is launch operations, and the corresponding time line is shown in Figure 5-13. The total time for the final countdown is two hours. The two-hour countdown capability provides fast response for missions such as space rescue. A little more than one hour of this time is taken up by propellant loading, with approximately one-half hour required for launch checkout.

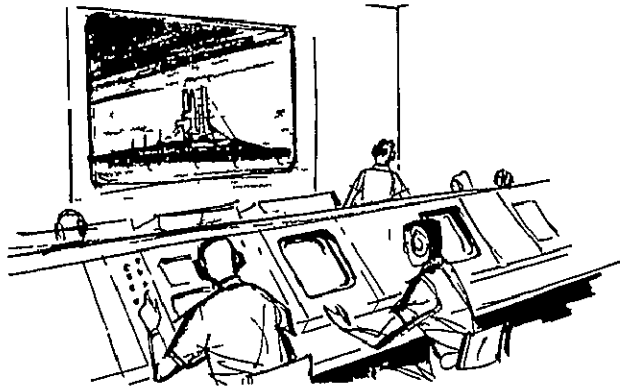
Since it is one of the critical factors in the two-hour countdown, the propellant loading operation is further expanded in Figure 5-14. The simultaneous flow of both liquid oxygen and liquid hydrogen from ground storage facilities to the vehicle must be a design consideration for vehicle propulsion system plumbing, and for propellant loading system design and operation procedures. Launch operations are then followed by flight operations for both the booster and orbiter, as depicted by the last two bars of Figure 5-1.

## FLIGHT OPERATIONS

After liftoff, the booster main propulsion system continues to operate for approximately three minutes to a staging velocity of 2865 meters per second (Figure 5-15). The vehicle goes through a maximum dynamic pressure of 2865 kilograms per square meter at approximately 65 seconds. After separation, the booster glides hypersonically for approximately 10 minutes and then cruises back to the launch site subsonically. The cruise takes approximately one and a half hours.

The orbiter goes to orbit after staging and can remain in orbit for approximately seven days before deorbit, entry, and return to the launch site. The baseline mission for the orbiter is resupply of a space station, which is in a circular orbit inclined 55 degrees from the plane of the equator and at an altitude of approximately 500 kilometers. After rendezvous with the space station, docking operations are initiated (Figure 5-16).

The total flight operation time line for both orbiter and booster is summarized in Figure 5-17. The total operational cycle for the orbiter is approximately 21 days, and 14 days for the booster. The difference is the seven-day on-orbit operation of the orbiter. Even before the orbiter is docked to the space station, the booster has landed at the launch site (Figure 5-4), thus marking a return to the start of the operational cycle as shown on the first bar of Figure 5-1.



INITIATE FINAL COUNTDOWN  
PROPELLANT LOADING  
BOARD CREW/PASSENGERS  
LAUNCH CHECKOUT  
COUNTDOWN & LAUNCH

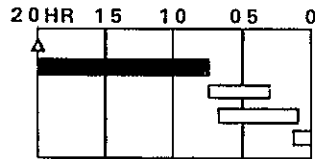
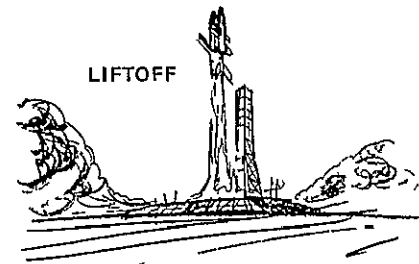
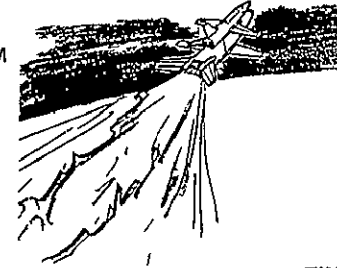
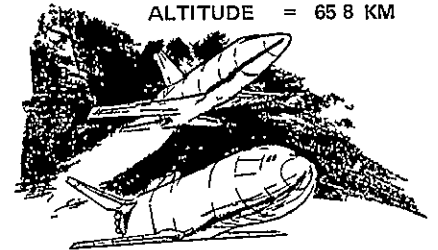


Figure 5 13 Launch Operations Time Line

MAX Q  
MAX DYNAMIC  
PRESS = 2 626 KG/SQ M  
TIME = 65 SEC  
VELOCITY = 335 M/SEC  
ALTITUDE = 97 KM



LIFTOFF



STAGING  
TIME = 32 MIN  
VELOCITY = 2 846 M/SEC  
ALTITUDE = 65 8 KM

Figure 5 15 Ascent Flight Operations

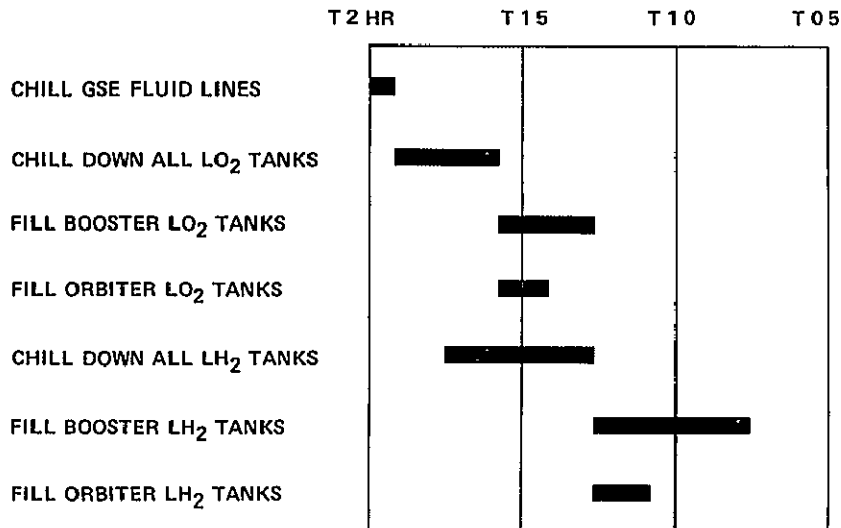


Figure 5 14 Propellant Loading Operations

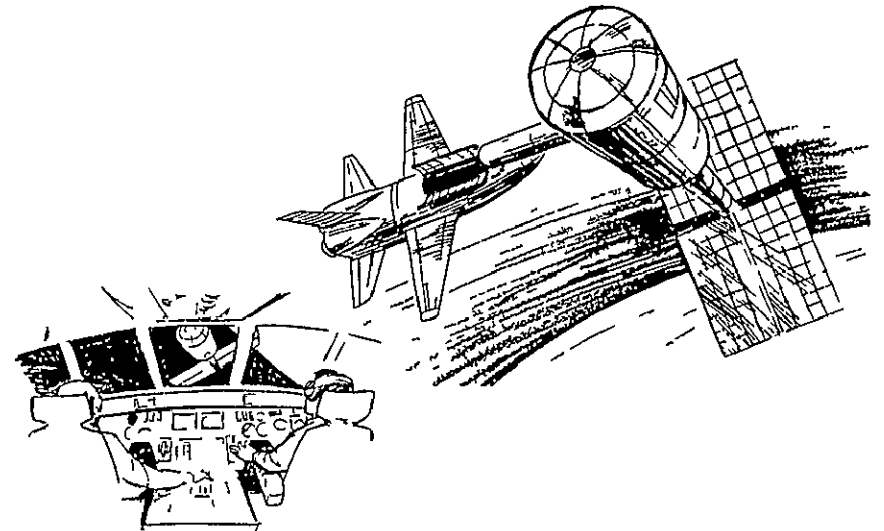


Figure 5 16 Docl mg Operations

OPERATIONS	BOOSTER	ORBITER
LIFTOFF	T=0	T=0
STAGING	0 05	0 05
DOCK WITH SPACE STATION		24 5
UNDOCK WITH SPACE STATION		153 4
TRANSFER TO PHASING ORBIT		154 0
ENTRY	0 10	167 5
INITIATE CRUISE PHASE	0 20	167 8
LANDING	1 85	168 0

*Figure 5-17 Flight Operations Time Line (Hours)*



## 6. DEVELOPMENT PLAN

The development test philosophy for both booster and orbiter is outlined in Figure 6-1. Subsystems and structural subassemblies will be qualified by ground tests. No complete booster or orbiter vehicle will be manufactured for ground tests. The first orbiter vehicle and the first booster vehicle manufactured will be used for horizontal flight tests. Vehicles 2 and 3 (of both orbiter and booster) will be used for vertical flight tests: first, launches of single stages (both booster and orbiter launches), and finally launches of the mated booster/orbiter space shuttle. For both booster and orbiter vehicles, the first horizontal flight tests begin in 1975, vertical launch of single stages in 1976, and vertical launch of the mated configuration in 1977. After flight test requirements have been satisfied, orbiter and booster vehicles 1 through 3 will be modified as required and delivered to the operational fleet.

The development program functional flow plan is diagrammed in Figure 6-2. In addition to the production of flight test vehicles,

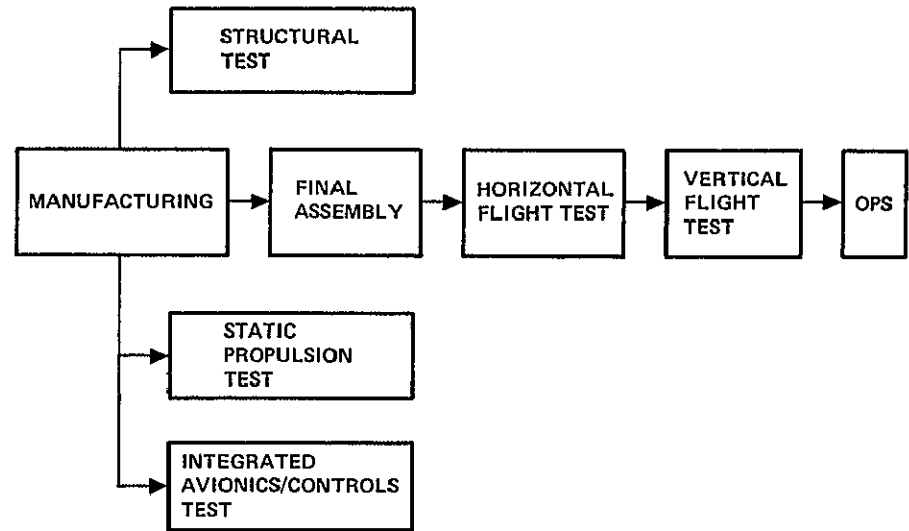


Figure 6-2 Program Functional Flow Plan

QUALIFICATION LEVEL	TEST ARTICLES	COMMENTS
SUBSYSTEMS & STRUCTURES	SUBASSEMBLIES	GROUND TESTS
SUBSONIC CHARACTERISTICS	BOOSTER VEHICLE 1 ORBITER VEHICLE 1	HORIZONTAL FLIGHT TESTS (1975)
TRANSONIC/SUPERSONIC CHARACTERISTICS	BOOSTER VEHICLE 2 & 3 ORBITER VEHICLE 2 & 3	SEPARATE VERTICAL LAUNCHES BOOSTER AND ORBITER (1976)
INTEGRATED SYSTEM OPERATIONS	BOOSTER VEHICLE 2 & 3 ORBITER VEHICLE 2 & 3	VERTICAL LAUNCH OF MATED BOOSTER/ORBITER (1977)

Figure 6-1 Development Test Philosophy

production of structural test articles, static propulsion test hardware, and hardware for integrated avionics and controls testing will be required. The program elements defined in the functional flow plan that lead to operations (discussed in the last section) will be briefly discussed in sequence.

### MANUFACTURING AND ASSEMBLY

The assembly breakdown for the booster liquid hydrogen tank is depicted in Figure 6-3. Since the tank structure will be fabricated from conventional aerospace materials, detailed parts and components can be fabricated in existing aerospace facilities. However, it may be desirable to use currently available specialized facilities such as those available at NASA-Seal Beach and NASA-Michoud for tank welding and hydrostatic testing. These facilities have unique capability for assembly and testing of large propellant tanks.

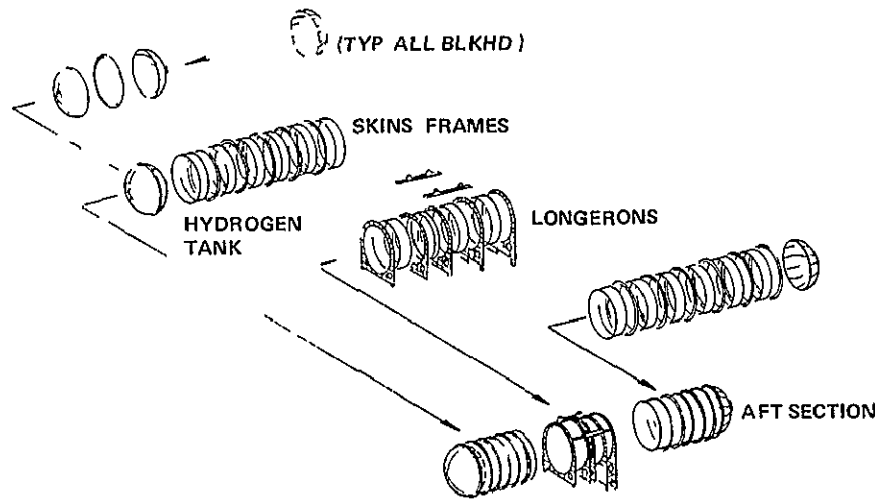


Figure 6 3 LH<sub>2</sub> Tank Assembly Breakdown

The assembly of the mated LH<sub>2</sub> and LO<sub>2</sub> tanks that form the structural backbone of the basic booster body is shown in Figure 6-4

The assembly breakdown for the booster fuselage is shown in Figure 6-5. The sequence of assembly is indicated in the flow diagram. Most of the various subsystems and subassemblies are readily transportable to the fuselage assembly site and can be manufactured at other appropriate sites. It is expected that many of these will be subcontracted. The mated tank assembly, however, is too large for transport, except by barge. It would probably be fabricated at the same site used for the fuselage assembly.

The mated tank structure is the major load carrying member of the booster, to which the rocket engine thrust structure is attached, along with 12 high-pressure, LO<sub>2</sub>/LH<sub>2</sub>, 180,000-kilogram-thrust rocket engines. The flyback air-breathing engine support structure is attached at the forward end of the main tank, along with the engine compartment structure housing for these deployable turbofan engines. The metallic radiative thermal protection system (TPS) is

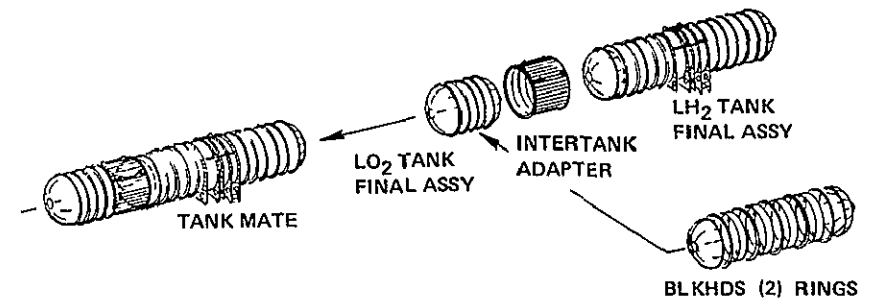


Figure 6 4 Mated Tank Assembly Breakdown

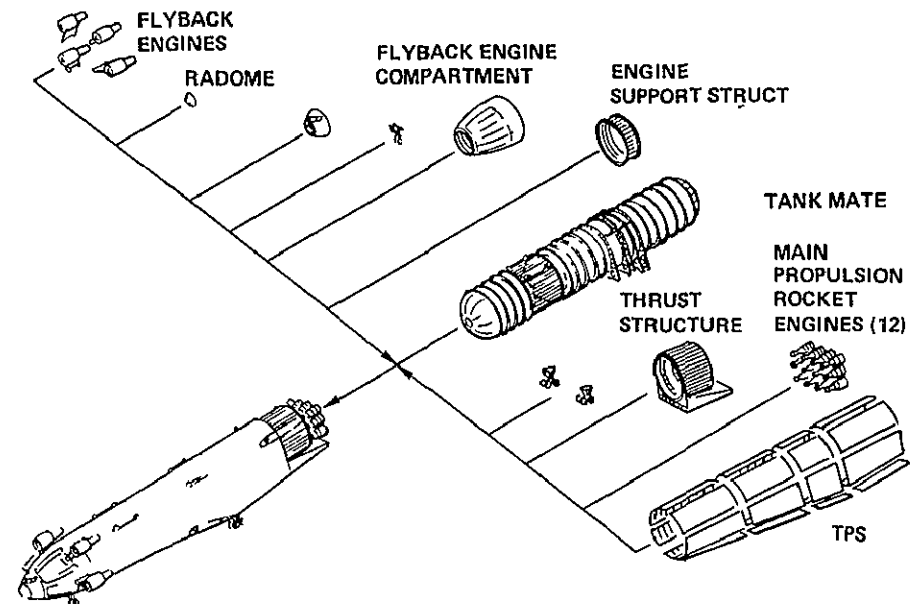


Figure 6 5 Fuselage Assembly Breakdown

then attached to the main tank structure by a system of support links that permits differential expansion of the TPS and the tank structure. Final steps in the sequence are installation and checkout of the landing gear and deployment of the air-breathing engines. These steps require a building with vertical clearance in excess of the 40

feet, which is typical of the high-bay sections of most existing aerospace industry factories

The sequence for final mating, assembly, and checkout of the booster is shown in Figure 6-6. The location at which the final mate and assembly operations are performed must have a satisfactory landing and takeoff strip so the vehicle can be self-ferried to the point of flight test or operations, if these are not carried out at the final assembly site. If circumstances dictate that the final mating operations take place at a site different from that of fuselage final assembly, barge transportation probably will be needed to transport the fuselage from the final assembly to the final mate location. Its size precludes overland transportation. Phase B studies will consider various candidate assembly, final mating, and flight test sites to determine the most economical approach. The studies also will establish whether it is desirable to perform the final mating, assembly, and checkout operations at the same site where the flight test program is conducted and will determine whether this should be the operational site as well.

The final orbiter assembly is depicted in Figure 6-7. The orbiter is smaller than the booster, and its final assembly can be carried out in facilities compatible with the production of vehicles such as large commercial aircraft or expendable launch vehicles. The assembly site should have ready access to a 3050-meter runway for initial flight tests and ferry operations. The propellant tanks in the orbiter are suspended within the load-carrying structure and are smaller and therefore easier to transport than the large load-carrying propellant tanks of the booster. This allows more flexibility in the choice of final assembly site for the orbiter.

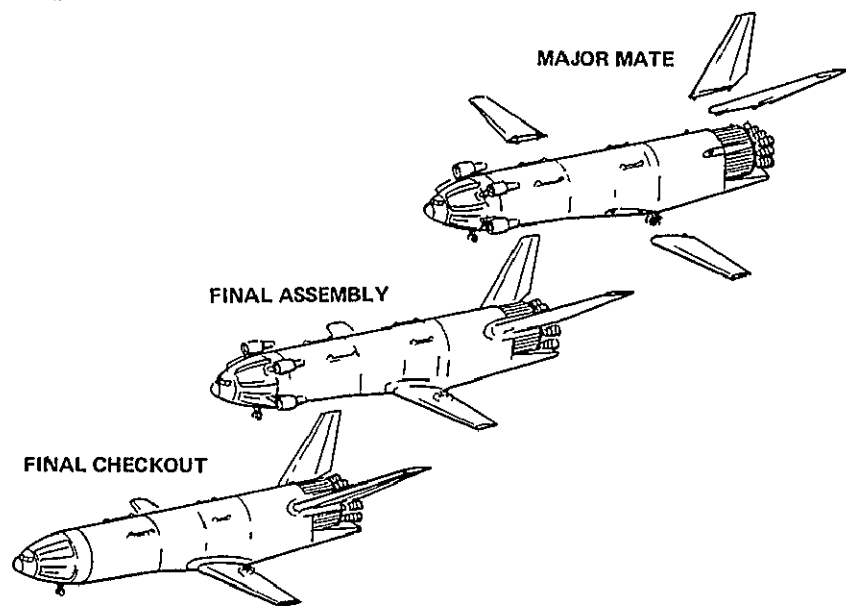


Figure 6-6 Final Mating, Assembly, and Checkout

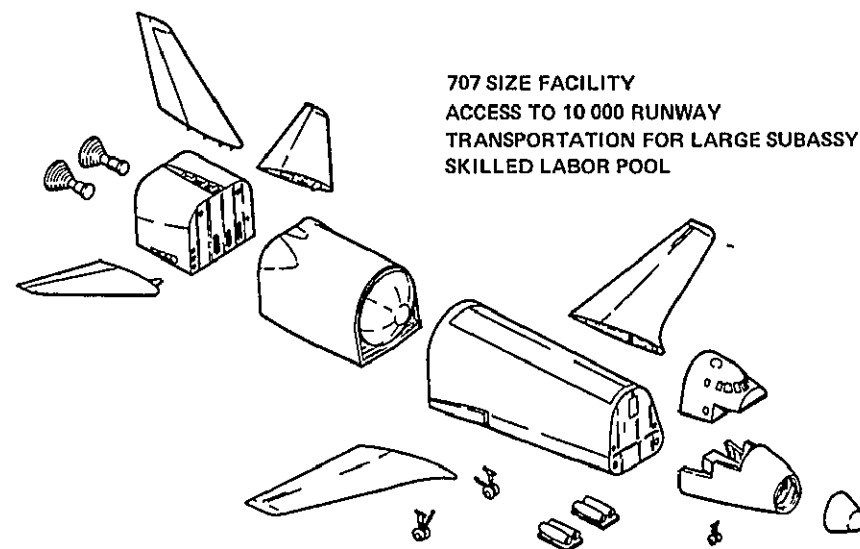


Figure 6-7 Final Orbiter Assembly

### GROUND TESTS

A large variety of ground tests of major subsystems and subassemblies is required (Figure 6-8). Wind tunnel tests must be conducted at a number of government and industry facilities to explore completely the flight regimes of the vehicle. A large number of design development tests will be required to verify the selection of materials and detail design concepts. Subsystem and structural subassembly tests will be required.

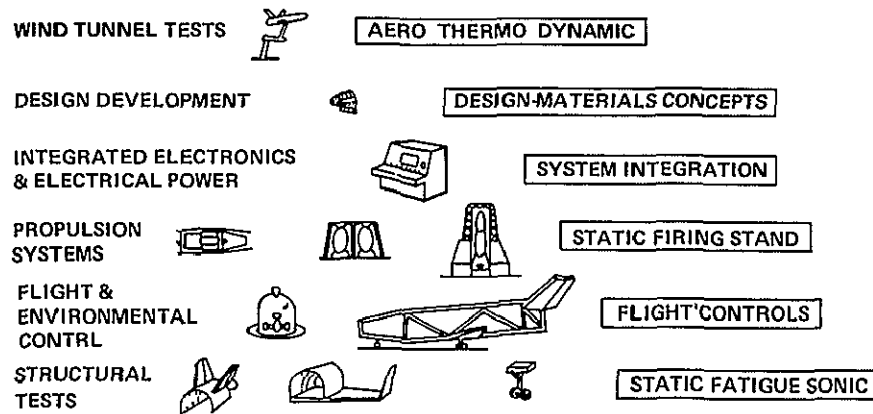


Figure 6 8 Major Ground Tests

Major structural tests must be conducted on critical booster structural subassemblies (Figure 6-9) Typical of this very extensive test program are the tests of the wing and carry-through section. The structural integrity and leak tightness of the crew compartment under pressure loads must also be demonstrated. Because of the large thermal gradients experienced by many of the sections, it will be necessary to test at elevated temperatures simulating flight environment as well as at 100m temperature. Because the shuttle vehicles are reusable aerodynamically recovered vehicles, the final proof testing will, of course, be conducted in flight tests to subject the structure to its final flight environment in an incremental fashion.

A similar set of major structural tests must be conducted on the orbiter (Figure 6-10). These tests again will verify the structural integrity and check out the operation of all mechanical equipment such as landing gear and deployment of jet engines. Where thermal stresses are a problem, tests must also simulate the flight environment to the extent necessary to check out the design at operating conditions.

Existing test facilities such as the Marshall Space Flight Center static test facility can be used for major space shuttle structural static and fatigue tests as shown in Figure 6-11. (It should be noted that

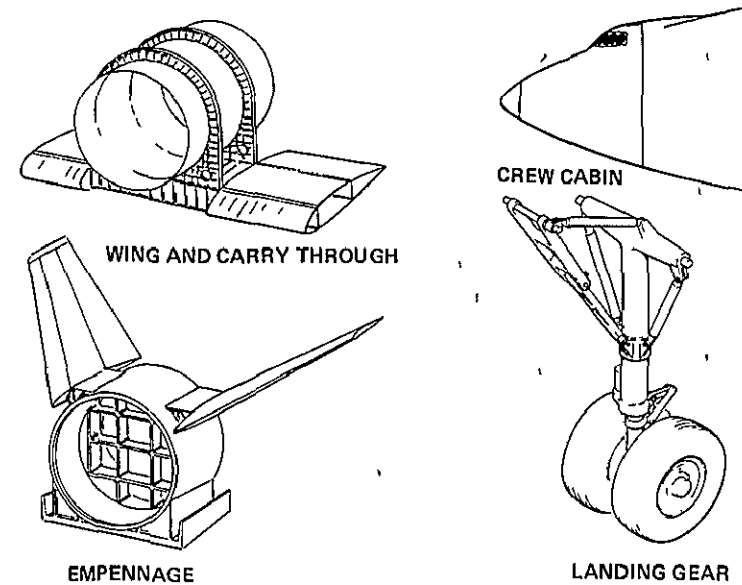


Figure 6 9 Major Structural Tests (Booster)

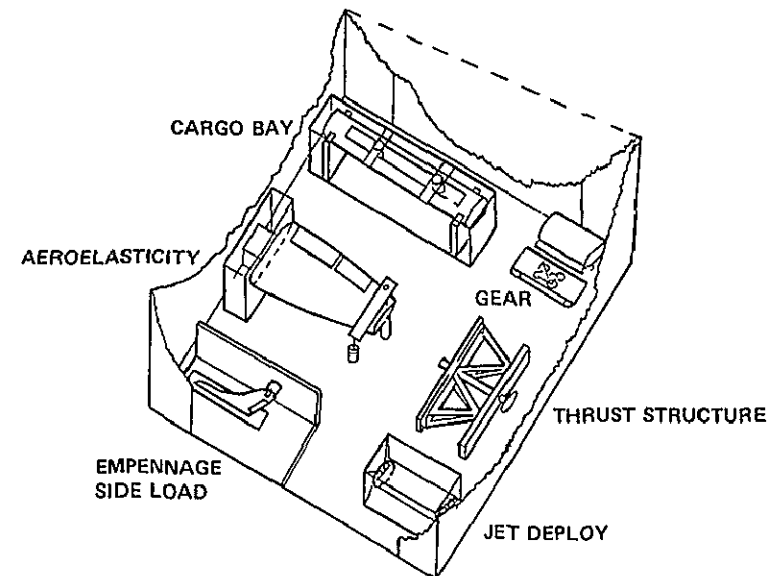
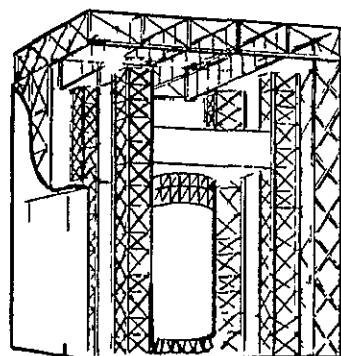


Figure 6 10 Major Structural Tests (Orbiter)



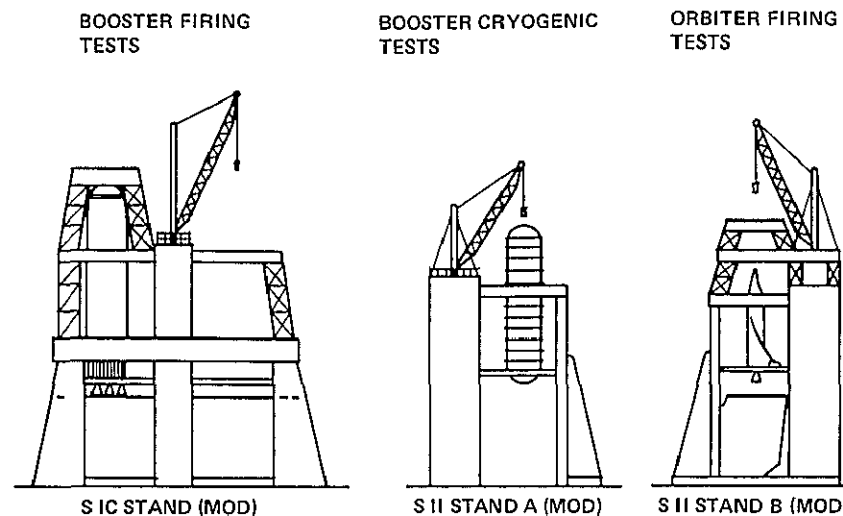


MARSHALL SPACEFLIGHT CENTER STATIC TEST FACILITY

*Figure 6 11 Structural Static/Fatigue Test of  
Booster Thrust Barrel*

the specific development facilities referenced in this section have only been selected as baseline for the start of Phase B. During Phase B, tradeoff studies will be conducted in which all feasible development facilities are considered. Final selection of major development facilities will be made by NASA. Large components such as the booster thrust barrel, as well as numerous smaller structural static and fatigue test specimens, could be handled in this facility. The booster tankage is comparable in size to that of the Saturn first stage. Therefore, this facility is well suited to the experimental work.

Static propulsion system tests could be conducted at existing facilities at the NASA Mississippi Test Facility (Figure 6-12). Only modest modifications would be required to the Saturn first-stage stand to permit static firing of the booster propulsion system to be carried out there. Cryogenic fatigue tests of the booster load-carrying propellant tanks could also be carried out at one of the Saturn second-stage test stands at the Mississippi Test Facility with only



*Figure 6 12 Static Propulsion Test, Mississippi Test Facility*

moderate modification. The second Saturn stage-two test stand at the Mississippi Test Facility could support the static propulsion system firings for the orbiter propulsion system with only minor modifications of the facilities required. Other test sites such as the NASA Rocket Propulsion Laboratory in California are being evaluated.

Detailed ground tests of the integrated avionics and control systems could be carried out using a test setup such as shown (Figure 6-13). Interface of the integrated avionics with the flight control hardware could be checked out in development tests by connecting the avionics components to a flight deck mockup and an "iron horse" fuselage and wing with the flight controls installed, and a vehicle thrust section with the engine gimbaling provisions. Flight crews and engineers could then simulate typical flight situations, checking the operation of the system and the interfaces between avionics and mechanical systems.

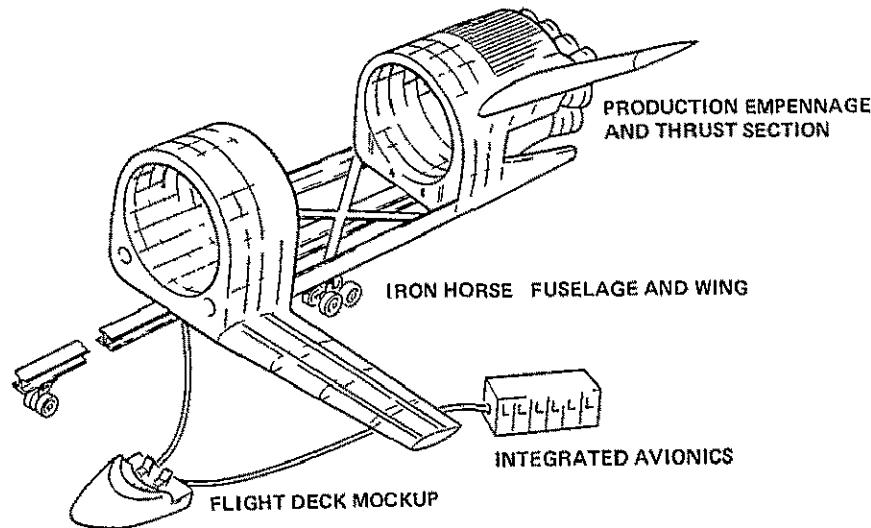


Figure 6 13 Integrated Avionics/Control Test

## HORIZONTAL FLIGHT TESTS

The NASA Flight Research Center in California, well suited for horizontal flight tests of both the booster and orbiter, has been selected as a baseline for these tests (Figure 6 14). The orbiter and booster will be flight-tested separately as subsonic aircraft, going through all the steps traditionally followed in aircraft testing beginning with low-speed taxi tests and progressing up through low-speed flights until the entire speed and altitude spectrum of the vehicle operating with its airbreathing engines has been satisfactorily checked out. Since the orbiter and booster are relatively simple subsonic vehicles with rather modest performance requirements, as compared to conventional aircraft such as the C-5A, the subsonic phase of flight testing will be much shorter and will be directed primarily at demonstrating the flightworthiness of the vehicles.

Specific horizontal flight test objectives are summarized in Figure 6-15. The primary objective is to demonstrate the flight-

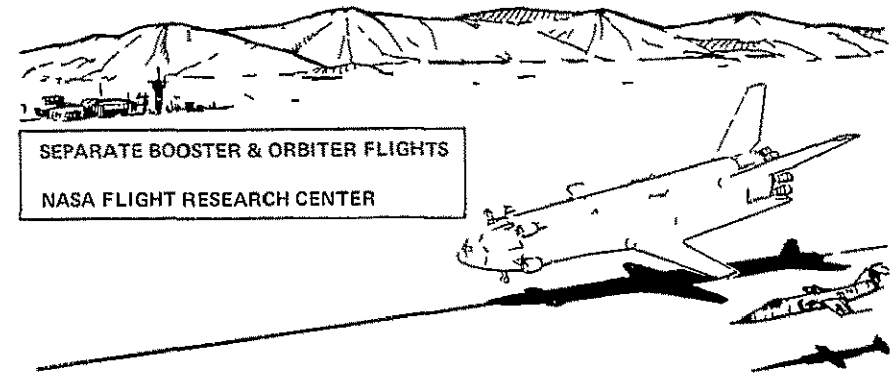


Figure 6 14 Horizontal Flight Test

### GROUND HANDLING CHARACTERISTICS

AIRSPED CALIBRATION

TAKEOFF & LANDING PERFORMANCE

STALLS & SLOW FLIGHT CHARACTERISTICS

VIBRATION FLUTTER & STRUCTURAL LOADING DATA

CLIMB & CRUISE PERFORMANCE

SUBSYSTEMS FUNCTIONAL CHECKS & PERFORMANCE

FLYING QUALITIES

Figure 6 15 Horizontal Flight Test Objectives

worthiness of the orbiter and booster in the subsonic flight mode. Tests will be conducted in an incremental fashion to permit modifications and corrections in procedures to be made as the tests progress. In the interests of flight testing at the earliest practical time, many subsystems not essential to this phase of flight (such as rocket engines) could be left out, simulated by mockup, or installed

as inactive hardware to simulated mass properties. This would permit tests to concentrate on the hardware involved in the subsonic regime only.

## VERTICAL FLIGHT TESTS

The booster and orbiter will be tested separately in vertical flight tests, as indicated (Figure 6-16). After satisfactory completion of separate tests, they will be mated for integrated system tests, which will be conducted in incremental steps until the entire performance envelope is explored. The chart indicates typical tests to be accomplished in these three test modes. The vehicles would initially be flown at reduced thrust levels (engines throttled) and with reduced propellant loads so that their flight envelopes could be expanded incrementally. Independent tests of the booster impose no particular recovery problems. The booster has cruise-back capability, and the flights could be conducted so as not to exceed cruise-back

range of the booster. Orbiter vertical flight tests will be somewhat constrained by the recovery problem. Since the orbiter does not have cruise capability, the flight-test trajectories must be compatible with the availability of appropriate down-range landing fields. Orbiter tests could progress to increasing flight velocities, with landing at down-range sites at increasing distances from the launch sites. The vehicle would then be flown back with a "strap-on" ferry kit that had air-breathing engines and fuel. Prime purpose of these single-vehicle tests will be to verify the vehicle aerodynamic and flight control characteristics and to demonstrate integrity of the heat shields and structure.

Major objectives of the integrated system tests would be to determine the interference effects of the mated vehicles up to the staging point. The verification of the staging maneuver is a major milestone in these tests. The tests would also permit the full performance envelope of the system to be explored. Final tests would simulate typical operational modes to establish the operational readiness of the system. These tests would establish the operational procedures to be used and would provide firm cost data on the projected operational costs of the system. This information would be vital to mission and payload planners for planning use of the shuttle for future operations.

The summary program development plan is presented in Figure 6-17, with dates as specified for the Phase B study. Phase C/D go-ahead is specified as 1 October 1971, and the date of initial operational capability is 1 October 1977. Major intermediate milestone dates are as indicated. It is not anticipated that this schedule could be significantly compressed. Therefore, if the Phase C/D go-ahead slipped from the date shown, all milestone dates indicated would slip by the same time interval. This is regarded as a tight, but realistic, schedule that could be met if funding is provided throughout as planned and no major program redirections are imposed as the program progresses.

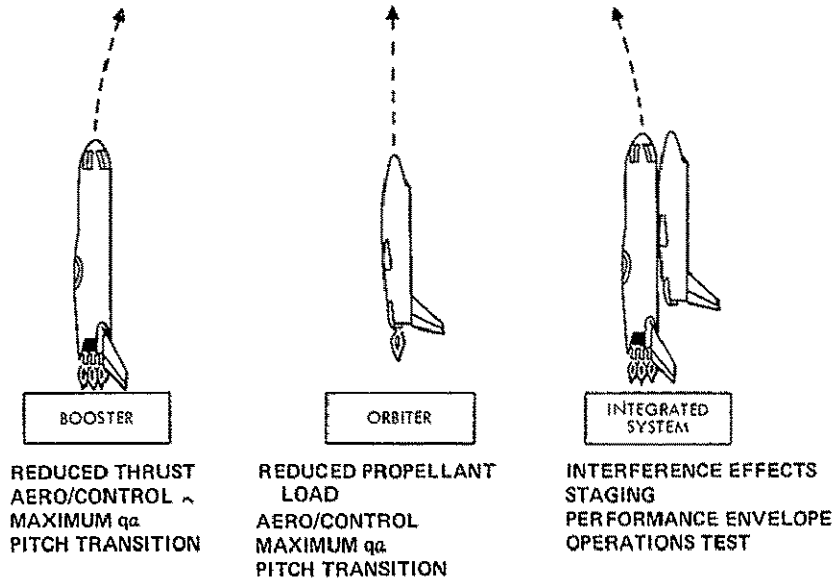


Figure 6-16 Vertical Flight Test

MILESTONE	CALENDAR YEARS						
	71	72	73	74	75	76	77
PHASE C/D GO AHEAD	▼						
MOCKUPS COMPLETE			▼				
FIRST BOOSTER HORIZ FLT					▼		
FIRST ORBITER HORIZ FLT					▼		
FIRST MATED FLT						▼	
IOC							▼

Figure 6 17 Summary Program Plan

More detail on the baseline program development plan is given in Figure 6-18. Hardware manufacture will start on both booster and orbiter vehicles in the second quarter of 1973, with first horizontal flights in the third quarter of calendar 1975. Deliveries of production vehicles would commence in mid-1977, with vehicles delivered at six-month intervals. It is anticipated that three production boosters and four production orbiter vehicles would be delivered at the times

shown to support an assumed operational program of 25 flights per year. Additional vehicles would be delivered to support a higher rate of flights.

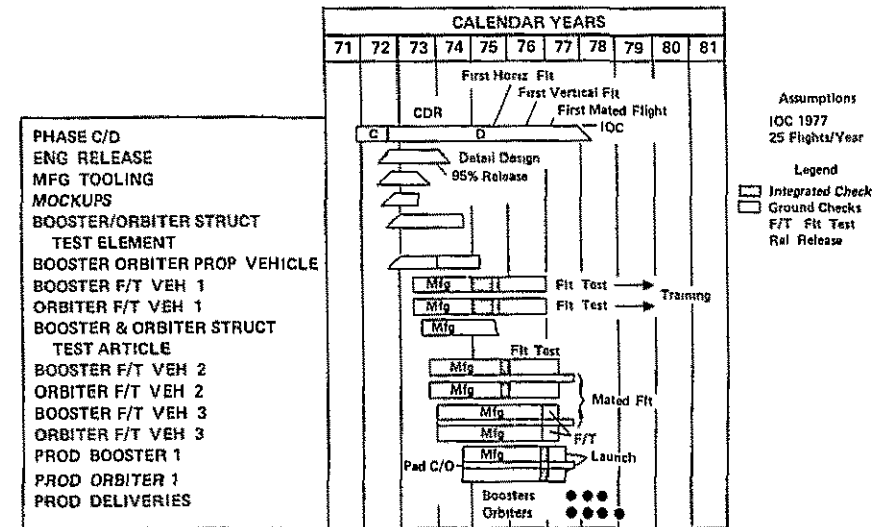


Figure 6 18 Baseline Program Plan



## 7. SUMMARY

The essential features of the Phase B shuttle program have been presented. Also, some of the technical aspects of the baseline system have been discussed. These baselines represent a going-in position, or a starting point, for the study. We will be endeavoring to improve these initial approaches in order to develop a system that meets the performance, mission flexibility, and cost objectives that NASA has defined.

We have attempted to present here sufficient detail to indicate the major program issues associated with shuttle. All design options and issue solutions are not yet fully developed. One of the main objectives of Phase B is to develop the best shuttle system through design, analysis, and test. The three most critical issues that are being faced in the Phase B and through the shuttle development are:

1. Maintaining the vehicle weight targets and, therefore, the performance capability that we currently predict.
2. Achieving the currently projected total program, production, and operational costs.
3. Developing the system on a schedule consistent with the initial operational capability goals. Meeting this target is most important. Time is money and the unavailability of a shuttle could have significant impact on other manned and unmanned programs.

Success in meeting these three objectives is directly related to the approach used in critical development or risk areas. The solutions to risk items must be balanced off against the parameters of weight and performance, cost, and schedule. Examples of the major risk areas seen at this time are shown in the upper right quadrant of Figure 7-1.

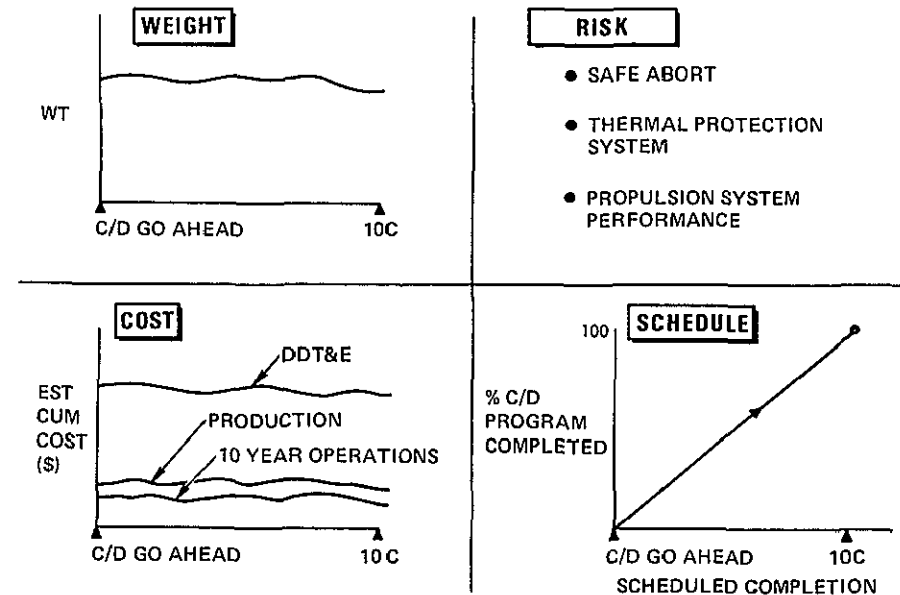


Figure 7-1 Most Critical Issues

Through recent space program achievements, industry and NASA have demonstrated the ability to meet performance and schedule goals despite many technology and management hurdles. Thus, with confidence in these areas, it is now of utmost importance that we devote equal energy to improving our cost performance. In the shuttle program, we are implementing management techniques that will assure the cost and cost risk are included in all design and program decisions down to the component level. We are confident this will lead to a shuttle design that meets the low development and operational cost objectives that have been established.

There is a common purpose in our meeting here today. It is the combined development of an international shuttle. By combined

development is meant the actual development of the hardware by the United States and European industry under common direction from NASA

At Space Division our team members have given considerable thought to potential systems that might be developed by European partners. These are categorized in Figure 7-2. As will be seen, a wide spectrum of areas of participation has been considered, ranging from avionics development to major propulsion system elements and primary structure. These items represent a substantial portion of the development program. They also would provide a challenge from a management and technology development viewpoint. In addition, it is necessary to now start mission planning for non-U.S. payloads. This is required so that we can incorporate at an early time the unique mission application and payload interface requirements that might be generated by European payloads.

The schedule for various participation in the shuttle program is outlined in Figure 7-3. As the figure shows, it is necessary to initiate

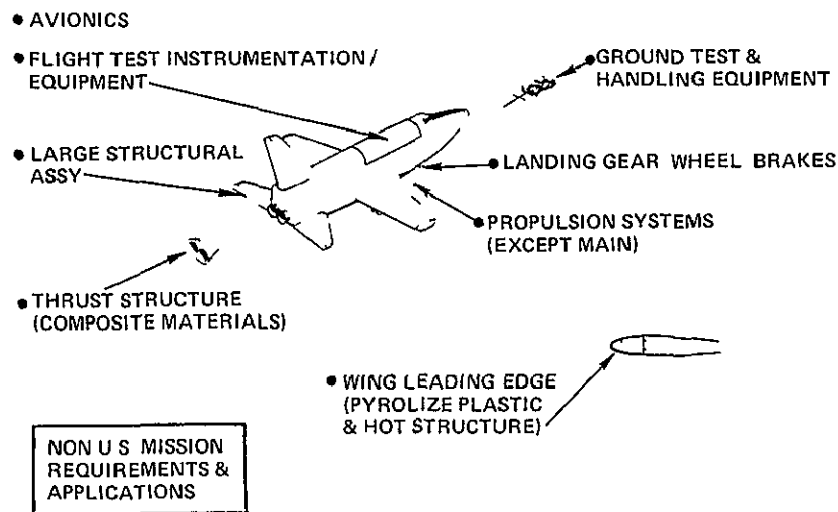


Figure 7-2 Candidates for Participation

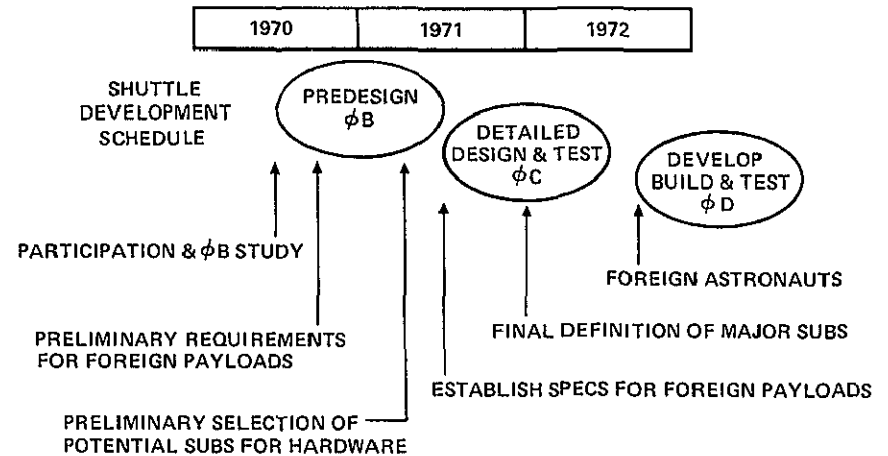
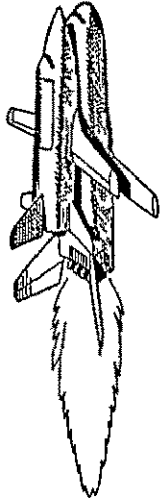


Figure 7-3 Timetable

agreements soon if European industry is to be directly involved in the decisions and design details of Phase B. Before the midpoint of the Phase B contract, i.e., before the end of 1970, the requirements for launch of non-U.S. payloads should be integrated into the vehicle designs. Approximately 12 months from now we will be selecting prime contractors for development of major subsystems on the shuttle. These organizations will work with us in Phase C and on into the final development and operation of the shuttle vehicles. As is also shown in the figure, decisions regarding detailed specifications on non-U.S. payloads and final selection of subcontractors will probably be required in 1971.

In summary (Figure 7-4) our Phase A and in-house studies lead us to project with confidence that the baseline shuttles we had described today are technically feasible and can be developed to meet the low cost transportation objectives.

Through the Phase B contract, we will, during the next year, develop high confidence in our designs, their performance, and in our cost and schedule projections. Finally, we believe that the shuttle



- PHASE A STUDIES HAVE SHOWN BASELINES TECHNICALLY FEASIBLE & WILL MEET LOW COST TRANSPORTATION OBJECTIVES
  
- PHASE B WILL YIELD HIGH CONFIDENCE BECAUSE
  - PRELIMINARY DESIGNS
  - PERFORMANCE/MASS FRACTIONS
  - SOLUTIONS TO KEY ISSUES
  - COST SCHEDULE PROJECTIONS
  
- THERE ARE REAL OPPORTUNITIES FOR INTERNATIONAL PARTICIPATION

*Figure 7 4 Summary*

will ultimately develop into the international space transportation system of the 70's and 80's We also feel that there is a real opportunity for the European industries represented here today to become directly involved in the development of this most necessary next step towards the space program of the future



Rept No. SD 70-9  
or Space Division North American Rockwell  
Author Space Shuttle Program Review  
Title Oct 81

Temp No  
6930  
16697

Presents the essential features of the Phase B Shuttle  
Program and, ~~as well~~<sup>as</sup> some of the technical aspects  
of the baseline system <sup>as presented</sup> - configurations and mission profiles  
for the shuttle ~~orbit~~<sup>orbit</sup> and boosters, subsystems and  
operations, and the development plan and testing  
program are the main items touched.

MOC  
= 0

REVIEWS ESSENTIAL FEATURES OF  
PHASE SPACE SHUTTLE SYSTEM PROGRAM

NASA SPACE SHUTTLE PROGRAM

KEY WORDS NASA SPACE PROGRAMS P  
SPACE SHUTTLES P  
INTERNATIONAL COOPERATION P  
SPACE MISSIONS  
~~MANEUVERS~~  
PROPULSION SYSTEM CONFIGURATIONS  
AEROSPACE SYSTEMS  
AVIONICS GROUND STATIONS  
~~TESTS COST ESTIMATES~~  
MANAGEMENT PLANNING  
CONFERENCES  
COST ESTIMATES  
OPERATIONAL PROBLEMS